

Function analysis of *Xenopus* Numbl in the context of primary neurogenesis

Dissertation

for the award of the degree

"Doctor rerum naturalium"

Division of Mathematics and Natural Sciences
of the Georg August University Göttingen

submitted by

Frank Nieber

from Celle, Germany

Göttingen 2010

Dr. Kristine A. Henningfeld

Department of Developmental Biochemistry, University of Göttingen

Prof. Dr. Ernst A. Wimmer

Department of Developmental Biology, University of Göttingen

Prof. Dr. Andreas Wodarz (Reviewer)

Department of Stem Cell Biology, University of Göttingen

Prof. Dr. Tomas Pieler (Reviewer)

Department of Developmental Biochemistry, University of Göttingen

Date of the oral examination:

Affidavit

Herewith I declare that I prepared the PhD thesis "Function analysis of *Xenopus* NumbL in the context of primary neurogenesis" on my own and with no other sources and aids than quoted.

29.10.2010

Submission Date

Frank Nieber

List of Publications

1. **Frank Nieber**, Tomas Pieler, Olaf Jahn, and Kristine A. Henningfeld. NumbL is essential for *Xenopus* primary neurogenesis and functions independent of Notch signaling. In preparation
2. **Frank Nieber**, Tomas Pieler, and Kristine A. Henningfeld. Comparative Expression Analysis of the Neurogenins in *Xenopus tropicalis* and *Xenopus laevis*. *Dev Dyn.* 2009 238:451–458

Table of Contents

Table of Contents	I
Acknowledgements	IV
List of Figures	V
Abbreviations	VII
1. Introduction	
1.1 Neural Induction	1
1.2 Neuroectoderm maturation	4
1.3 Neuronal Differentiation	6
1.4 Lateral Inhibition	9
1.5 Numb as cell fate determinant in neurogenesis	11
1.6 Numb acts as scaffold protein	13
1.7 Numb and Numbl like isoforms	14
1.8 Multiple functions of Numb	16
1.9 Regulation of Numb	16
1.10 <i>Xenopus</i> Numb and Numbl like	17
1.11 Aims	18
2. Materials and Methods	
a. Organisms	
2.1.1 <i>Xenopus laevis</i> and <i>Xenopus tropicalis</i>	19
2.1.2 <i>Escherichia coli</i>	19
2.2 Oligonucleotides	
2.2.1 RT-PCR oligonucleotides	19
2.2.2 General oligonucleotides	21
2.2.3 Morpholino oligonucleotides	21
2.3 Constructs	
2.3.1 Overexpression	22
2.3.2 Markers for whole mount in situ hybridization	27

2.4 Total RNA extraction and cDNA synthesis	29
2.5 RT-PCR analysis	29
2.6 In vitro synthesis of RNA	
2.6.1 Capped sense RNA	30
2.6.2 Antisense RNA	30
2.7 T _N T in vitro translation	30
2.8 Embryo culture and microinjections	31
2.9 X-Gal staining	32
2.10 Whole mount in situ hybridization	33
2.11 Phosphorylated Histone 3 (pH3) staining	35
2.12 Sections	35
2.13 Fluorescent labeling of animal caps	36
2.14 Tandem affinity purification (TAP)	37
3. Results	
3.1 <i>Xenopus</i> Numb isoforms switch during neural development	39
3.2 <i>NumbL</i> is expressed in the territories of primary neurogenesis	40
3.3 <i>NumbL</i> is positively regulated by Neurogenin 1-3	43
3.4 <i>NumbL</i> gain-of-function leads to an increase in neural tube size	45
3.5 <i>NumbL</i> knockdown does not activate the Notch pathway	46
3.6 Notch inhibition does not rescue <i>NumbL</i> knockdown	47
3.7 A knockdown of <i>NumbL</i> leads to an increase in neural progenitors	49
3.8 <i>NumbL</i> knockdown increases the number of mitotically active cells in the ectoderm at early gastrula stages	50
3.9 <i>NumbL</i> knockdown promotes neural crest formation at tailbud stages	52
3.10 <i>Ngn</i> expression patterns are disturbed in <i>NumbL</i> morphants	53

3.11 NumbL knockdown leads to an increase in early neural gene expression	54
3.12 <i>Zic</i> expression is increased in a Notch independent manner upon NumbL knockdown	56
3.13 <i>Xenopus</i> Numb and NumbL are located in the cytoplasm	57
3.14 NumbL interacts with the AP-2 complex	61
3.15 Interaction with the AP-2 complex is essential for NumbL function	62
4. Discussion	
4.1 <i>NumbL</i> has a dual function during <i>Xenopus</i> primary neurogenesis	64
4.2 NumbL function during <i>Xenopus</i> primary neurogenesis is independent of Notch signaling	66
4.3 NumbL is localized in the cytoplasm and interacts with the AP-2 complex	69
5. Summary	72
6. Bibliography	73
7. Appendix	87
Curriculum vitae	90

Acknowledgements

I would like to thank Prof. Pieler for providing me the opportunity to perform my PhD thesis in his laboratory. In addition, I would like to thank Prof. Wimmer and Prof. Wodarz for helpful discussion during my thesis committee meetings. I also thank Prof. Doenecke, Prof. Bucher and Dr. Stoykova, who kindly agreed to be part of my extended thesis committee.

Especially, I thank my supervisor Dr. Kristine Henningfeld for her all-time support. I appreciate her enormous personal effort in guiding and teaching me during my thesis. So Kris, thank you a lot for discussion, ideas and help with any kind of problems!

Further, I thank the members of the department and particular the members of the Neuro-Group, Barbara, Katja, Marie and Patrick for the motivating and inspiring working atmosphere in the laboratory.

I express my gratitude to Dr. Olaf Jahn and Dr. Ivan Manzini who supported me in different aspects of my project and the Göttingen Graduate School for Neurosciences and Molecular Biosciences for funding of my thesis.

List of Figures

Figure 1: Organizing centres during neural induction	2
Figure 2: Overview of excreted signaling inhibitors expressed by the Spemann organizer and the pathways inhibited	2
Figure 3: Neural Induction	4
Figure 4: Neuroectoderm maturation	6
Figure 5: Domains of primary neurogenesis	7
Figure 6: Neuronal differentiation	8
Figure 7: Lateral inhibition by the Delta Notch signaling pathway	10
Figure 8: Lateral inhibition defines the number of neurons in the neuroectoderm	11
Figure 9: Numb as cell fate determinant in <i>Drosophila</i> SOP	12
Figure 10: Protein-protein interaction domains of Numb	14
Figure 11: Numb isoforms	14
Figure 12: NumbL knockdown inhibits proneural factors downstream of Ngn	18
Figure 13: Temporal expression analysis of <i>X.tropicalis</i> Numb and NumbL isoforms	40
Figure 14: Comparison of spatiotemporal expression of <i>X. laevis</i> Numb and NumbL	42
Figure 15: NumbL is positively regulated by the neurogenins	44
Figure 16: NumbL overexpression promotes neurogenesis and enlarges the neural tube	46
Figure 17: NumbL knockdown does not cause an increase of the Notch signaling pathway in the open neural plate	47
Figure 18: Notch signaling does not rescue NumbL knockdown	48
Figure 19: NumbL knockdown leads to an increase in early neural gene	

expression	49
Figure 20: NumbL knockdown leads to increased proliferation during gastrula stages and loss of cell cycle regulators	51
Figure 21: NumbL knockdown promotes neural crest fate at tailbud stages	53
Figure 22: NumbL knockdown influences Neurogenin expression	54
Figure 23: NumbL knockdown leads to an increase in Zic gene expression	55
Figure 24: Zic genes are activated by Notch but Notch inhibition does not rescue the NumbL knockdown phenotype	57
Figure 25: Subcellular localization of mouse MT-Numb1, <i>X.laevis</i> MT-NumbL and <i>X.tropicalis</i> MT-Numb3	59
Figure 26: Subcellular localization of <i>X. laevis</i> NumbL and <i>X. tropicalis</i> Numb under wildtype and neuralized conditions	60
Figure 27: NumbL interacts with components of the AP-2 complex	62
Figure 28: Interaction with the AP-2 complex is crucial for NumbL function	63
Figure 29: Scheme of NumbL dual function during primary neurogenesis	72
Appendix Figure 1: Genomic structure of <i>X. tropicalis</i> <i>Numb</i> and identified insert sequences	87
Appendix Figure 2: Tandem affinity purification of NumbL(DLA)-CTap	89

Abbreviations

AP	alkaline phosphatase
ATP	adenosine triphosphate
BCIP	5-bromo-4-chloro-3-indolyl phosphate
BMB	Bohringer Mannheim blocking reagent
BMP	bone morphogenetic protein
bp	base pairs
BSA	bovine serum albumin
°C	Celsius degree
CIAP	calf intestine alkaline phosphatase
Dig	dioxigenine
DNA	deoxyribonucleic acid
DTT	dithiothreitol
EDTA	ethylenediaminetetraacetic acid
EGTA	ethyleneglycol-bis(2-aminoethylether)-N,N-tetraacetate
et al.	et alii
g	gramm
h	hours
HCG	human chorionic gonadotropin
kb	kilobase
l	liter
LB	Luria-Bertani
μ	micro
m	milli
M	molar
MAB	maleic acid buffer
MEM	MOPS-EGTA-MgSO ₄ buffer
MEMFA	MOPS-EGTA-MgSO ₄ formaldehyde buffer

min	minutes
mm MO	mismatch MO
MO	morpholino oligonucleotide
mRNA	messenger RNA
n	nano
NaAc	sodium acetate
NBT	nitro-blue tetrazolium
Ngn	neurogenin
Ngnr	neurogenin related
PAGE	polyacrylamid gel electrophoresis
PBS	phosphate buffered saline
PCR	polymerase chain reaction
pH	negative decade logarithm of hydrogen ion concentration
PTB	phosphor-tyrosine-binding
PRR	proline rich repeat
RNA	ribonucleic acid
rpm	rounds per minute
RT	room temperature, reverse transcriptase
RT-PCR	reverse transcriptase PCR
sec	second
SSC	standard saline citrate buffer
<i>Taq</i>	<i>Thermus aquaticus</i>
TAP	Tandem affinity purification
T_m	melting temperature
U	units
Vol.	volume
X-Gal	5-bromo-4-chloro-3-indolyl- β -D-galactoside
<i>X. laevis</i>	<i>Xenopus laevis</i>

X. tropicalis

Xenopus tropicalis

Abbreviations of Deoxynucleic Acids

A Adenine
C Cytosine
G Guanine
T Thymine

Abbreviations of Amino Acids

A	Alanine	C	Cystein
D	Aspartate	E	Glutamate
F	Phenylalanine	G	Glycine
H	Histidine	I	Isoleucine
K	Lysine	L	Leucine
M	Methionine	N	Asparagine
P	Proline	Q	Glutamine
R	Arginine	S	Serine
T	Threonine	V	Valine
W	Tryptophane	Y	Tyrosine

1. Introduction

1.1 Neural Induction

In *Xenopus*, the majority of neurons are born in two main waves. In the first wave, called primary neurogenesis, the early nervous system required for movements and responses of the larvae is established (Hartenstein, 1989). In the second wave, which begins at the onset of metamorphosis, the majority of primary neurons are replaced with secondary neurons to generate the nervous system of the adult animal (Wullimann *et al.*, 2005). The molecular mechanisms of both phases of neurogenesis may be conserved, as genes involved in the process of primary neurogenesis are also active during secondary neurogenesis (Wullimann *et al.*, 2005).

During gastrulation, the dorsal ectoderm acquires the competence for a neural fate in a process called neural induction. Cells of the dorsal ectoderm receive inducing signals from the mesoderm and adopt a neural fate at the expense of an epidermal fate (De Robertis and Kuroda, 2004). Prior to the onset of gastrulation at blastula stages the combined activity of two signaling centers predisposes the prospective neuroectoderm to neural induction (Kuroda *et al.*, 2004) (Figure 1). One is the blastula Chordin and Noggin expressing centre (BCNE), which is located in dorsal animal cells and expresses the BMP antagonists *Chordin* and *Noggin*, as well as *Xnr3* and the homeobox gene *Siamois* (Kuroda *et al.*, 2004). The other is the Nieuwkoop center, which is localized in dorsal vegetal cells and expresses *Cerberus*, an inhibitor of Wnt, BMP and Nodal signaling (Piccolo *et al.*, 1999) and the Nodal-related endomesodermal inducers *Xnr1*, *Xnr2*, *Xnr4*, *Xnr5* and *Xnr6* that induce the Spemann organizer in overlying mesodermal cells (Nieuwkoop, 1969; Agius *et al.*, 2000; Takahashi *et al.*, 2000; Shivdasani, 2002; Kimelman, 2006).

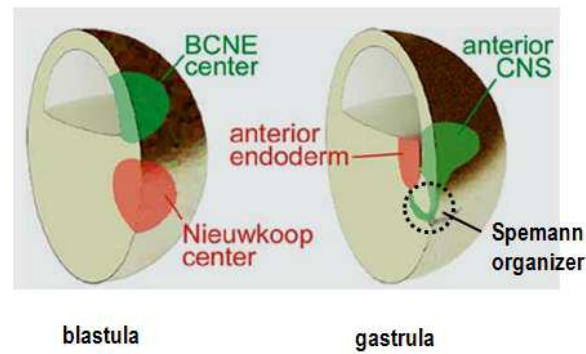


Figure 1: Organizing centers during neural induction. During gastrula stages, the Nieuwkoop center is found in the dorsal vegetal region while the blastula Chordin/Noggin expressing cells (BCNE) are located in the animal region. Both centers induce the Spemann organizer during gastrula stages and give rise to the anterior-most endoderm or the ectodermal anterior CNS, respectively (after Kuroda *et al.*, 2004, modified).

During gastrulation, the Spemann organizer expresses and secretes several organizer-specific proteins such as the Wnt inhibitors *Frzb-1*, *Dickkopf-1*, *Crescent* (Leyns *et al.*, 1997; Glinka *et al.*, 1998; Pera *et al.*, 2000; Piccolo *et al.*, 1999), the TGF/Nodal inhibitors *Lefty* and *Antivin* (Meno *et al.*, 1996; Thisse *et al.*, 1999), the BMP antagonists *Chordin*, *Noggin* and *Follistatin* (Piccolo *et al.*, 1996; Zimmerman *et al.*, 1996; Iemura *et al.*, 1998) and *Cerberus*, which inhibits Nodal, Wnt and BMP signals (Piccolo *et al.*, 1999) (Figure 2).

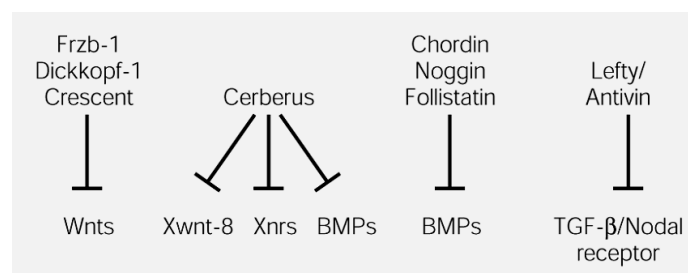


Figure 2: Overview of excreted signaling inhibitors expressed by the Spemann organizer and the pathways inhibited. The secreted factors of the Spemann organizer antagonize an epidermal fate in ectodermal cells and therefore enable a neural induction of the ectoderm (De Robertis *et al.*, 2000).

The Spemann organizer is not a homogeneous structure and can be separated in three subregions that possess different inducing potentials: the head organizer, the trunk/tail organizer and the deep yolky endoderm (Spemann and Mangold, 1921; Spemann, 1931; Nieuwkoop *et al.*, 1952; Saxen *et al.*, 1962;

Gerhart, 2001). With the onset of gastrulation, the first tissue to invaginate through the early blastopore lip contains cells of the vegetal marginal zone (ventral band), which form the yolky endoderm subregion of the organizer (Sasai *et al.*, 1995). These cells express *Dickkopf* and *Cerberus* and induce the most anterior neural structures and the cement gland. The head organizer originates in the ventral marginal zone and gives rise to mesodermal tissue of the organizer (Harland and Gerhardt, 1997; Kodjabachian, 1998). The head organizer expresses anti-BMPs, such as *Chordin*, *Noggin* and *Follistatin*, as well as the Wnt-inhibitor *Frzb-1* and *Crescent*, and induces the anterior neural plate that will give rise to the forebrain and midbrain. The trunk/tail organizer originates in the dorsal band of the marginal zone (Gerhardt, 2001) and induces the posterior neural plate through *Chordin*, *Noggin* and *Follistatin* expression. FGF signaling was also found to be essential for establishment and maintenance of the trunk/tail organizer (Mitchel and Sheets, 2001; Delaune *et al.*, 2005; Fletcher and Harland, 2008).

For the induction of a neural fate in the ectoderm, bone morphogenetic protein (BMP) signaling levels have to be lowered, as BMPs induces genes like the zinc-finger transcription factor *GATA-1* drive ectodermal tissue to an epidermal fate (Shibata *et al.*, 1998; Gawantka *et al.*, 1995). The secreted BMP antagonists expressed by the Spemann organizer inhibit BMP signaling by binding BMPs and preventing their interaction with BMP-receptors (*Chordin* and *Noggin*) or by blocking activation of the receptor (*Follistatin*). Another inhibitor of BMP signaling is *Derriere* (or *GDF3*), which like BMP belongs to the TGF- β family of ligands (Levine *et al.*, 2006; Levine *et al.*, 2009), and is expressed already before gastrulation in the BCNE. However, BMP inhibition alone is not sufficient to induce a neural fate in the ectoderm; it has been shown that low levels of FGF signaling are also required (Delaune *et al.*, 2005). FGF inhibits BMP signaling by downregulating the activity of Smads, intracellular transducers of the BMP pathway via the Ras/MAPK pathway (Pera *et al.*, 2003; Kuroda *et al.*, 2005). Although an inhibition of BMP is sufficient to induce early neural markers like *Zic1*, FGF4 activity was found to be essential for the induction of early neural genes like *Zic3* and *FoxD5a* that were not induced by BMP inhibition alone (Marchal *et al.*, 2009). Recently, the necessity of simultaneous BMP inhibition

and FGF signals for stable induction of neural genes was demonstrated. FGF activation could induce the neural markers *Sox2* and *Sox3* in *Xenopus* ectodermal explants, but BMP signals were able to revert the tissue to an epidermal fate (Wills *et al.*, 2010). In addition to BMP inhibition and FGF signaling, inhibition of Wnt signaling is needed to allow the establishment of the neural ectoderm. Wnt inhibition strongly increases the neuroectoderm size and activation of the canonical Wnt pathway impairs the expression of neural markers (Heeg-Truesdell *et al.*, 2006).

1.2 Neuroectoderm maturation

The process of neural induction results in the expression of a large number of genes that coordinately promote a neural fate, limit the size of the neural plate and regulate the onset of neuronal differentiation (Sasai *et al.*, 1996; Moody *et al.*, 2002). Although the transcriptional regulation of most panneural genes has not been characterized to date, FGF4-mediated calcium influxes via DHP-sensitive Ca^+ channels in the cells of the presumptive neural ectoderm were shown to be essential and sufficient for the induction of early neural genes (Moreau *et al.*, 2008; Lee *et al.*, 2009) (Figure 3).

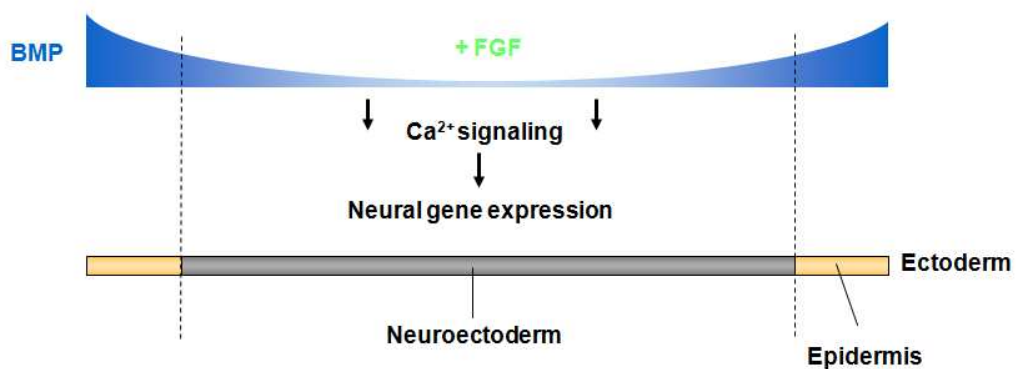


Figure 3: Neural Induction. Absence of BMP signaling together with low levels of FGF signaling lead to a calcium dependent induction of neural genes in the ectoderm. High levels of BMP inhibit a neural fate and promote an epidermal fate.

The genes induced during neural induction include the forkhead transcription factor *FoxD5* (Sölter *et al.*, 1999), coiled-coil domain containing DNA replication inhibitor *Geminin* (Kroll *et al.*, 1998), the HMG-box genes *Sox2*, *Sox3*, *SoxD* and *Sox11* (Uwanogho *et al.*, 1995; Mizuseki *et al.*, 1998a; Kishi *et al.*, 2000; Wegner and Stolt, 2005; Dee *et al.*, 2008), the zinc finger transcription factors *Zic1*, *Zic2* and *Zic3* (Nakata *et al.*, 1997; Brewster *et al.*, 1998; Mizuseki *et al.*, 1998b) and the Iroquois genes *Xiro1*, *Xiro2* and *Xiro3* (Bellefroid *et al.*, 1998). While BMP antagonism alone is sufficient to induce *Zic1*, which like *Zic3* promotes expression of downstream neural genes, activation of *FoxD5* and *Zic3* and their downstream targets *Geminin* and *Sox11* requires FGF4 activity (Marchal *et al.*, 2009). The activation of *Zic2*, downstream of *FoxD5*, was in turn found to be dependent on Notch signaling (Yan *et al.*, 2009a). *Sox11*, *Geminin* and *Zic2* were found to be sufficient to induce the downstream targets *Sox2* and *Sox3* (Yan *et al.*, 2009b). Upon maturation of the neuroectoderm, additional panneural markers like the *neural cell adhesion molecule (NCAM)* and *SoxD* are expressed (Kintner *et al.*, 1987; Mizuseki *et al.*, 1998b). In contrast to *Sox2* and *Sox3*, which enhance the sensitivity of ectodermal cells to inducing signals, *SoxD* has been shown to induce neuronal differentiation through the activation of *Ngn2* (Mizuseki *et al.*, 1998b, Hardcastle *et al.*, 2000) (Figure 4).

Nodal related genes as targets of *Wnt-8*, *VegT* and *Vg1* are proposed to restrict a neural fate at the borders of the neural plate and thereby define the size of the neuroectoderm (Heeg-Tuesdell *et al.*, 2006).

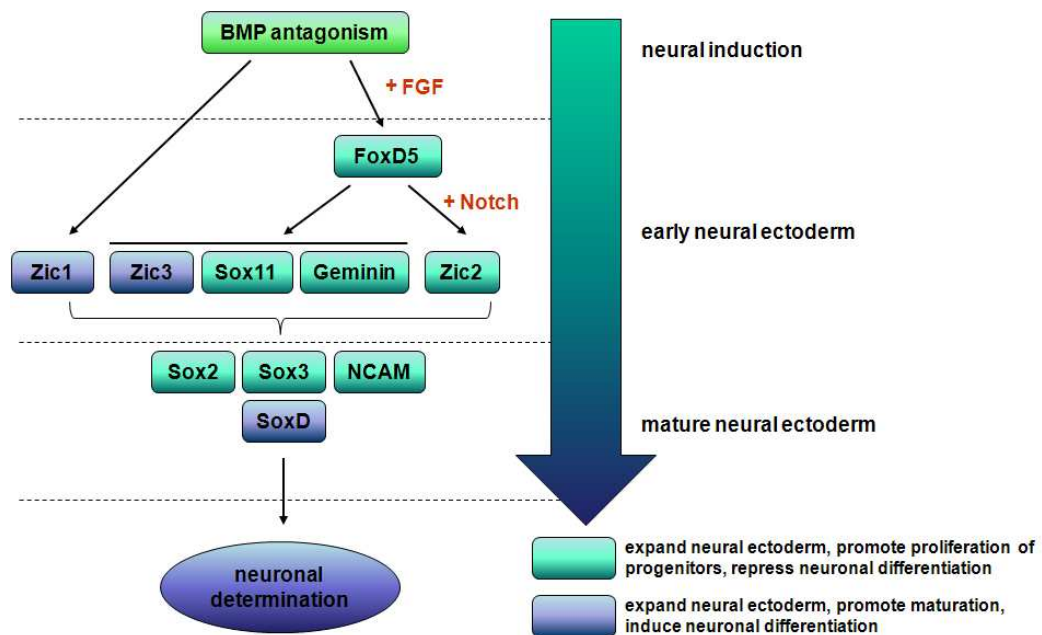


Figure 4: Neuroectoderm maturation. Upon BMP inhibition and low levels of FGF signaling, the forkhead transcription factor *FoxD5* is induced. *Zic1* is induced independently of FGF signalling. *FoxD5* induces Notch dependent and independent further downstream neural genes like *Zic3*, *Sox11*, *Geminin* or *Zic2*. Upon maturation of the neuroectoderm, the neural markers *Sox2*, *Sox3*, *NCAM* and *SoxD* are expressed. *Zic1*, *Zic3* and *SoxD* promote single cells in the mature neuroectoderm to express neuronal determination factors and undergo differentiation.

1.3 Neuronal Differentiation

The primary neurons are born in three bilateral longitudinal domains in the posterior neural plate and can be visualized by the expression of *neural specific type II β -tubulin (N-tubulin)* (Oschwald *et al.*, 1991). With the exception of the trigeminal placodes, neurogenesis in the anterior neural plate is delayed until late neurula stages (Papalopulu and Kintner, 1996). The neuroectoderm at the open neural plate stage is bilayered. While the primary neurons mainly arise from the deeper sensorial layer, the cells in the superficial epidermal layer stay in a proliferative state and undergo differentiation in a later phase of development (Chalmers *et al.*, 2002; Hartenstein, 1989) (Figure 5). As the neural plate folds and forms the neural tube, the medial, intermediate and lateral stripe will give rise to motor neurons, interneurons and sensory neurons, respectively (Chitnis *et al.*, 1995; Hartenstein, 1989) (Figure 5).

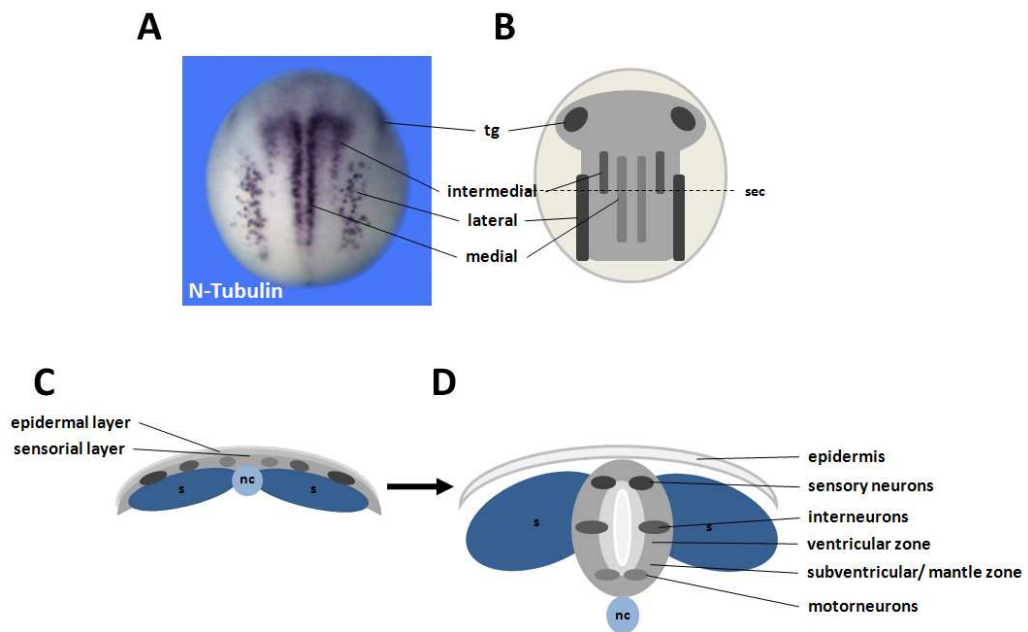


Figure 5: Domains of primary neurogenesis. (A) Stage 15 embryo stained for *N-tubulin* by whole mount in situ hybridization to mark postmitotic neurons. The embryo is shown in a dorsal view, anterior up. (B) Schematic representation of the domains of primary neurogenesis at the open neural plate stage (light grey). The characteristic domains are depicted in the three longitudinal domains on both sides of the midline and the trigeminal placodes. (C) Schematic representation of a transversal section of the open neural plate of the embryo as indicated with the dashed line (sec) in (B). The neuroectoderm consists of a superficial and a deep cell layer. Primary neurons are located in the deep layer. (D) Schematic representation of a transversal section of a stage 30 posterior neural tube. The neural plate has folded up to form the neural tube, the medial, intermediate and lateral stripe of primary neurons give rise to motorneurons, interneurons and sensory neurons, respectively. While proliferating progenitor cells are located in the ventricular zone, differentiating neurons are located in the subventricular and mantle layer. tg, trigeminal placodes; s, somite; nc, notochord; sec, plane of section.

The first proneural genes expressed in the areas of primary neurogenesis belong to the neurogenin family of bHLH transcription factors (*Ngn*), *Ngn1*, *Ngn2* (originally referred to as *Ngnr-1*) and *Ngn3*, which are distantly related to the *Drosophila* proneural transcription factor *Atonal* (Jarman *et al.*, 1993; Ma *et al.*, 1996, Nieber *et al.*, 2009). Neurogenins are proposed to act as neuronal determination factors (Sommer *et al.*, 1996; Ma *et al.*, 1996; Mizuseki *et al.*, 1998b) and several panneural genes like *Zic1*, *Zic3* and *SoxD* have been shown to induce *Ngn2* expression. *Zic2* is instead expressed in between the stripes of *Ngn1* and *Ngn2* and inhibits *Ngn* expression and function (Brewster *et al.*, 1998), thereby refining the territories of neurogenesis. *Ngn2* instructs neural as non-

neural ectoderm to undergo neuronal differentiation by activating a network of downstream differentiation factors, such as *NeuroD*, *Coe2*, *Xebf3*, *Mxi1* and *MyT1* (Bellefroid *et al.*, 1996; Ma *et al.*, 1996; Dubios *et al.*, 1998; Klisch *et al.*, 2006; Pozzoli *et al.*, 2001). In addition, Ngn2 induces the cell cycle inhibitors p21 activated kinase 3 (*Pak3*) and the growth arrest and DNA damage induced gene gamma (*Gadd45-y*) to enable cell cycle exit and differentiation of progenitor cells (Souopgui *et al.*, 2002; De la Calle-Mustienes *et al.*, 2002). An additional cell cycle regulator, the Cip/Kip cyclin dependent kinase inhibitor $p27^{Xic1}$ is also highly expressed in neuronally determined cells and was found to be required for activation of downstream differentiation factors (Vernon *et al.*, 2005; Carruthers *et al.*, 2003) and stabilization of Ngn2 by presumably preventing its phosphorylation by CDK and subsequent degradation (Vosper *et al.*, 2009 and Philpott, unpublished data) (Figure 6). Ngn2 was additionally described to activate transcription of genes that encode proteins involved in chromatin remodeling like Brg1 and the proneural RNA binding protein Seb4R, which are essential for neuronal differentiation (Seo *et al.*, 2005; Boy *et al.*, 2004). More recently, it has been shown that Ngn2 also induces genes encoding a variety of other transport proteins, signal pathway components and transcription factors; the underlying functionalities of the mainly uncharacterized genes remain to be elucidated (Seo *et al.*, 2007).

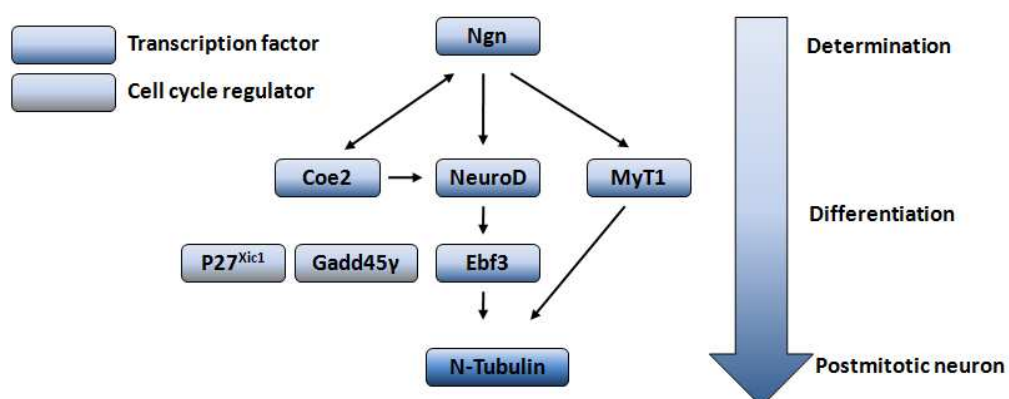


Figure 6: Neuronal differentiation. Schematic representation of genes that are activated by Ngn2. Color code for transcription factors and cell cycle regulators is indicated on the left. Ngns define neuronal determined cells and activate a network of downstream transcription factors like Coe2, NeuroD, MyT1 and Ebf3, which finally leads to the expression of N-tubulin in postmitotic neurons. The cell cycle regulators $p27^{Xic1}$ and Gadd45y are also necessary for differentiation.

1.4 Lateral Inhibition

Neurogenins not only induce downstream differentiation factors, they also activate the Notch pathway, which inhibits neurogenesis in a process called lateral inhibition (Figure 7). This is achieved by induction of *Delta-1*, a single pass membrane ligand for the Notch receptor (Chitnis *et al.*, 1995). Delta-2 and Serrate-1 are additional Notch ligands that were shown to function in *Xenopus* primary neurogenesis (Peres *et al.*, 2006; Kiyota *et al.*, 2004). Upon Delta-1 binding the Notch receptor of a neighboring cell, a series of proteolytic cleavages occurs that releases the intracellular domain of the Notch receptor (NICD) into the cytoplasm (Louvi *et al.*, 2006). NICD translocates into the nucleus, where it replaces a co-repressor at the suppressor of hairless (Su(H)) transcription factor, acts as a co-activator and drives expression of target genes (Louvi *et al.*, 2006; Wettstein *et al.*, 1997). Some of the best-characterized Notch target genes are the bHLH repressors of the enhancer of split-related (ESR) and Hairy family. The ESR proteins inhibit Ngn2 expression and function. Thus, the signal-receiving cell is prevented from undergoing neuronal differentiation (Chitnis *et al.*, 1996, Dawson *et al.*, 1995) and a salt and pepper like pattern of primary neurons is created (Figure 8A-D). If Notch signaling is artificially activated by expression of NICD, neuronal differentiation is blocked in every cell of the neuroepithelium, resulting in a loss of postmitotic neurons (Figure 8E,F). Vice versa, if Notch activity is blocked by expression of a dominant negative Su(H), lateral inhibition is blocked and all cells in the territories of primary neurogenesis undergo neuronal differentiation (Figure 8G,H).

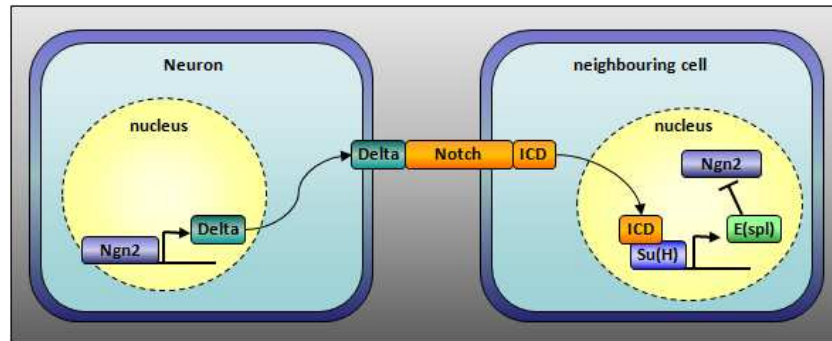


Figure 7: Lateral inhibition by the Delta Notch signaling pathway. Expression of Ngn2 in the cell fated to become a neuron activates Delta, a ligand of the Notch receptor. Upon Delta binding to the Notch receptors of the neighbouring cell, a series of proteolytic cleavages releases the intracellular domain of the receptor (NICD) which translocates to the nucleus and acts as a co-activator in inducing expression of Enhancer of split related genes (ESR). The ESRs inhibit Ngn2 expression and function in the signal-receiving cell and prevent it from undergoing neuronal differentiation.

How a single cell within the territories of primary neurogenesis can escape lateral inhibition, enter neuronal differentiation and inhibit all surrounding cells from differentiating remains unclear. It has been proposed, that once a cell activates the transcription of downstream proneural genes through elevated levels of Ngn, it becomes refractory to lateral inhibition in a process that requires MyT1 (Van Doren *et al.*, 1992; Bellefroid *et al.*, 1996). This is supported by the finding that ectopic neurogenesis induced by Ngn overexpression can be blocked by Notch activation (Ma *et al.*, 1996), while the neuroectoderm of embryos injected with *Ngn2* and *MyT1* mRNA becomes resistant to lateral inhibition by Notch (Bellefroid *et al.*, 1996).

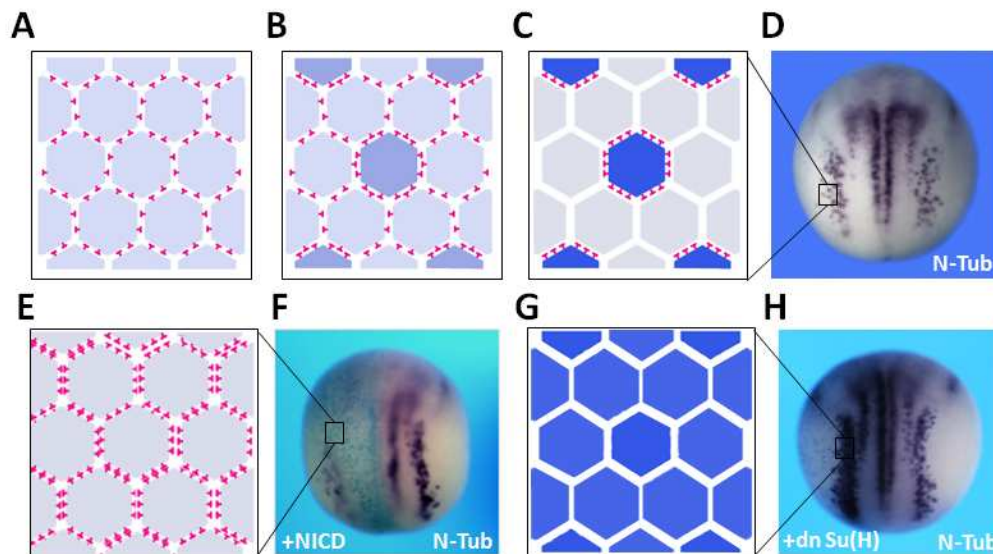


Figure 8: Lateral inhibition defines the number of neurons in the neuroectoderm. (A) Upon initial induction of neuronal determination factors like Ngn, the cells in the neuroectoderm express Delta-1 and mutually inhibit each other from undergoing differentiation. (B) Some cells express higher levels of Delta or become refractory to inhibitory signals. (C) Neuronal determined cells suppress differentiation in neighbouring cell and undergo neuronal differentiation. (D) Salt and pepper like pattern of primary neurons in a stage 15 embryo (E, F) Ectopic activation of Notch signaling by the constitutively active NICD. All cells inhibit each other from undergoing differentiation. (G, H) Inhibition of Notch signaling by Su(H)^{DBM}, a dominant negative form of Su(H). Lateral inhibition does not occur, all cells in the territories of cell neurogenesis undergo neuronal differentiation (modified from Molecular Biology of the Cell, 2005).

1.5 Numb as cell fate determinant in neurogenesis

Numb was originally identified as a cell fate determinant in dividing *Drosophila* sensory organ precursor cells (SOPs) (Uemura *et al.*, 1989). In the development of a sensory hair in *Drosophila*, a single SOP undergoes two subsequent divisions, giving rise to four cells of different types: a hair cell, two outer supporting cells and a neuron. While a loss of Numb generated four outer supporting cells, Numb overexpression generated four neurons (Rhyu *et al.*, 1994) (Figure 9). Numb was found to be asymmetrically distributed to one daughter cell upon cell division and inhibit Notch signaling in this cell, thereby determining different cell fates in the daughters (Wang *et al.*, 1997).

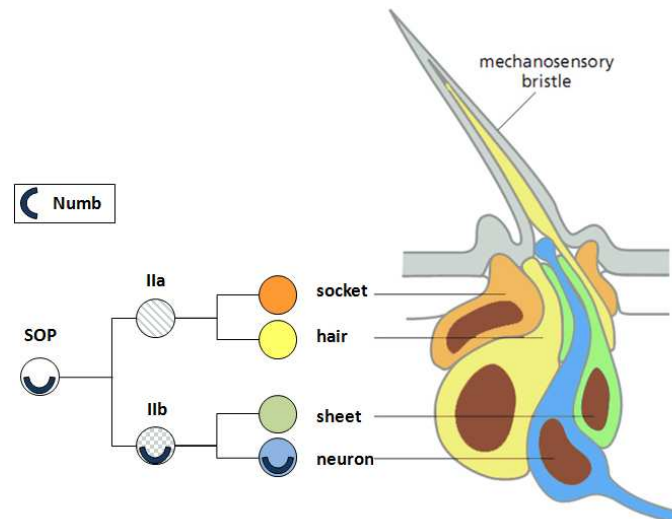


Figure 9: Numb as cell fate determinant in *Drosophila* SOP. Numb is asymmetrically distributed upon division of the SOP and the subsequent division of the IIb cell, acting as intrinsic cell fate determinant to inhibit Notch signaling and enable neuronal differentiation (modified from Rhyu et al., 1994).

The Numb proteins are highly conserved in their sequence throughout species. In contrast to *Drosophila*, which has only one *Numb* gene, two closely related *Numb* genes have been identified in vertebrates, *Numb* and *Numbl* (*Numbl*) (Verdi et al., 1996; Zhong et al., 1996). The murine and the human Numb homologues, mNumb and hNumb can substitute dNumb function and similarly induce ectopic neuron formation when overexpressed in *Drosophila* (Verdi et al., 1996; Toriya et al., 2006) suggesting Numb function is conserved through evolution.

In mice, *Numb* and *Numbl* were also shown to function in vertebrate neurogenesis, as a loss of both results in an overall loss of differentiated neurons (Petersen et al., 2002; Li et al., 2003; Petersen et al., 2004). *Numb* and *Numbl* were found to act in a partially redundant manner and to be essential for neural development in the mouse. While a homozygous knockout of *Numbl* in mouse causes no severe phenotype (Petersen et al., 2002), *Numb* depleted mice showed defects in cranial neural tube closure and die around E11.5 (Zhong et al., 2000). Conditional *Numb* knockout mice are viable and exhibited a loss of differentiated neurons in the forebrain, an effect that could be enhanced in a *Numbl* null background (Petersen et al., 2002; Li et al., 2003). Contradictory

results were obtained with respect to the mechanism of the loss of differentiated neurons. A double knockout of *Numb* and *NumbL*, using nestin-Cre mediated excision at E8.5 prior to the onset of neurogenesis, resulted in a depletion of neural progenitors and reduced number of differentiated neurons, suggesting a function in progenitor cell maintenance at this early stage (Petersen *et al.*, 2002). Vice versa, a knockout of both genes, using Emx-Cre at E9.5 – E12.5, was found to cause hyperproliferation of neural progenitors in the forebrain, impairing differentiation (Li *et al.*, 2003). Knockout of *Numb* at E10.5 in a *NumbL* deficient background, using D6-Cre, similarly resulted in depletion of neural progenitors (Petersen *et al.*, 2004). Thus, *Numb* was shown to be essential for neurogenesis, but playing two distinct roles, one in maintaining the proliferative state of progenitors and a second in enabling differentiation of these cells.

1.6 Numb acts as scaffold protein

Numb contains several protein-protein interaction domains and correspondingly, has been shown to interact with a wide variety of different proteins. A highly conserved phosphotyrosine binding domain (PTB) is localized in the N-terminus and a proline-rich repeat domain (PRR) more C-terminally. The *Numb* PTB domain was shown not only to bind proteins containing phosphotyrosine residues (Blaikie *et al.*, 1994), but also mediate interaction with PDZ-domain containing proteins like LNX or even more distinct peptide ligands like putative serine/threonine kinase NAK (Chien *et al.*, 1998). The PRR was found to interact with a wide variety of proteins containing SH3 interaction domains (Verdi *et al.*, 1996). Located in the most distal C-terminus are DPF AP-2 and NPF Eps-15 interaction motifs, which mediate interactions with the endocytotic machinery (Santolini *et al.*, 2000) (Figure 10).

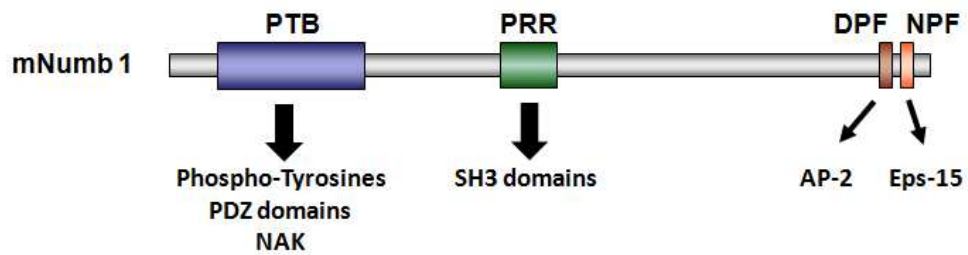


Figure 10: Protein-protein interaction domains of Numb. Scheme of mNumb1 protein with protein-protein interaction domains and interacting protein domains/ proteins.

1.7 Numb and Numblike isoforms

Four different isoforms of Numb (Numb1-4), which are generated by alternative splicing, have been described. The isoforms differ by the presence or absence of an 11 amino acid insert in the PTB domain or the PRR domain (Dho *et al.*, 1999) (Figure 11). NumblL lacks both inserts and isoforms for NumblL have not been reported.

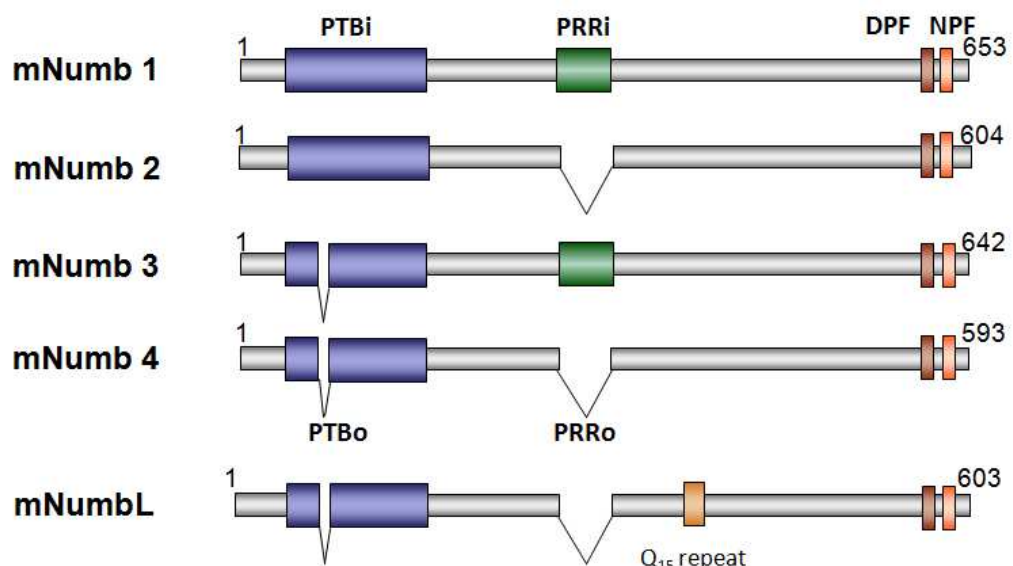


Figure 11: Numb isoforms. Four different Numb isoforms are generated due to different splicing. The isoforms differ from each other in the presence or absence of an insert in the PTB domain and the PRR domain. NumblL lacks both inserts.

The PTB insert was found to be crucial for membrane localization of Numb (Verdi *et al.*, 1996). Membrane localization of Numb can be achieved by either binding phosphotyrosine residues of tyrosine kinase receptors via the PTB domain (Verdi *et al.*, 1996) or with assistance of an adaptor protein, Partner of Numb (Pon) (Lu *et al.*, 1998). Numb isoforms that are localized to the membrane are able to be asymmetrically distributed upon cell division and therefore distinguish between different cell fates. Asymmetric segregation of Numb is a consequence of phosphorylation of Numb by the asymmetrically localized Bazooka/Par-6/aPKC complex (Par-3/Par-6/aPKC) (Wirtz-Peitz *et al.*, 2008; Smith *et al.*, 2007) or phosphorylation of Pon by Polo, a cell cycle connected kinase (Wang *et al.*, 2007). Both events trigger Numb release from the cortex and therefore its localization to the opposite side of the cell.

The Numb isoforms have also been shown to exhibit different biological activities. Specific expression of PRRi isoforms of Numb in murine neural progenitors resulted in increased proliferation and decreased differentiation, while expression of PRRo isoforms resulted in the opposite effect (Verdi *et al.*, 1999; Bani-Yaghoub *et al.*, 2007). These results suggest that not only different targets of Numb, but different context-specific downstream isoform responses exist. This is in agreement with the changing expression patterns of the Numb isoforms during mouse cortical development. In contrast to the differentiation promoting PRRo isoforms, the proliferating promoting PPRi isoforms are expressed mainly between E7 and E10 and become undetectable by E13 during a rapid expansion of the neural progenitor cell population (Dho *et al.*, 1999; Verdi *et al.*, 1999; Bani-Yaghoub *et al.*, 2007). The divergent functions of the mammalian Numb isoforms were further demonstrated by their overexpression in the *Drosophila* optic anlage (OOA) (Toriya *et al.*, 2006). Even in *Drosophila*, where no endogenous splice variants of Numb are present, the PRRi Numb constructs promoted proliferation, while the PRRo isoforms strongly increased neuronal differentiation in the OOA. Independent of the presence of the PRR domain, Numb isoforms lacking the insert in the PTB domain were shown to increase the sensitivity of transfected *Drosophila* PC12 cells to

neurotrophic growth factors and therefore to undergo neuronal differentiation (Pedersen *et al.*, 2002).

1.8 Multiple functions of Numb

The most well characterized function of Numb is its ability to negatively regulate Notch signaling (Rhyu *et al.*, 1994). Two mechanisms are known by which Numb can inhibit Notch. Numb and NumbL can antagonize Notch signaling through simultaneous interaction with the AP-2 complex and the Notch receptor, which results in endocytosis of the receptor (Santolini *et al.*, 2000). Numb also activates the E3 ligase Itch, which was found to target the Notch receptor as well as the cleaved NICD for ubiquitination and subsequent proteasomal degradation (McGill *et al.*, 2003). High levels of Notch signaling were found to downregulate *Numb* expression in the chick neuroepithelium (Chapman *et al.*, 2006), which is proposed as a mechanism to reinforce and maintain cell fate decisions.

In addition to Numb's ability to regulate Notch signaling levels, numerous distinct functions have been described. Numb was found to activate Itch, which targets Gli-1 for ubiquitination and degradation in mouse cerebellar granule cell progenitors (GCPs) and GCP derived cancer cell lines (Di Marcotullio *et al.*, 2006; Di Marcotullio *et al.*, 2010). As Gli1 is a downstream effector of SHH signaling, this results in an inhibition of SHH signaling. Numb was also shown to function in directional cell migration by mediating integrin endocytosis in the rear of migrating HeLa cells (Nishimura *et al.*, 2007). Furthermore, Numb was found to function in stabilization of the tumor suppressor p53 through the formation of a trimeric complex with p53 and the E3 ligase MDM2 (also known as HDM2). Complex formation prevents ubiquitination of p53, enabling cell cycle arrest and DNA repair (Colaluca *et al.*, 2008). A function of Numb in oncogenesis is also suggested by its frequent mutation in different cancer types (Westhoff *et al.*, 2009; Ostrakhovitch, 2009; Rennstam *et al.*, 2010).

1.9 Regulation of Numb

The critical role Numb plays during embryogenesis is underscored by the multiple mechanisms by which it is regulated at the post-transcriptional level. *Numb* was shown to be regulated on the translational level by Musashi, a neural RNA binding protein, which was shown to bind *Numb* mRNA and prevent its translation (Okano *et al.*, 2002). *Numb* mRNA translation was also inhibited by the micro-RNA miR146a in mouse satellite cells, where Numb promotes differentiation into muscle cells by inhibiting Notch signaling (Kuang *et al.*, 2009). Furthermore, Numb activity is regulated via phosphorylation of two specific serine residues, Ser²⁹¹ and Ser³¹⁰ (Tokumitsu *et al.*, 2006). If phosphorylated, these two serine residues trigger the binding of ubiquitously present 14-3-3 proteins to Numb, which mask the remaining protein-protein interaction sites and prevent Numb from binding its targets. Also, in the context of endocytosis, the adaptor-associated kinase 1 (aak1) was described to phosphorylate Numb, resulting in its redistribution to perinuclear endosomes in HeLa cells thereby regulating the endocytotic activity of Numb (Sorensen *et al.*, 2008).

1.10 *Xenopus* Numb and Numbl like

In a previous study, it could be shown that *X. laevis* *NumbL* was exclusively expressed in the presumptive neuroectoderm, the territories of primary neurogenesis and later throughout the nervous system (Nieber 2007). In whole embryos, *NumbL* was positively regulated by *Ngn2* and inhibited by the Notch pathway. A knockdown of *NumbL* using antisense MO inhibited neuronal differentiation demonstrating *NumbL* is essential for neurogenesis. The knockdown effect could be rescued by coinjection of *X. laevis* *NumbL* and mouse *NumbL* RNA. Of the four murine Numb isoforms, only the structurally related *Numb4* rescued the *NumbL* MO phenotype.

An expression analysis of proneural genes in *NumbL* morphant embryos revealed that the neuronal determination factor *Ngn2* was still expressed, but all

downstream targets were inhibited (Figure 12). Although NumbL exhibited in luciferase reporter assays the ability to decrease the activation of a Notch reporter, no increase in Notch target gene expression was observed upon NumbL knockdown.

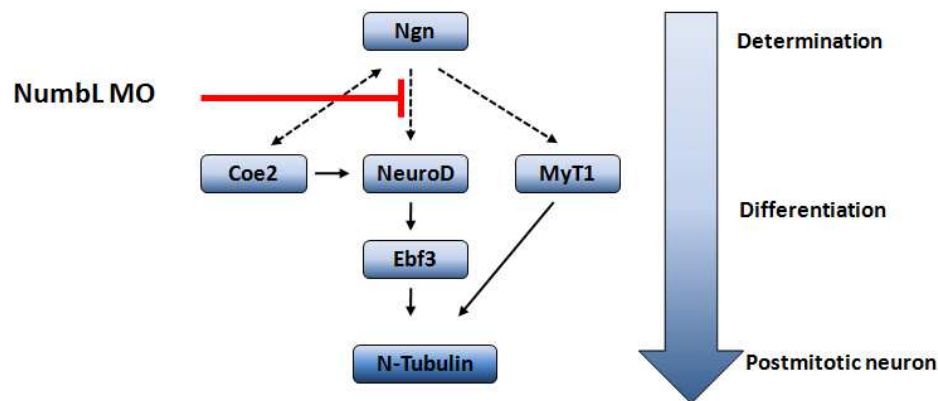


Figure 12: NumbL knockdown inhibits proneural factors downstream of Ngn. Upon injection of the NumbL MO, all proneural transcription factors downstream of Ngn were inhibited, suggesting a function for NumbL downstream of neuronal determination in the process of neuronal differentiation. (Nieber 2007)

1.11 Aims

NumbL was identified as an essential gene in the process of primary neurogenesis in *Xenopus*. However, a role for NumbL during neurogenesis could not be explained by the classical model of Numbs function as a Notch inhibitor during cell fate determination. Therefore, to understand NumbL role during primary neurogenesis, a detailed analysis of NumbL function during the development of the nervous system was performed.

2. Materials and Methods

2.1 Organisms

2.1.1 *Xenopus laevis* and *Xenopus tropicalis*

The African clawed frog *Xenopus laevis* (*X. laevis*) and the western clawed frog *Xenopus tropicalis* (*X. tropicalis*) were used as model organisms during this study. Pigmented or albino frogs were purchased from Nasco (Ft. Atkinson, USA). The developmental stages were distinguished according to Nieuwkoop and Faber (1967).

2.1.2 *Escherichia coli*

XL1-Blue *recA1*, *endA1*, *gyrA96*, *thi-1*, *hsdR17*, *supE44*, *relA1*, *lac[F' proAB, lacIqZDM15, TN10(Tetr)]^c* (Bullock *et al.*, 1987)

2.2 Oligonucleotides

2.2.1 RT-PCR oligonucleotides

RT-PCR oligonucleotides (primers) were purchased from Sigma-Aldrich. They were dissolved in HPLC H₂O to a concentration of 500 μM.

Xt Numb PTB	for	5'-AGGAATCAAGAGGGGATGCAC-3'	63°C, 35 cycles
	rev	5'-CATCCACAACCTCGAAGTCCA-3'	
Xt Numb PRR	for	5'-ACACTTTCAGCATGCCACCT-3'	65°C, 35 cycles
	rev	5'-CTTCTTCAAGCCAACGGTCT-3'	
Xt NumbL PTB	for	5'-AGGAGTCGAGGGGAATGC-3'	64°C, 35 cycles
	rev	5'-ACAACACGCAGCCCATCA-3'	

Xt NumbL PRR	for rev	5'-CTTCCACCACAACCAATGC-3' 5'-TCCTCAAGCCAGCGTTCC-3'	64°C, 35 cycles
XI Numb RT	for rev	5'-GAGGATATGGCAAGGCCAAAA-3' 5'-AACCACAGCCAGTCCAGTTC-3'	60°C, 30 cycles
XI NumbL RT	for rev	5'-AAGCCATCCTCTGGGTTTCT-3' 5'-CTGTCACCCCACACTCCTTT-3'	64°C, 32 cycles
Xt H4	for rev	5'-ATAACATCCAGGGCATCACC-3' 5'-AAAGAGCCTTTGGGTTCGAT-3'	60°C, 25 cycles
XI H4	for rev	5'-CGGGATAACATTCAGGGTATCACT-3' 5'-ATCCATGGCGGTAAGTGTCTTCCT-3'	56°C, 25 cycles
NeuroD	for rev	5'-GAAGGAGCAACAAGAGGAAG-3' 5'-TTCCCATATCTAAAGGCAG-3'	64°C, 32 cycles
N-tubulin	for rev	5'-ACACGGCATTGATCCTACAG-3' 5'-AGCTCCTTCGGTGTAAATGAC-3'	57°C, 30 cycles
Zic1	for rev	5'-GAGAAGTGGAAACAAATTGGC-3' 5'-GTCTGCGAAGGGATTGATG-3'	56°C, 29 cycles
Zic2	for rev	5'-GGGCAGACTTCTGCTTTCAC-3' 5'-ATCCCGGGGAATAGTAGGTG-3'	64°C, 29 cycles
Zic3	for rev	5'-TTCTCAGGATCTGAACACAT-3' 5'-CCCTATAAGACAAGGAATAC-3'	56°C, 27 cycles
NCAM	for rev	5'-CACAGTTCCACCAAATGC-3' 5'-GGAATCAAGCGGTACAGA-3'	50°C, 27 cycles
Sox2	for rev	5'-GAGGATGGACACTTATGCCAC-3' 5'-GGACATGCTGTAGGTAGGCGA-3'	56°C, 25 cycles
Sox3	for rev	5'-GCGCACATGAACGGCTGGACTA-3' 5'-GTGTGGGAGGTGATGGCTGGAG-3'	57°C, 28 cycles
Noggin	for rev	5'-AGTTGCAGATGTGGCTCT-3' 5'-AGTCCAAGAGTCTCAGCA-3'	57°C, 30 cycles
Xt Ngn1	for rev	5'-GCTGCACACCATCAAGAAGA-3' 5'-GCTGGAAGTGACACTGAGA-3'	60°C, 27 cycles
Xt Ngn2	for rev	5'-TTCCACCCTATCACCCATGT-3' 5'-GGTTGCCAGTACTCCAGCAT-3'	60°C, 27 cycles
Xt Ngn3	for rev	5'-CCCATATGCAGAGGAGAAGC-3' 5'-TCATCTGGGAAGGTGGGTAG-3'	60°C, 27 cycles
XI Ngn1	for rev	5'-CAGGAGGAGAAGGACACGAG-3' 5'-GGCTTCTCTTTGCACTGGTC-3'	60°C, 30 cycles

XI Ngn2	for	5'-GCGCGTTAAAGCTAACAACC-3'	60°C, 30 cycles
	rev	5'-G TTCAGGTGGAGCTCAGAGG-3'	
XI Ngn3	for	5'-AACGAGGTCTCCCCTCTCTC-3'	60°C, 30 cycles
	rev	5'-GAGTCCCATTCACTGGAGGA-3'	

2.2.2 General oligonucleotides

Oligonucleotides (primers) were purchased from Sigma-Aldrich. They were dissolved in HPLC H₂O to a concentration of 100 µM.

SP6	5'-TATTTAGGTGACACTATAG-3'	56°C
T7	5'-TAATACGACTCACTATAGGGCGA-3'	56°C
T7 (pCS2+)	5'-TCTACGTAATACGACTCACTATAG-3'	56°C

2.2.3 Morpholino oligonucleotides

Antisense morpholino oligonucleotides (Morpholinos, MO's) were purchased from Gene Tools, LLC (Philomath, USA). They were dissolved in RNase free water to a concentration of 10 µg/µl. MO were stored at -20°C. Prior to use, MO were heated to 65°C for 5 minutes.

NumbL MO: 5'-GCGCAGTAGTTGATGTTTGCCCTCA-3'

NumbL mmMO: 5'-GCCCAGTACTTCATCTTTGGCGTCA-3'

2.3 Constructs

2.3.1 Overexpression constructs

NumbLpCS2+ harbors the full open reading frame of XI NumbL, including ATG and stop codon. The fragment was generated by PCR amplification using NumbLpKBCMV (previously isolated by Dr. K. Henningfeld) as template, 5' NumbL (EcoRI/ATG) 5'- ATGAATTCATGAACAACTGCGTCAG-3' and 3' NumbL (XhoI) 5'- CGCTCGAGCTATCAATTCTATTTGAAAAGTC-3' as primers and inserted into EcoRI/XhoI linearized pCS2+ (D. Turner and R. Rupp, <http://sitemaker.umich.edu/dlturner.vectors>). For sense RNA, the construct was linearized with NotI and transcribed with SP6 RNA polymerase

MT-NumbLpCS2+ harbors the full open reading frame of XI NumbL, including ATG and stop codon. The fragment was generated by PCR amplification, using NumbLpCS2+ as template, NumbL MT sc for EcoRI 5'- ATGAATTCATGAACAACTGCGTCAG-3' and NumbL MT sc rev XhoI 5'- CGCTCGAGCTATCAATTCTATTTGAAAAGTC-3' as primers and inserted into EcoRI/XhoI linearized MTpCS2+. For sense RNA, the construct was linearized with NotI and transcribed with SP6 RNA polymerase.

NumbL(SA)pCS2+ harbors the full open reading frame of XI NumbL, including ATG and stop codon. The fragment was generated using the QuikChange XI Site-Directed Mutagenesis Kit (Stratagene), using NumbL pCS2+ as template and XLN S291A for 5'- GCTGGTGAGACAGGGAgCCTTTCGTGGATTCC-3', XLN S291A rev 5'- GGAATCCACGAAAGGcTCCCTGTCTCACCAGC-3', XLN S310A for 5'- CCTTTTAAACGGCAGCTTgCGCTGAACTCAATGAGC-3' and XLN 310A rev 5'- GCTCATTGAGTTTCAGCGcAAGCTGCCGTTTAAAAGG-3' as primers (introduced mutations in small letters) in two subsequent rounds of mutagenesis. For sense

RNA, the construct was linearized with NotI and transcribed with SP6 RNA polymerase.

NumbL(SD)pCS2+ harbors the full open reading frame of XI NumbL, including ATG and stop codon. The fragment was generated using the QuikChange XL Site-Directed Mutagenesis Kit (Stratagene), using NumbL pCS2+ as template and XLN S291D for 5'- GCTGGTGAGACAGGGAgcCTTTCGTGGATTCCCTGC-3', XLN S291D rev 5'- GCAGGGAATCCACGAAAGtcTCCCTGTCTCACCAGC-3', XLN S310D for 5'- CCTTTTAAACGGCAGCTTgacCTGAAACTCAATGAGCTCCCG-3' and XLN 310D rev 5'- CGGGAGCTCATTGAGTTTCAGgtcAAGCTGCCGTTTAAAAGG-3' as primers (introduced mutations in small letters) in two subsequent rounds of mutagenesis. For sense RNA, the construct was linearized with NotI and transcribed with SP6 RNA polymerase.

NumbL-CTappCS2+ harbors the full open reading frame of XI NumbL cloned upstream of the GS-TAP tag (Kyriakakis *et al.*, 2008). For cloning, the NumbL fragment was generated using XI NumbL pCS2+ as template and 5' NumbL EcoRI 5'- ATGAATTCATGAACAAACTGCGTCAG-3' and NL-CTap fusion rev 5'- CTTCTCGTCCAT CAATTCTATTTGAAAAGTC-3' as primers. CTap fragment was generated using pMK33-CTap (Kyriakakis *et al.*, 2008) as template and NL-CTap fusion for 5'-CAAATAGAATTGATGGACGAGAAGACCACC-3' and 3' XhoI CTap 5'- ATCTCGAG TCATTATTCAGTGACAGTG-3' as primers. Both fragments were fused a primerless PCR and then inserted into EcoRI/XhoI linearized pCS2+. For sense RNA, the construct was linearized with NotI and transcribed with SP6 RNA polymerase.

NumbL(DLA)pCS2+ harbors the full open reading frame of XI NumbL, including ATG and stop codon. The fragment was generated using the QuikChange XL Site-Directed Mutagenesis Kit (Stratagene), using NumbLpCS2+ as template and NL

mut AP2 for 5'-AGGAAGTGGACcTgGcTGAAGCTCAATGGG-3' and NL mut AP2 rev 5'-CCCATTGAGCTTCaGcCaGGTCCACTTCCT-3' as primers (introduced mutations in small letters). For sense RNA, the construct was linearized with NotI and transcribed with SP6 RNA polymerase.

MT-NumbL(DLA)pCS2+ harbors the full open reading frame of XI NumbL, including ATG and stop codon. The fragment was generated using the QuikChange XL Site-Directed Mutagenesis Kit (Stratagene), using MT-NumbL pCS2+ as template and NL mut AP2 for 5'-AGGAAGTGGACcTgGcTGAAGCTCAATGGG-3' and NL mut AP2 rev 5'-CCCATTGAGCTTCaGcCaGGTCCACTTCCT-3' as primers (introduced mutations in small letters). For sense RNA, the construct was linearized with NotI and transcribed with SP6 RNA polymerase.

NumbL(DLA-SA)pCS2+ harbors the full open reading frame of XI NumbL, including ATG and stop codon. The fragment was generated using the QuikChange XL Site-Directed Mutagenesis Kit (Stratagene), using NumbL(SA)pCS2+ as template and NL mut AP2 for 5'-AGGAAGTGGACcTgGcTGAAGCTCAATGGG-3' and NL mut AP2 rev 5'-CCCATTGAGCTTCaGcCaGGTCCACTTCCT-3' as primers (introduced mutations in small letters). For sense RNA, the construct was linearized with NotI and transcribed with SP6 RNA polymerase.

Xt Numb3pCS107 harbors the full Xt Numb3 open reading frame including ATG and stop codon. It was obtained from an EST Clone library (clone TEgg132I24) (Gene Service, Gilchrist et al., 2004): For sense RNA, the construct was linearized with ApaI and transcribed with SP6 RNA polymerase.

MT-Xt NumbpCS2+ harbors the full open reading frame of Xt Numb, including ATG and stop codon. The fragment was generated using the Xt Numb-pCS107 as template and MT-Xt Numb sc for 5'- GAATTCGATGAACAAACTGCGTCAG-3' and MT-Xt Numb sc rev 5'- CTCGAGCTACAATTCTATTTGAAAAGTCTTTTG-3' as primers and inserted into EcoRI/XhoI linearized pCS2+-MT. For sense RNA, the construct was linearized with NotI and transcribed with SP6 RNA polymerase.

mNumb1-4pCS2+ harbor the full open reading frames of the mNumb1-4 isoforms (Dho *et al.*, 1999). The clones mNumb1-4pEN clones were obtained from Dr. J. Mc Glade (Dho *et al.*, 1999). For cloning mNumb1-4 isoforms into pCS2+, the inserts were excised with EcoRI and ligated into EcoRI linearized pCS2+. For sense RNA, the constructs were linearized with NotI and transcribed with SP6 RNA polymerase.

MT-mNumb1pCS2+ harbors the full open reading frame of mNumb1, including ATG and stop codon. The fragment was generated using mNumb1-pCS2+ as template and mN1-MT sc for 5'-GAATTCAATGAACAAACTACGGCAA-3 and mN1-MT sc rev 5'- CTCGAGCTAAAGTTCTATTTCAAATGTTTTTC-3' as primers and inserted in EcoRI/XhoI linearized pCS2+-MT. For sense RNA, the construct was linearized with NotI and transcribed with SP6 RNA polymerase.

mNumbLpCS2+ harbors the full open reading frame of mNumbL (GenBank #U70674), including ATG and stop codon. It was excised with EcoRI and XhoI from mNumbL pBSK(-) (received from Dr. W. Zhong, Zhong *et al.*, 1997) and subcloned (EcoRI/XhoI) into pCS2+. For sense RNA, the construct was linearized with NotI and transcribed with SP6 RNA polymerase.

Xt Ngn1pCS2+ harbors the full open reading frame of Ngn1, including ATG and stop codon. The fragment was generated using Ngn1pCS108 (RZPD/imaGenes, CX475730) as template and Xt Ngn1 sc for 5'-CGGAATTCATGGCTTCCAACATGGACAG and Xt Ngn1 sc rev 5'-GCTCTAGATGTCATTGGAGTTAGCAGGC-3' as primers and inserted into EcoRI/XbaI linearized pCS2+. For sense RNA, the construct was linearized with NotI and transcribed with SP6 RNA polymerase.

Xt Ngn2pCS2+ harbors the full open reading frame of Ngn2, including ATG and stop codon. The fragment was generated using Ngn2pCS108 (RZPD/imaGenes, CX510880) as template and Xt Ngn2 sc for 5'-CGGAATTCATGGTGCTGCTGAAGTG-3' and Xt Ngn2 sc rev 5'-GCCTCGAGGTATGCAAGAACTCAAGTGGAA-3' as primers and inserted into EcoRI/XhoI linearized pCS2+. For sense RNA, the construct was linearized with NotI and transcribed with SP6 RNA polymerase.

Xt Ngn3pCS2+ harbors the full open reading frame of Ngn3, including ATG and stop codon. The fragment was generated using Ngn3pCS108 (RZPD/imaGenes, CX366256) as template and Xt Ngn3 sc for 5'-CGGAATTCATGGTGCTGCTGAAGTG and Xt Ngn3 sc rev 5'-GCTCTAGAGTATGCAAGAACTCAAGTGGAA-3' as primers and inserted into EcoRI/XbaI linearized pCS2+. For sense RNA, the construct was linearized with NotI and transcribed with SP6 RNA polymerase.

XI Ngn1pCS2P+ harbors the full open reading frame of XI Ngn1 including ATG and stop codon, 102bp 5'UTR and 227bp 3'UTR. XI Ngn1pCS2P+ was received from NIBB (XL267p21ex). For sense RNA, the construct was linearized with NotI and transcribed with SP6 RNA polymerase.

XI Ngn3pCS2P+ harbors the full open reading frame of XI Ngn3 including ATG and stop codon, 31bp of 5'UTR and 741bp of 3'UTR. XI Ngn3pCS2P+ was received from NIBB (XL265d10ex). For sense RNA, the construct was linearized with NotI and transcribed with SP6 RNA polymerase.

Following overexpression constructs have been described previously: **Su(H)^{DBM}pCS2+** (Wettstein *et al.*, 1997); **Delta-1^{STU}pCS2+** (Chitnis *et al.*, 1995); **NICDpCS2** (Coffman *et al.*, 1993); **NogginpGEM5ZF** (Smith *et al.*, 1993), **XI Ngnr-1 (Ngn2)pCS2+** (Ma *et al.*, 1996); **LacZpCS2+** (Chitnis *et al.*, 1995); **mGFPpCS2+** (Moriyoshi *et al.*, 1996, provided by A.Schambony, University of Erlangen, Germany).

2.3.2 Constructs for whole mount in situ

XI NumbLpBKCMV harbors the full open reading frame of XI NumbL including 98 bp of 5'UTR and 1233bp 3'UTR. XI NumbL-pBKCMV was isolated by Dr. K. Henningfeld in a λ Phage screen from a *X. laevis* tadpole head library (Holleman *et al.* 1999). For antisense RNA synthesis, the construct was linearized with EcoRI and transcribed with T7 RNA polymerase.

XI NumbpBLuescript SK- harbors 475 bp of the Numb 3'UTR and was received from the RZPD/imaGenes (BE189039). For antisense RNA synthesis, the construct was linearized with EcoRI and transcribed with T7 RNA polymerase.

Xt Ngn1pCS108 harbors the full Ngn1 open reading frame, including 362 bp of 3'UTR. It was purchased from the RZPD/imaGenes (CX475730). For antisense RNA synthesis, the construct was linearized with Sall and transcribed with T7 RNA polymerase.

Xt Ngn2pCS108 harbors the full Ngn2 open reading frame, including 260 bp of 3'UTR. It was purchased from the RZPD/imaGenes (CX510880). For antisense RNA synthesis, the construct was linearized with Sall and transcribed with T7 RNA polymerase.

Xt Ngn3pCS108 harbors the full Ngn3 open reading frame, including 529 bp of 3'UTR. It was purchased from the RZPD/imaGenes (CX366256). For antisense RNA synthesis, the construct was linearized with Sall and transcribed with T7 RNA polymerase.

XI Ngn1pCS2P+ harbors the full open reading frame of XI Ngn1 including ATG and stop codon, 102 bp 5'UTR and 227 bp 3'UTR. XI Ngn1pCS2P+ was received from NIBB (XL267p21ex). For antisense RNA synthesis, the construct was linearized with EcoRI and transcribed with T7 RNA polymerase.

XI Ngn3pCS2P+ harbors the full open reading frame of XI Ngn3 including ATG and stop codon, 31 bp of 5'UTR and 741 bp of 3'UTR. XI Ngn3pCS2P+ was received from NIBB (XL265d10ex). For antisense RNA synthesis, the construct was linearized with EcoRI and transcribed with T7 RNA polymerase.

Following constructs were previously described: **N-tubulin** (Oschwald et al, 1991); **Ngnr-1 (Ngn2)** (Ma et al., 1996); **MyT1** (Bellefroid et al., 1996), **NeuroD** (Lee et al., 1995); **NCAM** (Tonissen et al., 1993); **Sox3** (Penzel et al., 1997); **Sox2** (Mitzuseki et al., 1998); **Zic1** (Aruga et al., 2001); **Zic2** (Brewster et al., 1998); **Zic3** (Nakata et al., 1997); **XDelta1** (Chitnis et al., 1995); **XDelta2** (Jen et al., 1997); **ESR1** (Schneider et al., 2001); **ESR3/7** (Perron et al., 1998); **ESR5** (Jen et al.,

1997); **ESR8**; **ESR9**; **ESR10** (Gawantka *et al.*, 1998); **epidermal keratin** (Jonas *et al.*, 1985); **Twist** (Hopweed *et al.*, 1989)

2.4 Total RNA extraction and cDNA synthesis

Total RNA was isolated using the TRIZOL reagent (TriFast, Peqlab). To lyse the cells, 3-5 whole embryos or 30-50 animal caps were macerated with a 29-Gauge syringe in 500 µl TRIZOL reagent and centrifuged 10 minutes at maximum speed to remove debris. Further steps were performed according to the manufacturer's manual. The RNA was re-suspended in 30 µl RNase free H₂O and treated for 1 hour at 37°C with DNaseI to digest genomic DNA. DNaseI was inactivated by addition of 1/10 vol. of DNase inactivation solution (Ambion).

For cDNA synthesis, 100 ng total RNA was used in a 10 µl reaction containing 5 mM MgCl₂, 2.5 ng random hexamer, 5 mM dNTP mix, 0.8 units RNase out (Invitrogene) and 20 units reverse transcriptase (Roche) in 1X MgCl₂-free GoTaq incubation buffer (Promega). After a 20 minute annealing step at 20°C, the reaction was carried out at 42°C for 60 minutes and terminated by heating to 95°C for 5 minutes.

2.5 RT-PCR analysis

For semi-quantitative RT-PCR analysis, 5 µl cDNA was used in total reaction volume of 25 µl, containing 0.2 mM of each RT primer, 1.5 mM MgCl₂, 0.5 units GoTaq polymerase (Promega) in 1x MgCl₂-free GoTaq incubation buffer (Promega). Histone H4 was used as a loading control for equal cDNA concentrations and to test for cDNA contamination by genomic DNA.

2.6 In vitro synthesis of RNA

2.6.1 Capped sense RNA

The capped mRNA for microinjections was synthesized using the mMessage mMachineTM Kit (Ambion) according to the manufacturer's protocol. In 20 μ l total reaction volume, 1 μ g of linearized template plasmid was used. The transcription was incubated for at least two hours at 37°C. After incubation, template DNA was removed by addition of 5 units DNaseI followed by 30 minutes incubation at 37°C. The mRNA was purified using the RNeasyTM Mini Kit (Qiagen), eluted in 30 μ l of RNase-free H₂O, aliquoted in 2 μ l and stored at -80°C.

2.6.2 Antisense RNA

Labeled antisense RNA, used for probes in whole mount in situ hybridization, was synthesized in a total reaction volume of 25 μ l, containing 1 μ g of linearized template plasmid, 1 mM ATP, 1 mM GTP, 1 mM CTP, 0.64 mM UTP, 0.36 mM digoxigenin or fluorescein labeled UTP, 0.03 μ M DTT, 1.6 units RNase out (Invitrogene), 0.05 units Pyrophosphatase and 0.08 units RNA polymerase in 1x transcription buffer. After 3 hours of incubation at 37°C, the template DNA was removed by addition of 5 units DNaseI and subsequent incubation for 30 minutes at 37 °C. The labeled antisense RNA was purified using the RNeasyTM Mini Kit (Qiagen), eluting twice with 50 μ l of pre-heated RNase free H₂O (80°C) and stored in Hybridization Mix at -20°C.

2.7 T_NT in vitro translation

In vitro transcription and translation was performed using the T_NT[®] Coupled Reticulocyte Lysate System (Promega) according to the manufacturer's protocol. Proteins were separated by denaturing SDS-polyacrylamide gel electrophoresis (Sambrook and Russel, 2001). The dried gels were exposed to phosphorimager screens (Amersham) and scanned using a Typhoon Phosphorimager (Amersham).

2.8 Embryo culture and microinjections

10x MBS Salts: 880 mM NaCl, 1mM KCl, 10 mM MgSO₄, 25 mM NaHCO₃, pH 7.8

1x MBS: 1x MBS Salts, 0.7 mM CaCl₂

5x MBS AC (animal caps): 880 mM NaCl, 10 mM KCl, 10 mM MgSO₄, 25 mM NaHCO₃, 2.05 mM CaCl₂, 1.65 mM Ca(NO₃)₂, pH 7.8

Agar dishes: 60 mm petri dishes coated with 0.7% - 1.5% agar made with 0.8x MBS AC.

Dejelly solution: 2% (w/v) L-cysteine hydrochloride in H₂O, pH 8

Injection buffer: 1% (w/v) Ficoll in 1x MBS

Nile Blue staining solution: 0.01% (w/v) Nile Blue chloride, 89.6 mM Na₂HPO₄, 10.4 mM NaH₂PO₄, pH 7.8

X. laevis embryos were obtained by HCG-induced egg-laying, using 800 units of HCG per frog. Spawns were in vitro fertilized and embryos staged after Nieuwkoop and Faber, 1967. Embryos were injected in one blastomere of the two- or four-cell stage. For in situ analysis, 75 pg nuclear *LacZ* mRNA was coinjected. Embryos were injected in injection buffer, incubated for several hours and then incubated at 12.5 – 18 °C in 0.1x MBS until they reached the desired developmental stage. For ectodermal explants and pulldown experiments, the embryos were injected in both animal blastomeres at the two-cell stage.

Animal caps were dissected from stage 8-9 embryos in 0.8x MBS AC in agarose coated dishes and cultured in 0.8x MBS AC until control embryos reached the desired developmental stage.

X. tropicalis embryos were either obtained by natural mating or HCG-induced egg-laying, as well. For mating, male and female frog were pre-primed with 20 units of HCG, incubated for at least 12 hours and then boosted with 100 units of HCG. For in vitro fertilization, females were primed with 150 – 200 units of HCG.

X. tropicalis embryos were injected like *X. laevis* embryos and cultured in 0.11x MBS at room temperature until they reached the desired developmental stage.

2.9 X-Gal staining

10x MEM: 1 M Mops, 20 mM EGTA, 10 mM MgSO₄, pH 7.4 sterile filtered and stored in the dark

10x PBS: 1.75 M NaCl, 1 M KCl, 65 mM Na₂HPO₄, 18 mM KH₂PO₄, pH 7.4

Dent's solution: 20% (v/v) DMSO in methanol

K₃FE(CN)₆: 0.5 M in H₂O, stored in the dark

K₄FE(CN)₆: 0.5 M in H₂O, stored in the dark

MEMFA: 4% (v/v) formaldehyde (37%) in 1x MEM

X-Gal: 40 mg/ml 5-Bromo-4-chloro-3-indolyl-β-D-galactopyranoside in formamide, stored at -20°C in the dark.

X-Gal staining solution: 1 mg/ml X-Gal, 5 mM K₃FE(CN)₆, 5 mM K₄FE(CN)₆, 2 mM MgCl₂ in 1x PBS

Embryos were cultivated to the desired developmental stage and fixed for 30 minutes in MEMFA. After washing three times with 1x PBS, embryos were transferred to X-Gal staining solution and incubated in the dark until sufficient staining was observed (10-30 minutes). The staining was stopped by washing the embryos three times with 1xPBS, followed by a second fixation step in MEMFA for 30 minutes. For whole mount in situ, the embryos were dehydrated by washing several times in absolute ethanol and then stored at -20°C. For pH3 staining, embryos were dehydrated with absolute methanol and stored in Dent's solution for at least 24 hours at -20°C.

2.10 Whole mount in situ hybridization

10X PBS: 1.75 M NaCl, 1 M KCl, 65 mM Na₂HPO₄, 18 mM KH₂PO₄, pH 7.4

20X SSC: 3 M NaCl, 0.3 M NaCitrat, pH 7.2 - 7.4

5X MAB: 500 mM maleic acid, 750 mM NaCl, pH 7.5

Antibody solution: 2% BMB, 20% heat treated horse serum, 1:2000 dilution of anti-digoxigenin or anti-fluorescein antibody coupled to alkaline phosphatase (Roche) in 1X MAB

APB: 100 mM Tris-HCl, pH 9.0, 50 mM MgCl₂, 100 mM NaCl, 0.1% TWEEN-20

BCIP: 50 mg/mL in 100% Dimethylformamide; stored at -20°C

Color reaction solution: 80 µg/ml NBT, 175 µg/ml BCIP in APB

EtOH series: 100%, 75%, 50% ethanol in H₂O, 25% ethanol in PTw

Hybridization Mix (Hyb Mix): 50% Formamid, 1 mg/ml, Torula-RNA, 10 µg/ml Heparin, 1X Denhardt's, 0.1% Tween-20, 0.1% CHAPS, 10 mM EDTA in 5X SSC

MeOH series: 100%, 75%, 50%, 25% methanol in H₂O

MAB/BMB: 2% BMB in 1X MAB

MAB/BMB/HS: 2% BMB, 20% heat-treated horse serum in 1X MAB

NBT: 100 mg/mL in 70% Dimethylformamide; stored at -20°C

PTw: 0.1% Tween-20 in 1X PBS

PTw/FA: 4% (v/v) formaldehyde in PTw

Proteinase K: 5 µg/ml Proteinase K in 0.1X PBS

RNAse Solution: 10 µg/ml RNAse A, 0.01 U/ml RNAse T1 in 2X SSC

Whole mount in situ was performed as described (Harland, 1991, Hollemann et al., 1999), using antisense RNA probes labeled with digoxigenin-11-UTP or fluorescein-UTP. Double in situ hybridization was performed according to Knecht et al., 1995. All steps were performed at room temperature with mild shaking. The embryos were rehydrated in the EtOH series to PTw, washed three times with PTw for 10 minutes and the subjected to Proteinase K treatment for

several minutes to enhance penetration of the antisense probe. To stop Proteinase K digestion, embryos were washed twice in 0.1 M triethanolamine and pH 7.5 were acetylated by adding 25 μ l of acetic anhydride to the triethanolamine to reduce unspecific binding of the probe. After treatment, embryos were fixed in PTw/FA for 25 minutes, washed five times in PTw, transferred to HybMix and incubated for 5 hours at 65°C in a shaking incubator. Subsequently, HybMix was exchanged for the antisense probe, and hybridization took place overnight at 65°C.

On the second day, the RNA probes were recovered and stored at -20°C for further use. After washing the embryos for 10 minutes at 65°C in HybMix and three times 2x SSC for 15 minutes at 65°C, non hybridized RNA probe was removed by RNase digestion for 1 hour in RNase solution at 37°C. After washing once for 15 minute in 2x SSC and washing twice in 0.2x SSC for 30 minutes at 65°C, embryos were transferred to MAB for blocking. After 2 MAB washing steps, embryos were incubated for 20 minutes in MAB/BMB and 40 minutes in MAB/BMB/HS to reduce unspecific binding of the antibody. Antibody incubation took then place for 4 hours shaking at ambient temperature, followed by three MAB washing steps. Embryos were stored in MAB at 4°C overnight.

At the third day, embryos were washed twice with MAB and the caps of the vials exchanged followed by another three MAB washings. After transfer of the embryos to APB and three washing steps using APB, the embryos were transferred to the color reaction solution and incubated at 4°C in the dark until staining was sufficient. To stop the reaction, embryos were transferred absolute methanol and washed in the methanol series to reduce background staining. Samples were stored in MEMFA.

2.11 Phosphorylated Histone 3 (pH3) staining

10X PBS: 1.75 M NaCl, 1 M KCl, 65 mM Na₂HPO₄, 18 mM KH₂PO₄, pH 7.4

1° AB solution: 20% horse serum, 5% DMSO, 1:200 dilution rabbit anti-pH3 antibody (Biomol)

2° AB solution: 20% horse serum, 5% DMSO, 1:200 dilution goat anti-rabbit IgG horseradish peroxidase-coupled secondary antibody (Sigma)

MeOH series: 100%, 75%, 50%, in H₂O and 25% methanol in 1xPBS

PBS-TB: 0.05% Tween-20, 0.2% BSA in 1x PBS

PBS-TBN: 0.3 M NaCl in PBS-TB

The pH3 assay was performed as described (Dent *et al.*, 1989). All steps were performed at ambient temperature with mild shaking. After rehydration in the MeOH series to PBS, the embryos were pre-incubated in 20% horse serum in PBS for 2 hours. The solution was exchanged to the 1° AB solution and incubated for 3 hours. After washing twice with PBS-TB for two hours, the embryos were washed overnight in PBS-TB. On the second day, after incubation in PBS-TBN for 3 hours followed by a brief wash in PBS-TB, the embryos were transferred to the 2° AB solution and incubated for 5 hours. The embryos were washed twice in PBS-TB for 2 hours, once in PBS TBN for 2 hours and again in PBS-TB for 2 hours before they were washed overnight in PBS-TB. HRP activity was detected as for wmlSH.

2.12 Sections

Gelatin/albumin: 4.88 mg/ml gelatin, 0.3 g/ml bovine serum albumin, 0.2 mg/ml sucrose in PBS. The gelatin was dissolved by heating the solution to 60°C followed by the addition of Albumin and sucrose, filtered with a 0.45 µm filter (Sartorius) and stored at -20°C.

Mowiol: 5 g Mowiol was stirred overnight in 20 ml PBS. After addition of 10 ml glycerol, the solution was stirred again overnight. Mowiol that was undissolved was collected by centrifugation for 30 min at 20,000 g. The supernatant was pH adjusted to pH 7.0 (using pH strips) and stored at -20°C.

Samples were transferred to PBS and after equilibration in gelatin/albumin for 20 minutes mounted by addition of glutardialdehyde. Sections (30 µm) were cut on a Leica VT1000M vibratome and mounted in Mowiol (Holleman *et al.*, 1999).

2.13 Fluorescent labeling of animal caps

10X PBS: 1.75 M NaCl, 1 M KCl, 65 mM Na₂HPO₄, 18 mM KH₂PO₄, pH 7.4

1° AB solution: 1:100 goat anti-myc-Cy3 (Sigma) and 1:1000 rabbit anti-GFP (Abcam) in PTw

2° AB solution: 1:200 swine anti-rabbit IgG-FITC (DAKO) in PTw

DAPI solution: 1:1000 DAPI in 1xPBS

MEMFA: 4% (v/v) formaldehyde (37%) in 1x MEM

PTw: 0.1% Tween-20 in 1X PBS

For fluorescent labeling, animal caps were incubated until control siblings reached the desired developmental stage. The caps were fixed in MEMFA for 1 hour at ambient temperature or overnight at 4°C. After three 10 min washes of PTw, the first Antibody solution was applied for 2 hours at ambient temperature in the dark. After three 10 min washes of PTw, the second Antibody solution was applied for 1 hour at ambient temperature in the dark. Caps were then washed for 10 min once with PTw and once with PBS. To label nuclear DNA, DAPI solution was applied for 10 min. Caps were then transferred to PTw and stored up to one week at 4°C in the dark before evaluation at the confocal microscope.

2.14 Tandem affinity purification (TAP)

Lysis buffer: 5 mM Tris, 5% (v/v) Glycerol, 0.2% (v/v) NP-40, 1.5 mM MgCl₂, 125 mM NaCl, 25 mM NaF, 1mM NaVO₄, 1mM DTT, 1 mM EDTA, 1 protease inhibitor tablet (Roche) per 50 ml, pH 7.5

TEV cleavage buffer: 10 mM Tris, 100 mM NaCl, 0.1% NP-40, 1mM DTT, 0.5 mM EDTA, pH 7.5

Tandem affinity purification was essentially performed as described (Kyriakakis *et al.*, 2008). All steps were performed at 4°C. For tandem affinity purification of NumbL, 2000 embryos each were injected in both blastomeres at the 2-cell stage with NumbL-CTap or CTap alone (500 pg/injection), grown until they reached stage 15 and then shock frozen in liquid nitrogen. Embryos were lysed in 10 µl lysis buffer per embryo, using first a yellow pipette tip, then a 29-gauge syringe. After 30 minutes centrifugation at 4°C and maximum speed, the supernatant was transferred without any debris into new vials and mixed 1:1 with Freon to remove remaining yolk. After 10 minutes centrifugation at 4000 rpm at 4°C, the supernatant was again recovered into 15 ml falcon tubes (aliquots kept for “input”). 200 µl of IgG-sepharose beads were added in each tube and samples were incubated on a nutator for 2 hours at 4°C. After 1 minute centrifugation at 4°C, samples were three times washed with 2 ml of TEV cleavage buffer. For TEV cleavage, 1 ml of TEV cleavage buffer and 10 µl of TEV (AcTev, Invitrogen) were added and samples were incubated overnight on a nutator at 4°C.

For the second pulldown, samples were centrifuged 1 minute at 4000 rpm at 4°C, supernatant was recovered (aliquot saved for “1st pulldown”) into new tubes and 100 µl of streptavidin-beads were added, followed by a 2 hours incubation on a nutator at 4°C. After three washing steps with 2 ml TEV cleavage buffer, 500 µl of 2x SDS loading buffer were added and samples were boiled 5 minutes at 95°C to elute bound proteins. Samples were cooled on ice, centrifuged 1 minute at max speed and supernatant was recovered. To reduce

the volume of the eluate, samples were loaded on Amicon centrifugation columns (cut-off 5kDa) and were centrifuged 1 hour at 4000 rpm at 4°C until sample volume reached 100 µl. To separate the eluted proteins, 25 µl of each sample were loaded on 10% SDS gel.

Protein bands were visualized first by Colloidal Coomassie staining (Neuhoff, 1988, modified by Dr. O. Jahn, (Proteomics Unit, MPI for Experimental Medicine, Göttingen, Germany) and then subjected to mass spectrometry analysis using a Bruker Ultraflex MALDI-TOF-MS and a Thermo Finnigan LCQ Deca XP plus ES-IT-MS.

3. Results

3.1 *Xenopus Numb* isoforms switch during neural development

Mammalian *Numb* and *NumbL* have been shown to play an essential role during early development, particularly in the context of the nervous system (Gulino *et al.*, 2010). However, the functional role and molecular mechanism of action has been under debate. Therefore, to gain further insight into the function of this important class of proteins during early vertebrate development, the role of the *Numb* proteins during *Xenopus* embryogenesis was evaluated. Four different isoforms of mammalian *Numb*, which are generated by alternative splicing, have thus far been described (Verdi *et al.*, 1999; Dho *et al.*, 1999). These isoforms differ by the presence or absence of an insert in the PTB and PRR domain and were shown to exhibit different functional activities (Toriya *et al.*, 2006). Therefore, in a first approach to analyze the expression of the *Numbs* in *Xenopus*, RT-PCR analysis on staged embryos was performed as it can distinguish between the possible different isoforms.

X. tropicalis cDNA was used, as genomic sequence information is available allowing the design of primer sets spanning the putative insert regions of the splice variants. As shown in Fig. 13, multiple bands for *Numb* and a single size PCR product for *NumbL* were generated using the specific primers pairs. To unambiguously confirm that the observed PCR products indeed represent the different isoforms of *Numb* indicated, the amplified products were isolated and sequenced (see Appendix Fig. 1).

Starting at gastrula stages and throughout all later developmental stages analyzed, *NumbL* transcripts were detected that encode for a single protein lacking both the insert in the PTB and PRR domain (PTBo/PRRo). In contrast, PCR products corresponding to the PTBo/PTBi and PRRo/PRRi splice variants of *Numb* were detected, which is consistent with the previously described murine isoforms. Furthermore, a switch in *Numb* isoform expression occurs during development. In early cleavage stages the maternal transcripts encode for *Numb*

PTBo isoforms, which do not harbor the PTB insert (*Numb3* or *Numb4*). However, starting from stage 15 and during subsequent developmental stages, increasing levels of PTBi isoforms (*Numb1* or *Numb2*) with a simultaneous decrease in PTBo isoform levels are detected. Throughout development, most *Numb* isoforms contain the PRR insert (*Numb1*, *Numb3*) since only low but stable levels of PRRo transcripts (*Numb2*, *Numb4*) are detected. In contrast to the PTBi/PTBo ratio, the PRRi/PRRo ratio does not change during ongoing development. Thus during early developmental stages *Numb3* is the most abundant *Numb* transcript expressed and during later developmental stages transcripts encoding *Numb1* and *Numb3* are both present.

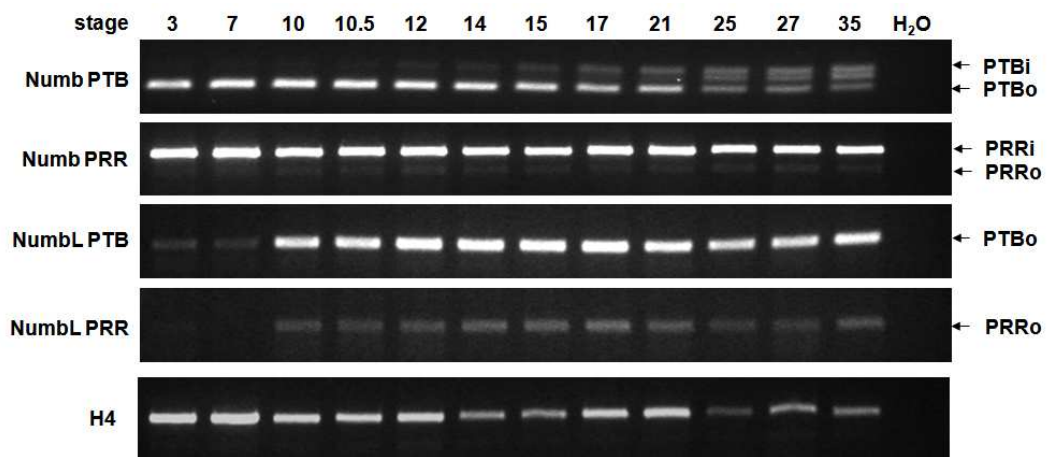


Figure. 13: Temporal expression analysis of *X. tropicalis* *Numb* and *NumbL* isoforms. Semi-quantitative RT-PCR analysis of staged embryo cDNA. Stages are indicated in the upper lane, the primer sets used at the left. To control for genomic DNA, a control RT-PCR reaction was done on the staged RNA in the absence of reverse transcriptase. Histone 4 was used as a loading control. Arrows at the right indicate the expected PCR product size of the isoforms.

3.2 *NumbL* is expressed in the territories of primary neurogenesis

Numb and *NumbL* are expressed in partially overlapping expression patterns in the mouse (Zhong *et al.*, 1996; Zhong *et al.*, 1997). Thus it is anticipated that they have common as well as distinct functions that correlate with their specific expression patterns. While *Numb* is expressed at low levels ubiquitously throughout the developing embryo, *NumbL* expression is highly restricted to the nervous system. Moreover, while *Numb* is found throughout all

layers of the neural tube, *NumbL* is only present in the mantle layer where cells are actively differentiating (Zhong *et al.*, 1997).

To evaluate their potential role in the development of the nervous system in *Xenopus* embryos, a detailed comparative expression analysis of *Numb* and *NumbL* was performed (Fig. 14). Whole mount in situ hybridization analysis was performed to determine the spatial expression of *Numb* and *NumbL* in *X. laevis* embryos. *Numb* is expressed at low levels throughout the embryo during early cleavage and gastrula stages (Fig. 14A, B). At open neural plate stages, *Numb* is weakly detected throughout the ectoderm and is enriched in a single longitudinal domain on both sides of the midline as well as in a horse-shoe domain that marks the panplacodal primordium (Schlosser 2006) (Fig. 14C, D). At stage 30, *Numb* transcripts are concentrated in the anterior region of the embryo including the brain and throughout the spinal cord. High expression levels of *Numb* are also found in the otic vesicle and the pronephros (Fig. 14J). As previously described (see Nieber 2007), during gastrula stages, *NumbL* is strongly detected above the blastopore lip, which demarcates the presumptive neural ectoderm (Fig. 14E, F). At the open neural plate stage, *NumbL* is detected in the midline and strikingly found in the territories of primary neurogenesis including the three longitudinal domains in the posterior neural plate, as well as in neurogenic trigeminal and olfactory placodes (Fig. 14G, H). At tailbud stages, *NumbL* continues to be expressed in the nervous system and is detected throughout the brain, spinal cord, eye and branchial arches (Fig. 14L).

The tissue-specific differences in *NumbL* and *Numb* expression in the neuroectoderm of open neural plate stage embryos are shown in transversal sections (Fig. 14I, K). *Numb* is found adjacent to the midline in the superficial epidermal layer of the bilayered neuroectoderm, which stays in a proliferative state and primarily undergoes differentiation in the later, secondary wave of neurogenesis (Chalmers *et al.*, 2002; Hartenstein 1989). In contrast, all three longitudinal expression domains of *NumbL* are located in the deep layer of the neuroectoderm, which mainly gives rise to the primary neurons (Fig 14K). The midline staining of *NumbL* is also located in the deeper sensorial layer in the

tissue that will give rise to the spinal cord floorplate. At tailbud stages, *Numb* is weakly expressed throughout the neural tube (Fig. 14M), while the expression of *NumbL* is more restricted (Fig. 14N) and is excluded from the ventricular zones where proliferating progenitor cells are located. In a double in situ for *NumbL* and *N-tubulin* (Fig. 14O), both expression domains partially overlap in the outer mantle zone, but in addition, *NumbL* is expressed in the intermediate zone, suggesting a function for *NumbL* during the onset of neuronal differentiation.

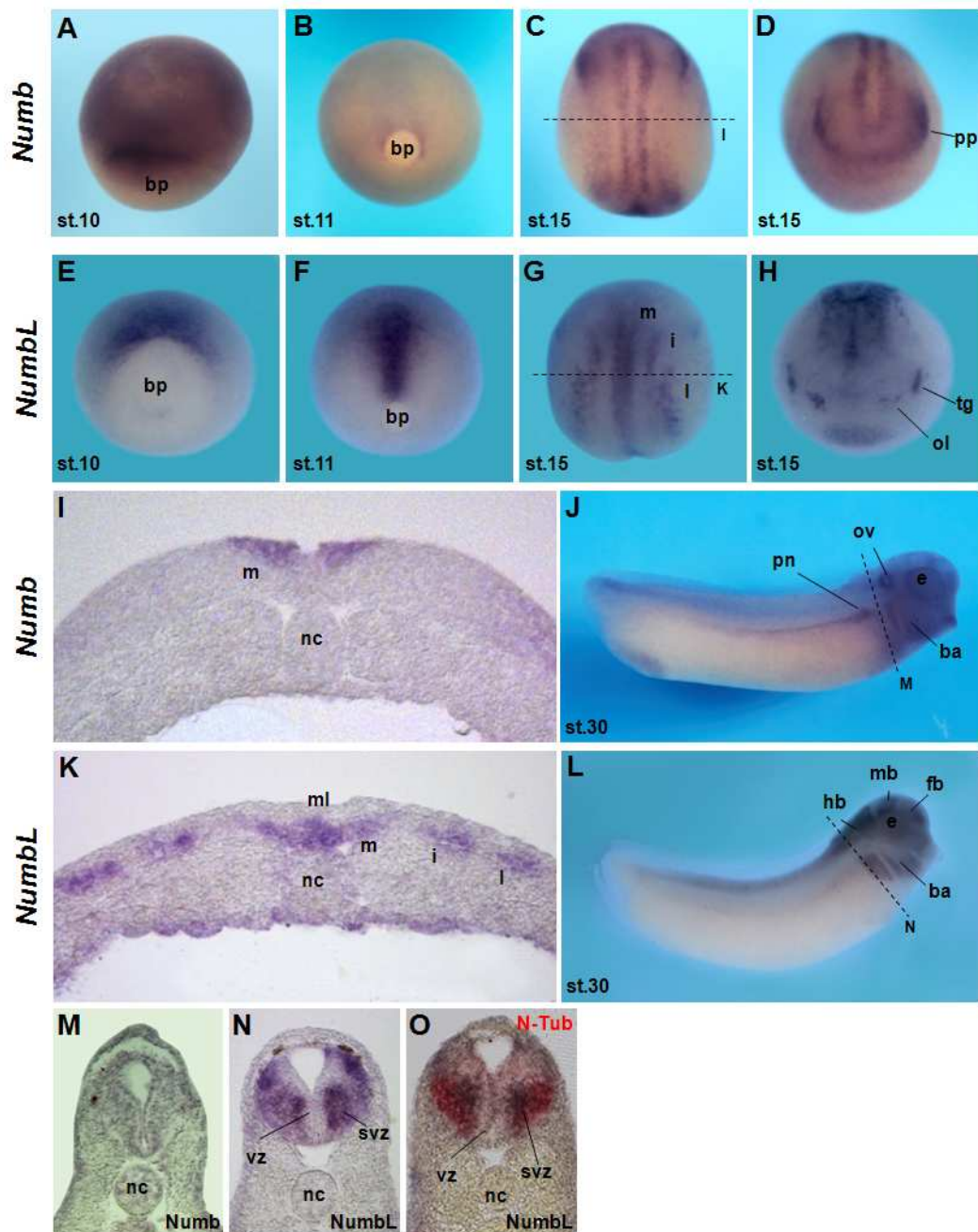


Figure 14: Comparison of spatiotemporal expression of *X. laevis Numb* and *Numbl*. Whole mount in situ expression analysis of *Numb* (A-D, I-J,M) and *Numbl* (E-H, K,L, N,O). (A,B and E,F) Gastrula stage embryo shown in view of the blastopore. (C and G) Neurula stage embryo, dorsal view, anterior up. Dashed line indicates plane of the transversal section shown below. (D and H) Neurula stage embryo, anterior view, dorsal up. (J and L) Tailbud stage embryo shown in a lateral view. Dashed line indicates plane of the transversal section shown below. (O) Transversal section of a stage 30 embryo hindbrain. Double in situ on *Numbl* (black) and *N-tubulin* (red). bp, blastopore; nc, notochord; st, stage; m, medial stripe; i, intermediate stripe; l, lateral stripe; ov, otic vesicle; pn, pronephros; ba, branchial arches; fb, forebrain; mb, midbrain; hb, hindbrain; ol, olfactory placode; pp, panplacodal primordium; tg, trigeminal placode; vz, ventricular zone; svz, subventricular zone.

3.3 *Numbl* is positively regulated by Neurogenin 1-3

As *Xenopus Numbl* exhibited a restricted expression in the areas of primary neurogenesis and loss-of-function experiments suggested an essential role of *Numbl* (Nieber 2007) in the process of primary neurogenesis, a detailed functional analysis of *Numbl* in this context was performed. A knockdown of *Numbl* has been shown to inhibit the expression of neuronal differentiation factors such as *MyT1* and *NeuroD*, which act downstream of the proneural determination factor *Ngn2* (Nieber 2007). Moreover, both the temporal expression of *Numbl* in the territories of primary neurogenesis, as well as the expression in the intermediate zone of the neural tube suggest a role for *Numbl* in *Xenopus* neurogenesis as cells have already started to initiate differentiation. It was therefore tested, if *Numbl* is indeed regulated by the Ngn family of proneural transcription factors. *X. laevis* embryos were injected in one of two cells with *Ngn1*, *Ngn2* or *Ngn3* mRNA and the influence on *Numbl* expression examined at stage 15 by whole mount in situ hybridization (Fig. 15). As shown in Fig. 15G-I, all three Ngns activate *N-tubulin* and *Numbl* in both the neural and nonneural ectoderm (Fig. 15A-C). Corresponding to the induction of *N-tubulin* only in the sensorial layer upon *Ngn2* overexpression (Chalmers *et al.*, 2002), *Numbl* is also exclusively activated in the sensorial layer of the epithelium (Fig. 15D-F).

In a second approach, the animal cap assay was used where both animal blastomeres of two-cell stage embryos were injected with *Ngn* mRNA. The animal caps were excised at the blastula stage, cultured until control siblings reached stage 15 and the expression level of target genes analyzed by semi-quantitative RT-PCR. As shown in Figure 15J, all three *Ngn*s strongly activated *N-tubulin* and *NumbL* in naïve ectoderm. This is consistent with the *Ngn*-induced activation in the nonneural ectoderm of the embryo. Moreover, *Numb* was not activated by *Ngn*, which further demonstrates that *NumbL*, but not *Numb*, is activated during neuronal differentiation downstream of the proneural factors.

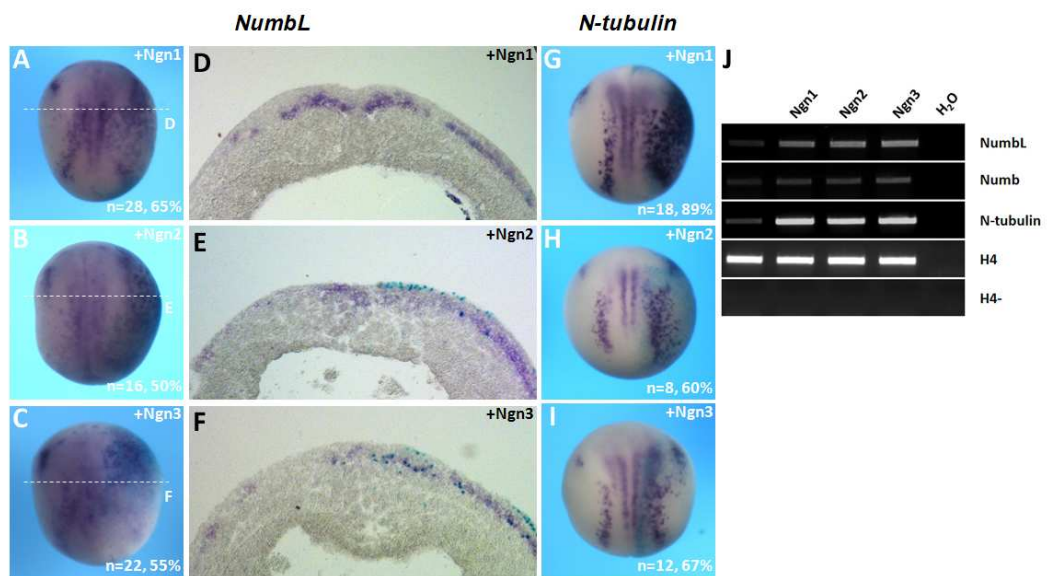


Figure 15: *NumbL* is positively regulated by the neurogenins. (A-C and G-I) Whole mount in situ hybridization analysis of neuronalized embryos. *X. laevis* embryos were injected with 20 pg of *Ngn1*, *Ngn2* or *Ngn3* mRNA, as indicated in the upper right corner, and fixed at stage 15 prior to analysis. 50 pg of β -Gal mRNA were co-injected as lineage tracer and mark the injected side, which is blue and always on the right. Embryos are shown in a dorsal view, anterior up. In situ probes are indicated at the top, statistics in the lower right corners. Dashed lines indicate plane of transversal sections adjacent to the embryos. All three Neurogenins induce *NumbL* as well as *N-tubulin*. (D-F) Transversal sections as indicated in A-C. (J) Semi-quantitative RT-PCR analysis of cDNA of *X. laevis* animal caps injected with 20 pg of *Ngn1*, *Ngn2* or *Ngn3* mRNA, as indicated. Explants were cultured until control siblings reached stage 15 and then total RNA was extracted. To control for genomic DNA a control RT-PCR reaction was done on the staged RNA in the absence of reverse transcriptase. H₂O represents a negative control where no RNA was added to the RT reaction. All three Neurogenins induce *NumbL* and *N-tubulin*, but not *Numb*.

3.4 *NumbL* gain-of-function leads to an increase in neural tube size

As the expression, regulation and loss-of-function analysis support a role for *NumbL* during *Xenopus* primary neurogenesis, a detailed analysis of *NumbL* function in this context was performed. At first, *MT-NumbL* mRNA was overexpressed in *X. laevis* embryos and the influence on primary neuron formation was monitored by whole mount in situ hybridization (Fig. 16). At the open neural plate stage, a slight increase in density of *N-tubulin* positive cells in the lateral stripe was observed (Fig. 16A). In a transversal section of the neural plate, all *N-tubulin* positive cells were located in the sensorial layer of the neuroepithelium (Fig. 18B). The same effect was obtained by overexpression of the *NumbL*(SA) double mutant, in which two serines (S264 and S281) that represent phosphorylation sites for negative post-translational regulation of *NumbL* (Kobayashi *et al.*, 2006) were exchanged to alanine (Fig. 16C). At tailbud stage, the embryos overexpressing *NumbL* do not exhibit an obvious phenotype except a slight bending of the embryo axis (Fig. 16D). In transverse, an increase in the size of the neural tube with a concomitant increase in *N-tubulin* positive cells is observed (Fig. 16E). Taken together, in gain-of-function analysis of *NumbL* in *X. laevis* embryos, *NumbL* is not sufficient to induce ectopic neurogenesis, but rather increases differentiation of primary neurons in the territories of primary neurogenesis.

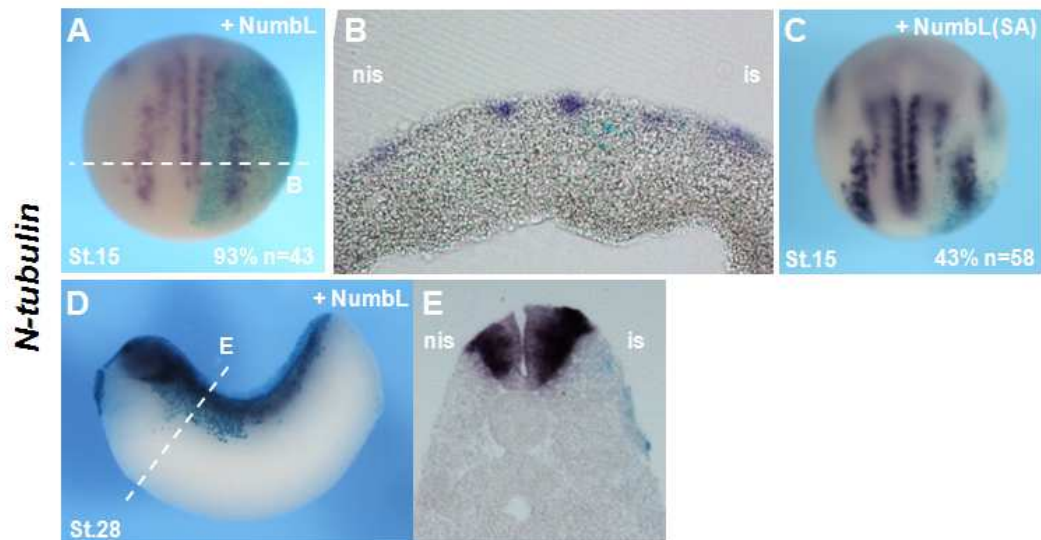


Figure 16: NumbL overexpression promotes neurogenesis and enlarges the neural tube. Whole mount in situ analysis of embryos that were injected with 500 pg of *NumbL* or *NumbL(SA)* mRNA as indicated in the upper right corner. β -Gal mRNA was co-injected as a lineage tracer. Embryos were cultured until the stage indicated in the lower left corner, fixed and probed for *N-tubulin*. Statistics are indicated in the lower right corner. **(A)** Embryo shown in a dorsal view, anterior up. Dashed line indicates the plane of the section shown in B. **(C)** Embryo shown in a dorsal view, anterior up. At open neural plate stage, overexpression of *NumbL* or *NumbL(SA)* results in a slight increase in *N-tubulin* positive cells on the injected side. **(D)** Embryo shown in a lateral view, anterior to the left. Dashed line indicated the plane of section shown in E. At tailbud stages, *NumbL* overexpression results an increased neural tube and an increased number of *N-tubulin* positive cells.

3.5 NumbL knockdown does not activate the Notch pathway

One of the best-described functions of members of the Numb family is their ability to act as an inhibitor of Notch signaling (Uemura *et al.*, 1989; McGill *et al.*, 2003). The loss of neuronal differentiation observed upon knock-down of NumbL in *X. laevis* (Nieber 2007) may therefore be the result of increased Notch signaling, which then suppresses neurogenesis. As described previously, neither the Notch target genes *ESR1* and *ESR9* nor the Notch ligand *Delta1* were found to be upregulated upon NumbL knockdown (Nieber 2007; Fig. 17A,B,F). To further provide evidence that Notch activity is indeed not increased by knock-down of NumbL, additional Notch target genes were analyzed by whole mount in situ in NumbL MO injected embryos (Fig. 17). The expression of all tested ectodermal

Notch target genes, *ESR3*, *ESR8* and *ESR10* (Fig. 17A-C, E-G), was not altered upon *NumbL* knockdown. The Notch target gene *ESR5* and the Notch ligand *Delta2* were shown to act in segmentation of the paraxial mesoderm (Sparrow et al., 1998). Corresponding with previous studies that demonstrated defects in somite formation in the mesoderm upon *Numb/NumbL* double knockout in mice (Petersen et al., 2005), *ESR5* and *Delta-2* were inhibited upon *NumbL* knockdown (Fig. 17D,H), indicating decreases in Notch signaling levels upon *NumbL* knockdown in the mesoderm.

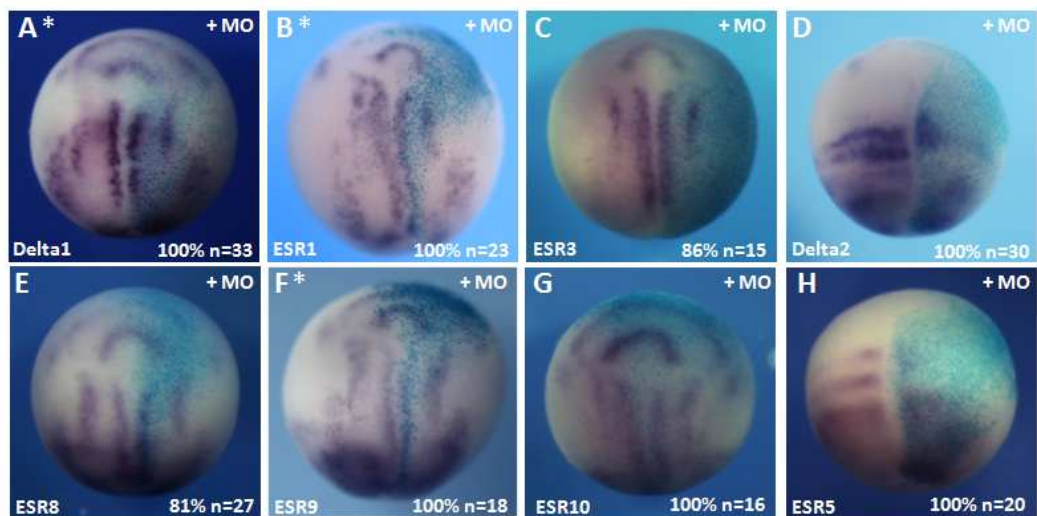


Figure 17: *NumbL* knockdown does not cause an increase of the Notch signaling pathway in the open neural plate. Whole mount in situ hybridization analysis of Notch target genes and Notch ligands in *NumbL* morphant embryos. Embryos were injected with 12.5 ng of *NumbL* MO and 50 pg of β -Gal mRNA as a lineage tracer in one blastomere of 2-cell embryos and cultured until stage 15. The injected side is marked by blue β -Gal staining and is always at the right. Embryos are shown in a dorsal view, anterior up. Probed genes are indicated in the lower left corner, statistics in the lower right corner. **(A-C; E-G)** *NumbL* knockdown does not upregulate ectodermal Notch target genes or the Notch ligand Delta-1. **(D,H)** *NumbL* knockdown results in an inhibition of the mesodermal Notch target gene *ESR5* and the Notch ligand Delta-2. *: previously published (Nieber, 2007)

3.6 Notch inhibition does not rescue *NumbL* knockdown

To further provide evidence that the *NumbL* knockdown phenotype in the neural ectoderm is not a result of elevated Notch levels, the Notch inhibitors *Delta-Stu* (Chitnis et al., 1996) and *Su(H)^{DBM}* (Wettstein et al., 1997) were

employed in co-injections with the NumbL MO. As a read-out, whole mount in situ on *N-tubulin* was performed, as it shows a strong phenotype upon NumbL knockdown (Nieber 2007). Injection of mRNA encoding both dominant-negative constructs induced the typical increase in neuronal density in the territories of primary neurogenesis (Chitnis *et al*, 1996; Wettstein *et al.*, 1997) as shown by the expression of *N-tubulin* (Fig. 18A,B). However, inhibition of Notch signaling by these constructs could not rescue the loss of *N-tubulin* positive cells in the NumbL knockdown embryos (Fig. 18C,D). These results further support the hypothesis that the function of NumbL is independent of Notch signaling in the context of primary neurogenesis

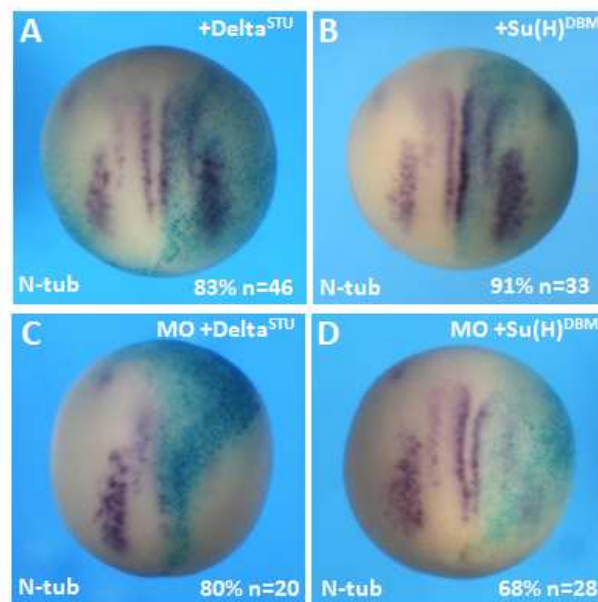


Figure 18: Notch inhibition does not rescue NumbL knockdown. Whole mount in situ analysis of *NumbL* morphants that were co-injected with 12.5 ng *NumbL* MO and 100 pg of the indicated Notch signaling inhibitor. β -Gal mRNA was co-injected as a lineage tracer. Inhibitors are indicated in the upper right corner, probed genes in the lower left corner. Statistics are shown in the lower right corner. Embryos were fixed at stage 15 prior to analysis. Embryos are shown in dorsal view, anterior up. **(A and B)** Notch pathway inhibition results in increase in *N-tubulin* density in the areas of primary neurogenesis. **(C and D)** Notch inhibition does not rescue the loss of *N-tubulin* upon a knockdown of *NumbL*.

3.7 A knockdown of NumbL leads to an increase in neural progenitors

The *Numb/NumbL* double knockout mice exhibit a severe influence on the neural progenitor cell population (Petersen *et al.*, 2002; Li *et al.*, 2003, Petersen *et al.*, 2004). Dependent on the stage of development that gene inactivation occurs, either depletion of neural progenitors as a consequence of premature differentiation, hyperproliferation of the neural progenitors or impaired differentiation of the progenitor population was observed. To determine, whether the observed loss of postmitotic neurons upon NumbL knockdown in *X. laevis* embryos was the consequence of alterations in the neural progenitor pool, the expression of the early neural genes Sox3 and NCAM was evaluated by whole mount in situ in NumbL knockdown embryos (Fig. 19). The expression domains of Sox3 and NCAM were significantly increased on the side of the embryo injected with the NumbL MO compared with the uninjected side (Fig. 19A and B). This demonstrates that the inhibition of neuronal differentiation is not due to the loss of the progenitor population and suggests that a loss of NumbL function may in fact increase proliferation of the neural progenitors and thereby impairing differentiation.

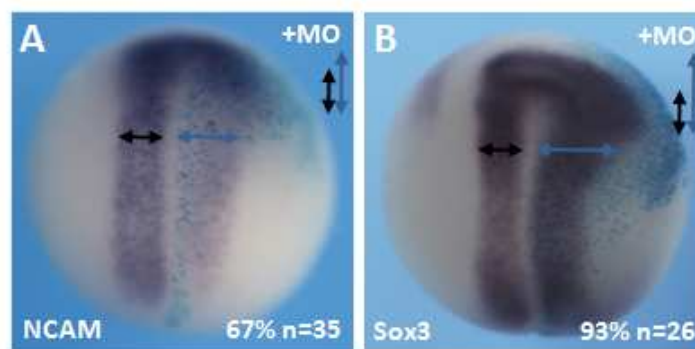


Figure 19: NumbL knockdown leads to an increase in early neural gene expression. Whole mount in situ analysis of *NumbL* morphant embryos. Embryos were injected with 12.5 ng *NumbL* MO and 50 pg β -Gal mRNA and cultured until stage 15 prior to analysis. The probed genes are indicated in the lower left corner, statistics in the lower right corner. The injected side is marked by blue β -Gal staining and is always at the right. Embryos are shown in a dorsal view, anterior up. Neuroepithelium size is represented by the double arrow for the injected site (blue) and the uninjected site (black). **(A)** *NumbL*

knockdown leads to a broadened expression domain of *NCAM*. **(B)** *NumbL* knockdown leads to an increased expression domain of *Sox3*.

3.8 NumbL knockdown increases the number of mitotically active cells in the ectoderm at early gastrula stages

As the expression domains of panneural genes like *Sox3* or *NCAM* were found to be increased in size upon NumbL knockdown, proliferation rates in the neuroectoderm were analyzed at different stages by immuno-labeling of phosphorylated Histone 3 (pH3), which marks mitotically active cells (Fig. 20). Embryos were unilaterally injected with the NumbL MO, cultured to the desired developmental stages and then subjected to pH3 staining. The stained embryos were sectioned and pH3 signals in a reference area on each side were counted in 15 consecutive sections. At neurula stages when loss of *N-tubulin* expression is observed, there was no difference in the number of pH3 positive cells on the NumbL MO injected side compared with the uninjected control side. Although, at stage 15 no significant difference in mitotically active cell number was observed, a knockdown of NumbL resulted in a thickening of the neuroectoderm on the injected site at this stage (Fig. 20F). Therefore to determine if increased proliferation was occurring during the establishment of the neural plate, we performed the pH3 assay on earlier stage embryos. While at stage 12 only a slight increase in pH3 positive cells could be detected (Fig. 20C, D and E), a significant increase in mitotically active cells in the prospective neuroectoderm was observed at the onset of gastrulation at stage 10 (Fig. 20A, B and E).

Differentiation of progenitor cells requires withdrawal from the cell cycle. This is achieved by the expression of cell cycle regulators like *Gadd45 γ* , *Pak3* and *p27^{Xic1}* (Souopgui *et al.*, 2002; De la Calle-Mustienes *et al.*, 2002; Vernon *et al.*, 2005). Consistent with the increase in mitotically active cells, a loss of *Gadd45 γ* and *Pak3* expression was observed in stage 15 NumbL morphants (Fig. 20G and H), thus raising the possibility that the neuronal progenitors are prevented from

undergoing differentiation and stay in a proliferative state because they are not able to exit the cell cycle.

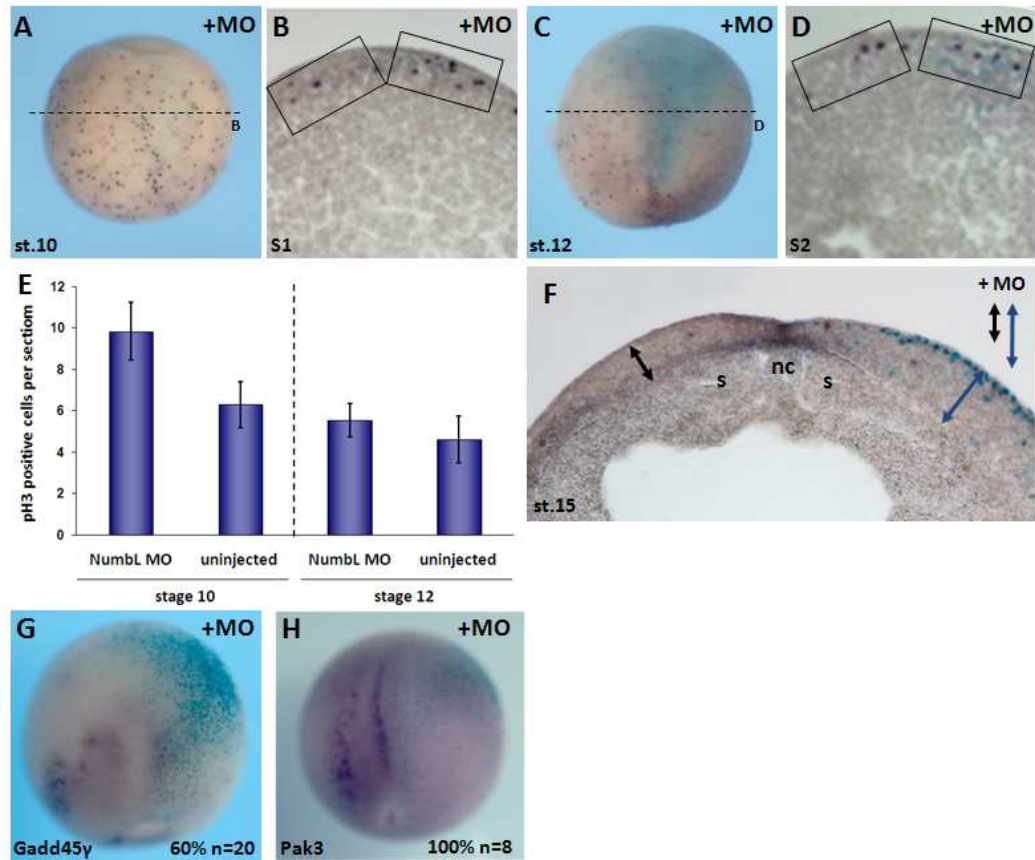


Figure 20: Numbl knockdown leads to increased proliferation during gastrula stages and loss of cell cycle regulators. Phosphoryllated Histone 3 staining of *Numbl* MO injected embryos. Embryos were injected with 12.5 ng *Numbl* MO and 50 pg β -Gal as lineage tracer. Embryos were cultured until they reached the indicated stage and then fixed for pH3 immuno-labeling. Stained embryos were sectioned and pH3 positive cells on injected and uninjected side were counted in 15 consecutive sections. **(A,C)** Embryos are shown in a dorsal view, anterior up. Dashed line represent plane of transverse sections shown in S1 and S2. Stage is indicated at the lower right corner. **(B, D)** Boxes indicate evaluated area on each side. **(E)** Graph summarizing the results. *Numbl* knockdown cause a significant increase in proliferation rates on the injected side during gastrula stages but not at later stages. **(F)** Transversal section of the neuroepithelium of a stage 15 *Numbl* morphant embryo. Epithelium thickness is represented by the double arrow for the injected site (blue) and the uninjected site (black). **(G,H)** In situ analysis of stage 15 *Numbl* morphants. Embryos are shown in a dorsal view, anterior up. The injected site is marked by blue β -Gal staining and is always on the right. Stained markers are indicated in the lower left corner, statistics in the lower right corner. nc, notochord; s, somite

3.9 NumbL knockdown promotes neural crest formation at tailbud stages

As described above, the knockdown of NumbL resulted in an increase in *Sox3* and *NCAM* positive cells at stage 15 (Fig. 19). To elucidate the fate of the observed increased progenitor population upon NumbL knockdown, the identity of the formed tissue was analyzed at stage 30 (Fig. 21). All NumbL MO injected embryos showed a thickened neuroepithelium on the injected side. The progenitor markers *Sox2* and *Sox3* were tested to ensure that the cells of the neuroepithelium were able to exit the progenitor state (Fig. 21A,B). While *Sox2* was only slightly expanded (Fig. 21A), *Sox3* appeared normal in comparison to the uninjected control side, indicating that the cells were not kept in a progenitor state. *N-tubulin* as marker for postmitotic neurons was found to be downregulated (Fig. 21C), with a slight recovery effect on expression on the MO injected side. *Epidermal keratin* expression was not altered upon NumbL knockdown (Fig. 21D). The head neural crest instead, marked by *Twist*, was found to be increased in NumbL morphants (Fig. 21E, E')

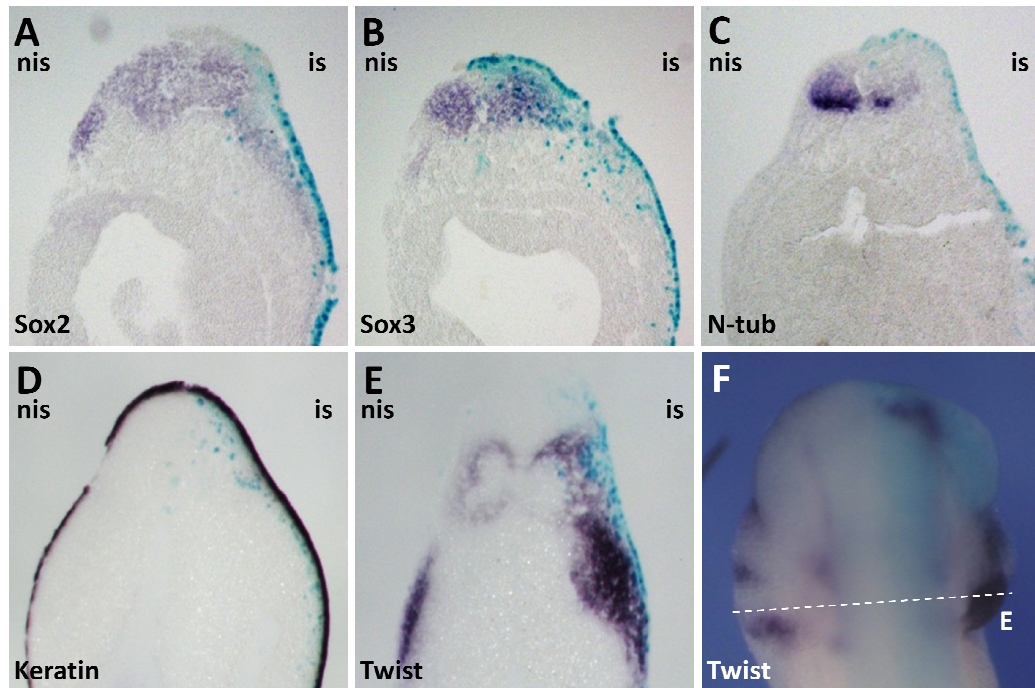


Figure 21: NumbL knockdown promotes neural crest fate at tailbud stages. Whole mount in situ analysis of *NumbL* morphants at tailbud stage. Embryos were injected with 12.5 ng MO, cultured until stage 30, fixed for in situ, probed for the genes that are indicated in the upper right corner and then transversally sectioned. The injected side is marked by blue β -Gal staining. Compared to the uninjected side, some additional tissue developed on the MO injected side. This tissue was weakly positive for *Sox2* and *Sox3* (A,B), negative for *N-tubulin* and epidermal *Keratin* (C,D) and strongly positive for *Twist* (E, F). is, injected side; nis, non-injected side.

3.10 *Ng*n expression patterns are disturbed in NumbL morphants

An expansion of neural progenitors marked by *Sox3* was detected and important cell cycle regulators that are induced during neuronal differentiation were lost upon knockdown of *NumbL*. Therefore, the question arose whether these cells were prevented from undergoing neuronal differentiation due to the loss of essential neuronal determination factors, thereby causing the loss of differentiated neurons. The best-characterized proneural factors expressed in the open neural plate are members of the *Ng*n family (*Ng*n1-3). We therefore tested the influence of *NumbL* MO on the expression of the *Ng*ns in *X. laevis* embryos by whole mount in situ hybridization. As observed previously, on the *NumbL* MO-injected side of the embryo (Nieber 2007), the expression of *Ng*n2

was still present, however, the expression domains appeared dispersed (Fig. 22B). The expression of *Ngn1* was also not inhibited by the presence of the NumbL MO. *Ngn1* expression domains were slightly extended and strongly increased in density on the injected side (Fig. 22A). The *Ngn3* expression domain was elongated on the NumbL MO injected side and at the same time appeared condensed in comparison to the uninjected control side (Fig. 22C). All together, all three *Ngns* are still expressed in NumbL morphants and loss of *Ngn* expression cannot be the reason for the complete loss of neuronal differentiation in the presence of the NumbL MO.

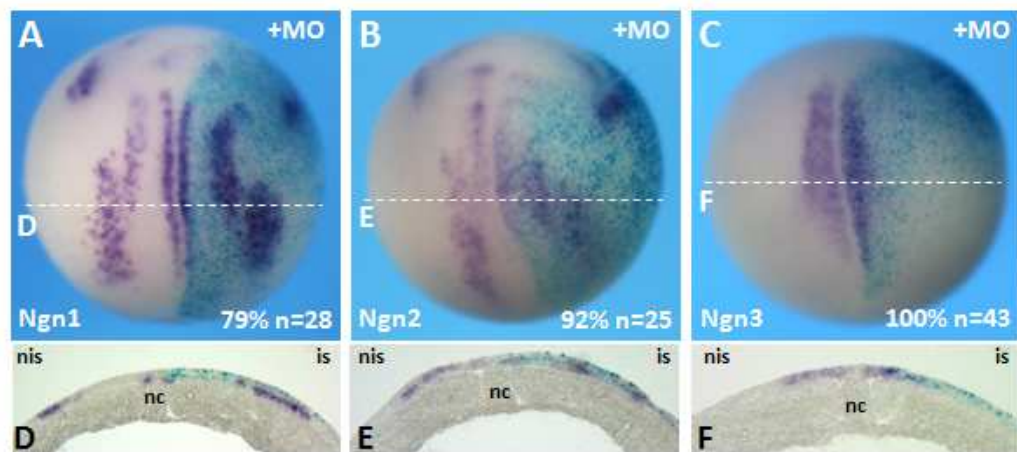


Figure 22: NumbL knockdown influences Neurogenin expression. Whole mount in situ hybridization analysis of NumbL morphants. Embryos were injected with 12.5 ng MO, cultured until stage 15, fixed for in situ and probed for the genes indicated in the lower left corner. Embryos are shown in a dorsal view, anterior up. The injected side is marked by blue β -Gal staining. Dashed lines represent the plane of the section shown below the embryo. Statistics are shown in the lower right corner. **(A, D)** *Ngn1* expression appears condensed upon *NumbL* knockdown. **(B, E)** *Ngn2* expression pattern is disturbed upon *NumbL* knockdown. **(C, F)** *Ngn3* expression domain appears condensed upon *NumbL* knockdown. nc, notochord; is, injected side; nis, non-injected side.

3.11 NumbL knockdown leads to an increase in early neural gene expression

In order to explain why a knockdown of NumbL prevented activation of neuronal differentiation factors downstream of *the Ngns*, the expression levels of negative regulators of neurogenesis were analyzed by whole mount in situ in

NumbL morphants (Fig. 23). We have already shown that expression of the ESR family of bHLH repressors is not increased upon knockdown of NumbL. An additional negative regulator is *Zic2*, which is a member of the *Zic* family of zinc-finger transcription factors. *Zic2* is expressed at the borders of the neural plate and in between the stripes of primary neurons (Brewster *et al.*, 1998). Functionally, *Zic2* was shown to promote a general neural fate in the ectoderm during neural induction and later to inhibit Ngn2 expression and function resulting in an inhibition of neuronal differentiation at the expense of a neural crest fate. Upon knockdown of NumbL, *Zic2* expression was strongly increased on the injected side (Fig. 23B). The other members of the *Zic* family, *Zic1* and *Zic3*, also promote a general neural fate, but distinguish themselves from *Zic2* by promoting neuronal differentiation (Nakata *et al.*, 1997; Mitzuseki *et al.*, 1998b). Both *Zic1* and *Zic3* were strongly increased upon NumbL knockdown (Fig. 23A,C). Remarkably, the increased *Zic* expression is predominantly found in the anterior neural plate and weaker in the posterior region of the embryo.

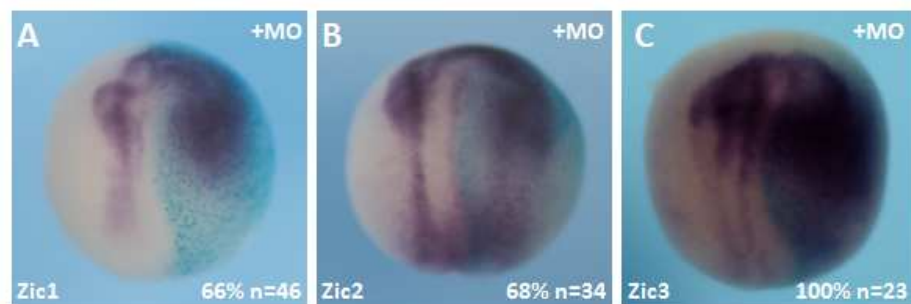


Figure 23: NumbL knockdown leads to an increase in *Zic* gene expression. Whole mount in situ analysis of NumbL morphant embryos. Embryos were injected with 12.5 ng *NumbL* MO and 50 pg β -Gal mRNA and cultured until stage 15 prior to analysis. The probed genes are indicated in the lower left corner, statistics in the lower right corner. The injected side is marked by blue β -Gal staining and is always at the right. Embryos are shown in a dorsal view, anterior up. **(A-C)** Expression domains of all three neural *Zics* are increased.

3.12 *Zic* expression is increased in a Notch independent manner upon NumbL knockdown

In mammalian cell lines, Numb and NumbL were shown to act as potent Notch inhibitors (McGill *et al.*, 2003), and also in *X. laevis* embryos NumbL has the ability to attenuate Notch activation of a luciferase reporter (Nieber 2007). In addition to its function in neuronal differentiation, Notch signaling has been shown to be involved in the activation of early neural genes like *Zic2* (Yan *et al.*, 2009a). Given two different modes of *Zic* activity depending on the developmental stage, the hypothesis was tested, whether NumbL could act as Notch inhibitor during gastrula stages where Notch signaling would influence *Zic* expression and thereby its function during neural induction. Embryos were injected with the constitutively active form of the Notch receptor, *NICD*, in one blastomere of the two-cell stage and the influence on *Zic* expression analyzed by whole mount in situ hybridization (Fig. 24). At stage 10, no alteration in *Zic1*, *Zic2* and *Zic3* expression was observed upon Notch activation (Fig. 24A, C and E). At stage 15, Notch activation by *NICD* injection lead to an increase in all three *Zics* (Fig. 24B, D and F), while *N-tubulin* was found to be inhibited (Fig. 24G), indicating that Notch pathway activation leads to increased *Zic* expression levels at the open neural plate stage, but does not influence early *Zic* expression during gastrulation.

To determine if the activation of *Zic* genes upon NumbL knockdown at stage 15 could be the result of Notch activation, *Zic3* expression was analyzed in NumbL morphants that were co-injected with the Notch signaling inhibitors *Delta^{Stu}* or *Su(H)^{DBM}* (Fig. 24I and K). The inductive effect of the NumbL knockdown on *Zic3* expression was not rescued by Notch inhibition, indicating Notch activation upon loss of NumbL is not the reason for the expansion of the *Zic3* expression domain. Notch inhibition alone did not influence *Zic3* expression, suggesting *Zic3* is regulated independent of Notch (Fig. 24H and J).

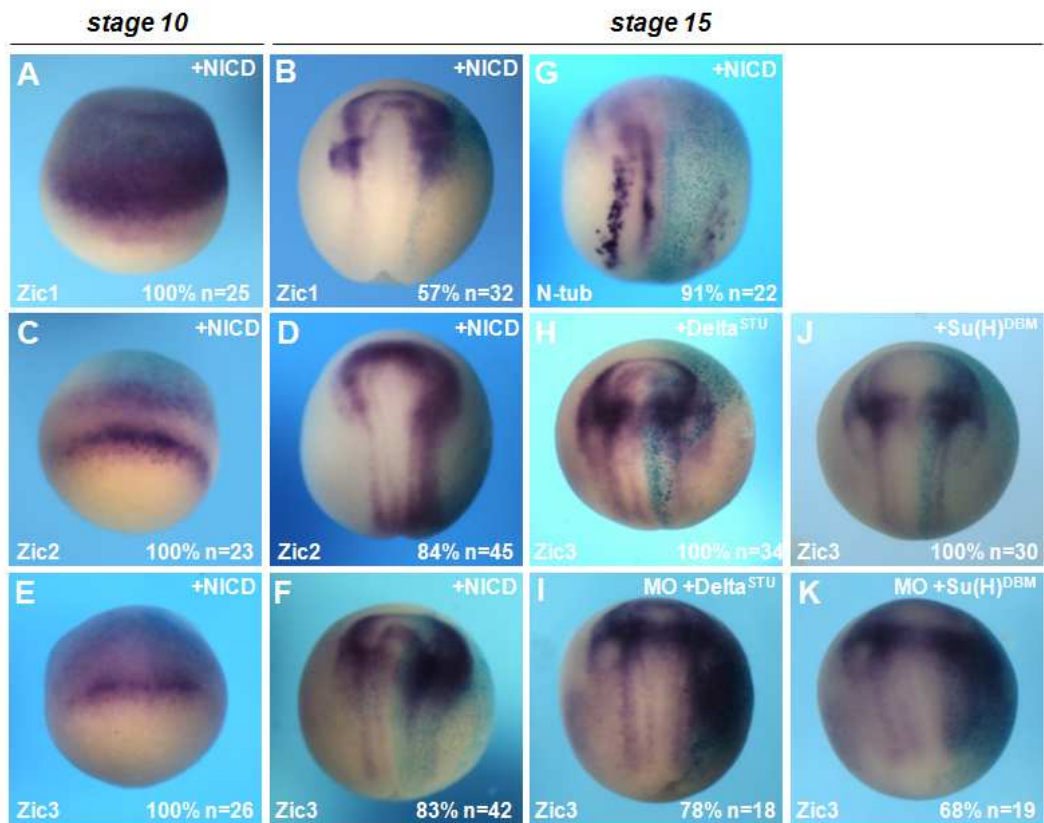


Figure 24: *Zic* genes are activated by Notch but Notch inhibition does not rescue the *NumbL* knockdown phenotype. Whole mount in situ analysis of embryos injected as indicated with 75 pg of *NICD*, 12.5 ng *NumbL* MO or 100 pg of the indicated Notch inhibitor. Embryos were cultured until they reached the stage indicated in the upper lane. Embryos were probed for the genes that are indicated in the lower left corner. Statistics are shown in the lower right corner. All embryos are shown in a dorsal view, anterior up. **(A,C,E)** *NICD* overexpression does not influence *Zic* gene expression during gastrula stages. **(B,D,F)** *NICD* overexpression causes an expansion of *Zic* expression domains at the open neural plate stage. **(G)** *NICD* inhibits *N-tubulin* expression at the open neural plate stage. **(H,J)** Inhibition of Notch signaling does not influence *Zic3* expression. **(I,K)** Notch inhibition does not rescue the *NumbL* MO effect on *Zic3* expression.

3.13 *Xenopus* Numb and NumbL are localized in the cytoplasm

Numb proteins have been shown to act as intrinsic cell determinants that are differentially inherited to daughter cells during cell division (Uemura *et al.*, 1989) or being asymmetrically distributed within single cells for example during migration (Nishimura *et al.*, 2007). These described functional activities of Numb

require its ability to localize to the membrane of a cell. Membrane localization of Numb can be achieved by either binding phosphotyrosine residues of tyrosine kinase receptors via the PTB domain (Verdi *et al.*, 1996) or with assistance of the adaptor protein Partner of Numb (Pon) (Lu *et al.*, 1998). In addition, studies in which the single Numb isoforms were overexpressed suggest different functions of the cytoplasmically and membrane localized isoforms (Bani-Yaghoub *et al.*, 2007; Kyriazis *et al.*, 2010).

Therefore, to gain insight in the possible function of *Numb* and *NumbL* in the ectoderm of developing *Xenopus* embryos, the subcellular localization of Myc-tagged (MT) versions of *X. laevis* NumbL and *X. tropicalis* Numb3 in animal caps (ectodermal explants) was analyzed. The *X. tropicalis* MT-Numb3 was used as it is the predominant Numb isoform during neurula stages (Fig. 13) and a full-length *X. laevis* Numb3 has not been isolated to date. Mouse MT-Numb1 was used as a control and was found to localize to the membrane (Fig. 25A-C) as described previously (Dho *et al.*, 1999). Neither MT-NumbL (Fig. 25D-F) nor MT-Numb3 (Fig. 25G-I) localized to the membrane and instead both were distributed symmetrically in the cytoplasm. The distribution of both constructs correlates with the structure of NumbL and Numb3, as the PTB insert, which was found to be essential for membrane localization of Numb is absent in both proteins (Verdi *et al.*, 1999; Dho *et al.*, 1999; Zhong *et al.*, 1997).

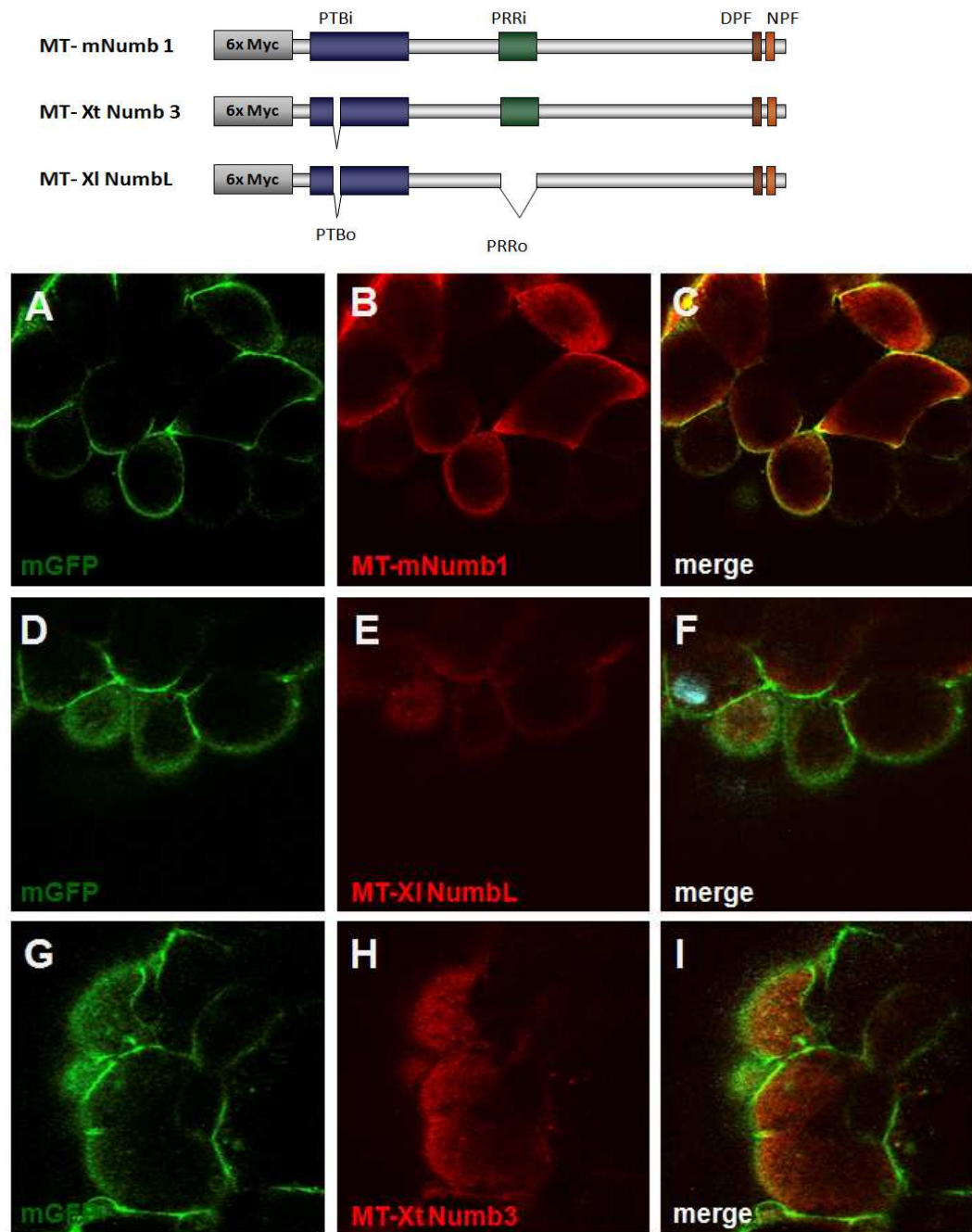


Figure 25: Subcellular localization of mouse MT-Numb1, *X.laevis* MT-NumbL and *X.tropicalis* MT-Numb3. Confocal images of labeled fluorescent proteins in animal caps. Caps were isolated from embryos injected with 500 pg of the indicated *MT-Numb* mRNA together with 100 pg mGFP mRNA and fixed at stage 15. Fluorescent labels are indicated in the lower left corner. Mouse *MT-Numb1* is localized at the membrane, while *X. laevis* *MT-NumbL* and *X. tropicalis* *MT-Numb3* are distributed in the cytoplasm. *X. laevis* *MT-NumbL* and *X. tropicalis* *MT-Numb3* form clusters at the cell membrane. The scheme at the top represents the domain structure of the isoforms used.

Numb and NumbL are adaptor proteins containing many protein-protein interaction domains (Verdi *et al.*, 1996). Therefore, we tested the hypothesis that the subcellular localization of the Numbs could change during the differentiation of the ectoderm to a neuron, depending on the presence or absence of regulatory proteins or signals. To examine this possibility, *X. laevis* animal caps were prepared from embryos injected with the indicated *MT-Numb* mRNA that were neuralized by co-injection of mRNA encoding the BMP inhibitor *Noggin* (*Nog*) or driven to undergo neuronal differentiation by the co-injection of mRNA encoding the proneural bHLH factor *Neurogenin2* (*Ngn2*) (Fig. 26). Both *MT-NumbL* (Fig. 26A-C) and *MT-Numb3* (Fig. 26D-F) were found to persist in the cytoplasm even when coinjected with *Noggin* or *Ngn2* mRNA, confirming the necessity of the PTB insert to localize to the membrane. Thus, a function of *Xenopus* *NumbL* or *Numb3* via asymmetrical distribution in dividing or polarized cells is unlikely.

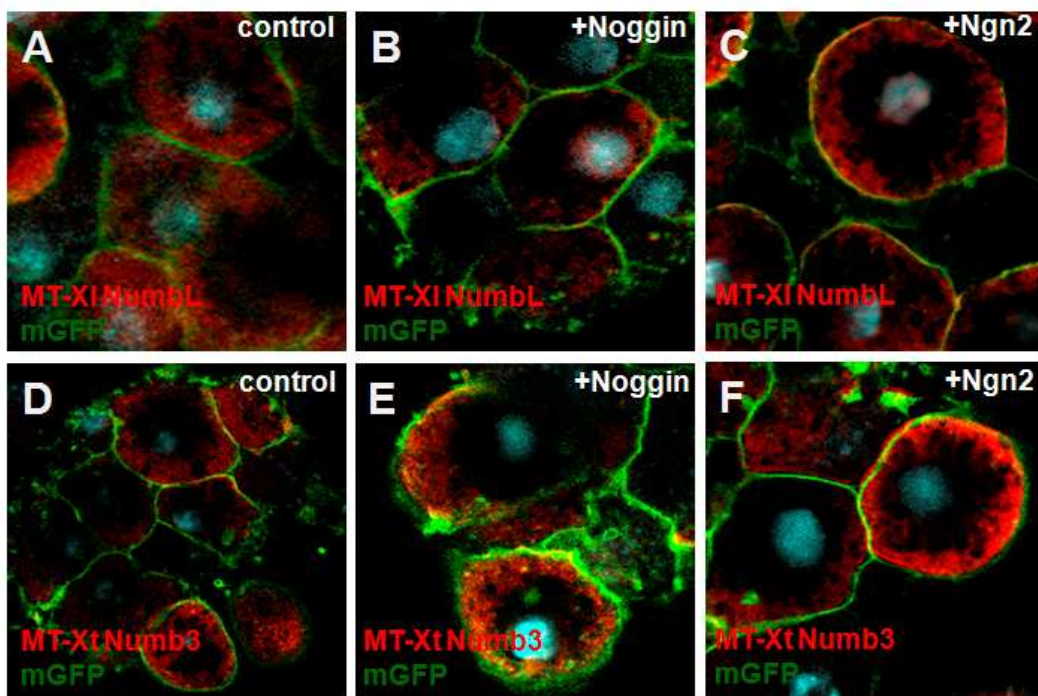


Figure 26: Subcellular localization of *X. laevis* NumbL and *X. tropicalis* Numb under wildtype and neuralized conditions. Confocal images of fluorescently labeled proteins in animal caps. *X. laevis* embryos were injected with 500 pg *MT-Numb* mRNA, 100 pg *mGFP* mRNA and 20 pg *Ngn2* mRNA or 50 pg *Noggin* mRNA. Fluorescent labels are indicated in the lower left corner, co-expressed mRNAs in the upper right corner.

Neuralization or neuronalization of the explanted tissue does not change the subcellular distribution of MT-NumbL and MT-Numb3.

3.14 NumbL interacts with the AP-2 complex

Numb family proteins are scaffold proteins containing multiple protein interaction domains. In order to understand NumbL function in the context of the developing nervous system, its direct interaction partners in this context have to be identified. To achieve this, a tandem affinity purification approach was used, by injecting mRNA encoding a double-tagged version of NumbL into *X. laevis* embryos. The TAP-tag containing a Streptavidin binding protein (SBP) and a ProteinG (ProtG), separated by 2 TEV precision protease cleavage sites, was cloned c-terminally to NumbL, creating NumbL-CTap (see Fig. 27 for scheme). *NumbL-CTap* or control *CTap* mRNA were injected in both blastomeres at the two-cell stage, the embryos cultivated until stage 15 and protein extracts prepared. In two subsequent pull-downs against ProtG and SBP, NumbL-CTap and CTap interacting proteins were isolated. The recovered proteins were separated by SDS-PAGE, first visualized by colloidal coomassie blue staining and then silver staining (Fig. 27).

As shown in the gel in Fig 27, two prominent bands are observed after the 2nd pull-down in both the CTap and Numb-CTap lanes that correspond to the streptavidine subunits. In addition, in the NumbL-CTap lane several protein bands were present that were not found in the CTap control lane. To identify the proteins, the bands were excised from the gel and analyzed by mass spectrometry (Fig. 27, table). The interacting proteins that were identified were the β 1 subunit of the AP-2 complex, the α 2 subunit of the AP-2 complex and the μ 1 subunit of the AP-2 complex. These results strongly indicate an interaction of NumbL with the Adaptor-related protein complex 2 (AP-2) in *Xenopus* embryos at the time primary neurons are differentiating.

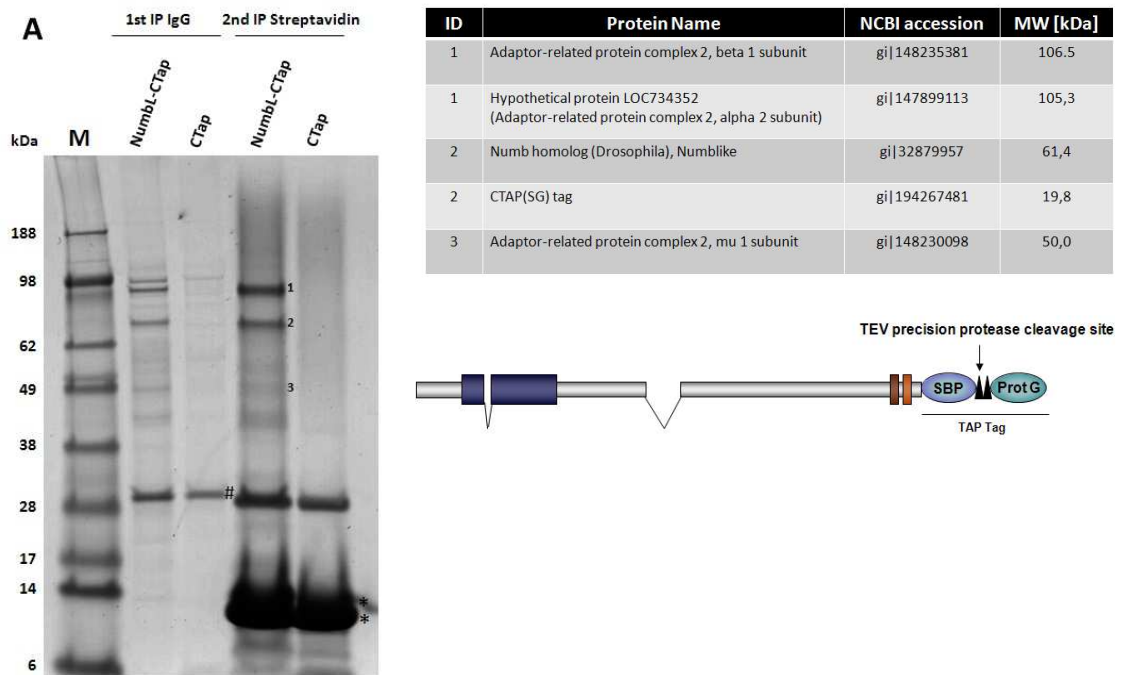


Figure 27: NumbL interacts with components of the AP-2 complex. Tandem affinity purification of NumbL-CTap from whole embryo lysates. Embryos were injected with 500 pg of NumbL-CTap oder CTap mRNA, cultured until stage 15 and frozen for protein extraction. The gradient gel is colloidal coomassie blue stained, loaded samples are indicated at the top. Marker sizes are indicated at the left. Identified bands are marked with numbers and described in the table at the right. Streptavidin subunit bands are marked by asterisks, TEV protease band by the pound sign on the gel.

3.15 Interaction with the AP-2 complex is essential for NumbL function

To determine if the identified interaction of NumbL with the AP-2 complex was of functional relevance, mutants of NumbL and NumbL(SA) were designed. In Numb, mutation of the DPF motif to DLA has been shown to abolish Numb binding to AP-2 (Santolini *et al.*, 2000). Therefore, the corresponding motif in NumbL, the DQF motif, was mutated to DLA. NumbL(DLA)-CTap was then used in a second TAP experiment that paralleled the one previously done with the wild-type NumbL. In this experiment, interactions with the AP-2 subunits were not observed (Appendix Fig. 2). These results suggest that this domain in NumbL is indeed responsible for interaction with the AP-2 complex. In vitro verification of NumbL interaction with the single AP-2 subunits by co-immunoprecipitation

were not performed as the isolated adaptins of the do not fold properly when expressed alone (Collins et al., 2002).

The NumbL DLA mutants were then tested for a possible dominant-negative effect by overexpressing them in *X. laevis* embryos and analyzing the influence on *N-tubulin* expression at stage 15 (Fig.28 A-C). Overexpression of mRNA encoding NumbL(DLA) and NumbL(SA-DLA) caused a phenotype, comparable to wild-type NumbL, exhibiting slightly increased numbers of *N-tubulin* positive cells in the lateral stripe. To show the necessity of the AP-2 interaction for NumbL function, rescue experiments were done. In these experiments, in contrast to the wild-type *NumbL*, the *NumbL(DLA)* mutants could not rescue the MO phenotype (Fig. 28,D-F). These results strongly suggest that the interaction with the AP-2 complex is essential for activity of NumbL during neuronal differentiation.

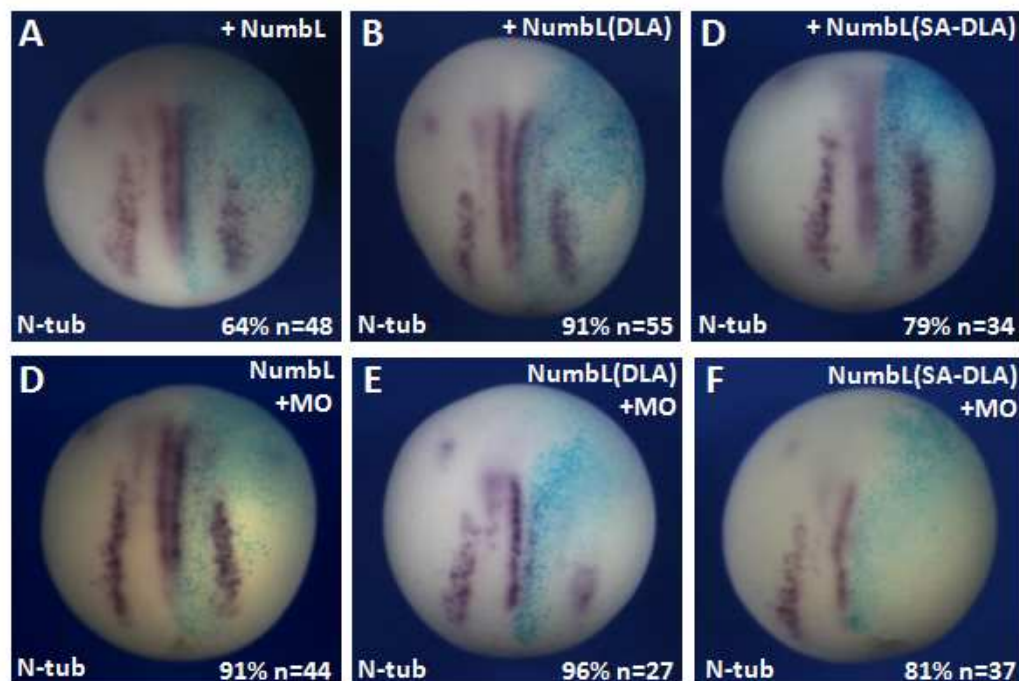


Figure 28: Interaction with the AP-2 complex is crucial for NumbL function. Whole mount in situ analysis of embryos that were injected with 500 pg *NumbL* construct mRNA and 12.5 ng *NumbL* MO, as indicated in the upper left corner. Embryos were cultured until stage 15, fixed and probed for *N-tubulin*. Statistics are shown in the lower right corner. Embryos are shown in a dorsal view, anterior up. **(A-C)** Overexpression of *NumbL*, *NumbL-DLA* or *NumbL SA DLA* does not show a dominant negative effect on *N-tubulin* expression. **(D-I)** The *NumbL* MO phenotype can be rescued by coinjection of mRNA encoding NumbL, but not by NumbL(DLA) or NumbL(SA-DLA).

4 Discussion

4.1 *Numbl* has a dual function during *Xenopus* primary neurogenesis

Numb and *Numbl* are expressed in the developing nervous system of mice, chicken and zebrafish (Zhong *et al.*, 1997; Niikura *et al.*, 2006; Wakamatsu *et al.*, 1999; Reugels *et al.*, 2006). *Numb* is expressed ubiquitously, including the mitotically active progenitor cells within the neural epithelium (Zhong *et al.*, 1996; Zhong *et al.*, 1997; Wakamatsu *et al.*, 1999; Reugels *et al.*, 2006), while *Numbl* is expressed specifically in the developing nervous system in post-mitotic differentiating cells (Zhong *et al.*, 1997). Correlating with its expression in other organisms (Zhong *et al.*, 1997), *X. laevis Numbl* is exclusively expressed in differentiating neurons in the open neural plate as well as in the closed neural tube, while *Numb* is more ubiquitously expressed. The conserved expression patterns of the *Numb* family genes already suggests that the functions of the *Numbs* in the context of neurogenesis may also be conserved. In addition to the expression of *Numbl* in the differentiating neurons, we also observe an early expression of in the dorsal ectoderm of gastrula stage embryos. At this stage when *Numbl* is expressed in prospective neural ectoderm, this tissue is characterized by BMP inhibition and FGF signals (Marchal *et al.*, 2009). Simultaneously, the first cells express the *Ngn* proneural genes and become determined to enter a neuronal fate (Sommer *et al.*, 1996; Ma *et al.*, 1998), however, downstream markers for neuronal differentiation are not yet present. Thus the expression of *Numbl* during *X. laevis* early embryogenesis suggests at least two unique functions of *Numbl* during the development of the nervous system (Fig.14); one early function during the establishment of the neural ectoderm and a later function in the process of neuronal differentiation.

Previously we showed that a knockdown of *Numbl* resulted in a complete loss of postmitotic neurons at the open neural plate stage (Nieber 2007). This differs from the mouse *Numbl* homozygous mutants that were reported to be viable but show no obvious phenotype (Petersen *et al.*, 2002).

The lack of phenotype was attributed to partial redundancy with other Numbs (Petersen *et al.*, 2002). Consistent with redundancy, Numb mutant mice exhibit severe cranial neural tube closure defects and die around E11.5, and double mutants of *Numb* and *NumbL* die earlier at around E9.5 with more widespread and severe defects than the single mutant (Petersen *et al.*, 2002). Moreover, several conditional knockouts (cKO) were created where *Numb* was eliminated at different time points from E8.5 to E12.5. While Numb cKO are viable and fertile and do not distinguish from wild-type animals, the Numb cKO in a *NumbL* deficient background results in embryonic lethality and a loss of differentiated neurons at E10.5 - 11.5. Taken together the mouse knockouts clearly demonstrate an essential role of the *Numbs* during neurogenesis. Furthermore, in *Xenopus* we could show that *NumbL* is essential for primary neurogenesis. The failure to observe a neural phenotype in mouse *NumbL* knockouts may be attributed to the incompleteness of the knockdown, as still low levels of *NumbL* are detectable in the homozygous mutants (Petersen *et al.*, 2002).

A knockdown of *NumbL* with a morpholino antisense oligonucleotide in *X. laevis* was found not only to inhibit differentiation of primary neurons but also to increase proliferation in the ectoderm specifically during gastrula and early neurula stages (Fig. 20). This results in a thickened neuroepithelium at stage 15. The expression domains of the neural progenitor gene *Sox3* and the panneural gene *NCAM* were increased at stage 15 following *NumbL* knockdown. This suggests a dual function of *NumbL* and is consistent with the results obtained in mouse. Depending on the developmental stage of gene inactivation in mouse, cDKO of *Numb* and *NumbL* either promoted premature differentiation and therefore depletion of the neural progenitor population (Petersen *et al.*, 2002; Petersen *et al.*, 2004) or impaired differentiation with concomitant hyperproliferation of these cells (Li *et al.*, 2003). This suggests a dual function for the *Numb* and *NumbL* in both progenitor cells maintenance and differentiation.

Similar to *Numb* proteins, the *Zic* zinc-finger transcription factors exhibit two different functions during neural induction and neuronal differentiation. In *X. laevis*, one early function of the *Zics* is to induce neural markers like *NCAM* and

to promote a general neural fate. During neuronal differentiation, *Zic1* and *Zic3* promote differentiation through activation *Ngn2* (Nakata *et al.*, 1997; Mitzuseki *et al.*, 1998). *Zic2*, in contrast, inhibits neuronal differentiation by inhibiting *Ngn2* expression and function (Brewster *et al.*, 1998) and is expressed between the stripes of primary neurogenesis. In addition, the *Zics* were described to function in patterning of the spinal cord by antagonizing SHH signals from the notochord and therefore confer dorsal neuronal and neural crest cell fates to neural progenitors (Nakata *et al.*, 1998; Aruga *et al.*, 2004). At the open neural plate stage, *Zic1*, *Zic2* and *Zic3* are strongly increased in *NumbL* morphants (Fig. 23). Corresponding to the strong activation in the anterior neural plate (Fig. 23) and the neural crest inducing activity of all three *Zic* genes (reviewed by Aruga, 2004), increased expression of the neural crest marker *Twist* is observed at tadpole stages (Fig. 21). Thus, the early activation of the *Zic* genes would explain the observed increase in proliferation in the neuroepithelium while the later increase in *Zic* expression could impair neuronal differentiation by promoting a neural crest cell fate in neural progenitors. However, since *Ngn* expression is not lost upon a *NumbL* knockdown (Fig. 22), the neuronal precursors exit the cell cycle and enter the differentiation pathway nevertheless. Therefore, the early function of *NumbL* to commit neuronal differentiation in the progenitors of the dorsal ectoderm may be independent of its later function during the process of neuronal differentiation itself.

Overexpression of *mNumb* in murine neural precursor cells caused isoform dependent either differentiation or proliferation of these cells (Bani-Yaghoub *et al.*, 2007). Consistent with the overexpression of *mNumb4*, the structurally most similar isoform to *NumbL*, *NumbL* gain-of-function in *X. laevis* does not promote ectopic formation of primary neurons, but rather a slight increase in neuronal density in the territories of primary neurogenesis at the open neural plate stage (Fig. 16). *NumbL* role during differentiation of primary neurons is further supported by its regulation through *Ngn1-3* (Fig. 15). The failure to obtain a strong gain-of-function phenotype may be due to post-transcriptional negative regulatory mechanisms. For example, the RNA binding protein Musashi inhibits translation of *Numb* transcripts (Okano *et al.*, 2002). As

Musashi, like most RNA-regulatory proteins characterized to date, bind within the untranslated regions of its target mRNA (Imai *et al.*, 2001), the used *NumbL* mRNA did not harbor its endogenous untranslated regions. However, one cannot exclude regulatory binding sites within the coding sequence for other regulatory proteins. Furthermore, translation of *Numb* mRNA was shown to be regulated by miR146a in mouse satellite cells (Kuang *et al.*, 2009), raising the possibility that *NumbL* mRNA translation might be regulated by micro RNAs, as well. Numb is also on a post-translational level by phosphorylation of two serine residues, Ser²⁹¹ and Ser³¹⁰ (Tokumitsu *et al.*, 2006). If phosphorylated, these two residues promote the binding of ubiquitous present 14-3-3 proteins, which mask Numb's protein-protein interaction domains and prevent it from binding its targets. Overexpression of phosphorylation mutants of NumbL in which the two conserved serines were exchanged to alanine (NumbL(SA)), did not result in a significantly stronger phenotype than wild-type gain-of-function (Fig. 16C). However, additional uncharacterized sites of negative regulation within NumbL may still be present. Alternatively, since NumbL functions as a scaffold protein, its activity is most likely dependent on the availability of its interaction partners. Therefore, the weak phenotype upon NumbL overexpression may also be explained by limiting amounts of interacting proteins.

4.2 NumbL function during *Xenopus* primary neurogenesis is independent of Notch signaling

Overexpression of *Drosophila* Numb results in an inhibition of Notch activity and an increased neuronal differentiation of SOP cells (Rhyu *et al.*, 1994; Guo *et al.*, 1996). As the comparable phenotype in *X. laevis* can be created by overexpression of Notch inhibitors and is much stronger than the effect observed for NumbL overexpression (compare Fig. 16A and Fig. 18A,C), it is likely that the increase in neuron density relies on a mechanism different from Notch signaling inhibition. Overexpression of distinct mouse Numb isoforms in murine neural

progenitor cells or *Drosophila* other optic anlage cells (OOA) revealed that although the different Numb isoforms possess different developmental potential in driving either proliferation or differentiation, Notch signaling was equally inhibited by the single isoforms (Toriya *et al.*, 2006; Bani-Yaghoub *et al.*, 2007). These results strongly support that the opposing isoform activities are independent of Notch signaling.

The knockdown of NumbL in *X. laevis* was shown to efficiently inhibit the formation of differentiated neurons (Nieber 2007). While the impaired neuronal differentiation upon a knockdown of NumbL phenocopies an activation of the Notch signaling pathway, no evidence for NumbL acting as an inhibitor of Notch signaling in this context was found. Neither were Notch target genes activated upon a loss of NumbL (Fig. 17), nor could the NumbL knockdown effect on neuronal differentiation be rescued by inhibition of Notch signaling (Fig. 18). These results further suggest a Notch independent function of NumbL during neuronal differentiation. Also, the underlying molecular mechanism of *Zic* activation is unclear as the induction of the *Zic* genes is subject to recent debate. Notch activation by overexpression of NICD resulted in an increase in *Zic* expression (Fig. 24). This could be either a direct effect, as Notch signals were shown to be essential for the induction of *Zic2* expression during neural induction (Yan *et al.*, 2009b), or an indirect effect as Notch activation increases proliferation of neural progenitors, leading to an enlarged neural plate (Louvi *et al.*, 2006). However, as shown for the NumbL knockdown phenotype on *N-tubulin* expression (Fig. 18), the increase in *Zic* expression was also found to be Notch independent. Inhibition of Notch did not rescue the knockdown phenotype in *Zic* gene expression (Fig. 24I and K).

Similar to the Notch activation upon Numb knockdown in *Drosophila* SOPs (Guo *et al.*, 1996), Notch signaling was suggested to be de-regulated and influence progenitor cell maintenance in the mouse Numb/Numbl double knockout, but no evidence for elevated Notch signaling has been demonstrated thus far. However, cNumb was described to bind and modulate Notch-1 activity upon overexpression in the chick neuroepithelium (Wakamatsu *et al.*, 1999). In

addition, NumbL overexpression in *X. laevis* embryos could decrease the activation of a Notch luciferase reporter by NICD (Nieber 2007). These data raise the possibility that Numb and NumbL can under certain developmental contexts act as Notch inhibitors.

Additional pathways that might be regulated by NumbL in the context of primary neurogenesis in *Xenopus* are BMP and FGF, as they are active in the ectoderm during neural induction. While BMP inhibition was shown to be sufficient for induction of *Zic1*, *Zic3* can only be activated if FGF4 signaling is not compromised at the same time (Marchal *et al.*, 2009). *Zic2* activation requires in turn Notch signaling downstream of the forkhead transcription factor FoxD5, an immediate target of *Zic1* and *Zic3* (Yan *et al.*, 2009b). Thus, candidate pathways for being regulated by NumbL at this stage are either BMP signaling, FGF signaling or events like calcium signals that might mediate the activation of target genes upon activation of FGF signals. Interestingly, Numb4, the structurally most similar isoform to NumbL, was recently described to influence calcium signaling in the context of neuronal differentiation. Numb4 was found to trigger neuronal differentiation upon overexpression in cultured mouse neuronal progenitor cells depending on a calcium influx via L-Type calcium channels and subsequent MAPK pathway activation (Lu *et al.*, 2009). Furthermore, a stress induced switch in Numb isoforms from PTBi (Numb1, Numb2) to PTBo (Numb3, Numb4) in PC12 cells specifically led to elevated Notch signaling levels and subsequent transcription of the *transient receptor potential channel 6 (TRP6)*, an L-Type calcium channel (Kyriazis *et al.*, 2010). These data suggest the possibility that NumbL might be involved in calcium signaling regulation downstream of FGF signaling and upstream of early neural gene expression as well as in the context of neuronal differentiation. However, the context specific regulation of the *Zic* genes has to be evaluated in further studies.

4.3 NumbL is localized in the cytoplasm and interacts with the AP-2 complex

Numb is known to act as asymmetrical distributed cell fate determinant in *Drosophila* SOPs and neural progenitor cells (Uemura *et al.*, 1989, Lu *et al.*, 1998). Numb has also been shown to function in mediating localized interactions between target proteins like the AP-2 complex and integrins (Nishimura *et al.*, 2007; Ezratty *et al.*, 2009). Both activities are dependant on Numbs ability to localize to the membrane, either prior to cell division or during a specific function carried out by the cell, i.e. migration. An insert within the PTB domain was found to be crucial for membrane localization of mammalian Numb (Verdi *et al.*, 1996). In this thesis, *Xenopus* Numb proteins lacking this insert (Numb3 and NumbL) were also found not to localize to the membrane in ectodermal explants (Fig. 25), even under neuralizing and neuronalizing conditions (Fig. 26). These results strongly suggest that NumbL protein will not be asymmetrically distributed during cell division. On the functional level, cytoplasmatic isoforms of hNumb were shown to specifically induce differentiation of rat PC12 cells upon growth factor withdrawal while cell expressing membrane localized isoforms stayed in a proliferative state (Pedersen *et al.*, 2002). Therefore, also the cytoplasmatic localization of *X. laevis* MT-NumbL would correlate with a possible function in neuronal differentiation.

Numb proteins were shown to interact with components of the AP-2 complex (Santolini *et al.*, 2000) and attach target proteins for endocytosis. Although the AP-2 interaction motif DPF in Numb is exchanged to a DQF motif in NumbL, strong interactions with AP-2 could nevertheless be detected in *Xenopus* open neural plate stage embryos (Fig. 27). As this interaction is crucial for NumbL ability to rescue the MO effect (Fig. 28), NumbL might act *in vivo* as an endocytotic protein, as well. The seemingly contradiction, that NumbL could act in endocytosis although it is not membrane localized per se can be explained by adaptor proteins that mediate interaction under certain conditions. Taking into account that mouse Numb was reported also to interact with adaptor proteins to

localize to the membrane (Lu *et al.*, 1998), this raises the possibility that *X. laevis* NumbL might nevertheless function as scaffold protein in membrane-associated processes like for instance endocytosis. Furthermore, Numb was shown to regulate not only endocytosis but also post-endocytotic trafficking and is localized to endosomes, as well (McGill *et al.*, 2009; Nishimura *et al.*, 2007). Therefore, a role for NumbL in downstream events of endocytosis in endosomal trafficking or recycling is possible.

Known targets endocytosed by Numb are the Notch receptor or integrins during directional cell migration (Santolini *et al.*, 2000; Nishimura *et al.*, 2007). Since Notch de-regulation could be excluded from causing the NumbL knockdown phenotype (Fig. 19; Fig. 20), NumbL target for promoting endocytosis remains to be identified. Possible targets for endocytosis by NumbL are FGF receptors (FGFR). FGFRs are tyrosine receptor kinases (TRKs) and dimerize to form an active ternary complex upon binding of an FGF ligand. They activate a downstream signaling cascade via mutual phosphorylation of both TRK domains (Ornitz *et al.*, 2001). After activation, the ternary complexes are endocytosed to terminate the signal and either degraded in lysosomes (mainly FGFR1-3) or recycled (mainly FGFR-4) (Haugsten *et al.*, 2005). Thus, since MAPK activation and calcium influx as readouts for FGF activation were observed upon mNumb4 overexpression in cultured neural progenitors (Lu *et al.*, 2009), mNumb4 could promote endocytosis and recycling of FGF receptors in this context. NumbL as closely related protein could possess similar activities and function in FGFR endocytosis or alternatively in recycling of the endocytosed membrane components, as it was suggested for Numb in the context of integrin recycling (Nishimura *et al.*, 2007). A knockdown of NumbL would then result in an increased number of ternary FGF/FGFR complexes that reside active at the membrane and increase FGF signaling levels, leading to increased neural gene expression but inhibited differentiation. The identification of the specific target proteins of NumbL will be an interesting topic of future studies. This is important not only due to the essential of NumbL during *Xenopus* neurogenesis, but also the emerging role of Numb proteins in cancer (Pece *et al.*, 2010).

5. Summary

In summary, two functions of NumbL were shown during neurogenesis. One in the context of neural induction, where NumbL is important for the activation of early neural genes upon inductive stimuli and a second function during the process of neuronal differentiation where NumbL is found in differentiating neurons and is essential for this process (Fig. 29). Mechanistically, one aspect of NumbL function lies in endocytosis by attaching targets to the AP-2 complex, which is essential for NumbL functionality. However, the specific targets and influenced signaling pathways could not be identified so far, also other possible functions of NumbL like interactions with E3 ligases remain to be revealed in future studies. Interestingly, NumbL functions, in contrast to what was expected, independent of Notch signaling since a loss of NumbL does not elevate Notch activity.

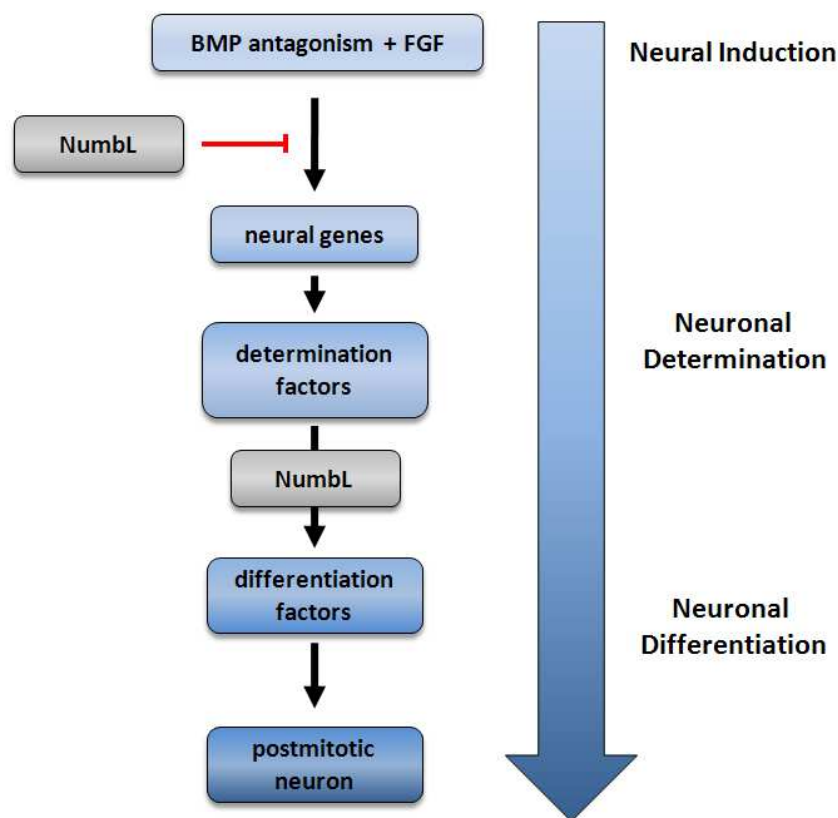


Figure 29: Scheme of NumbL dual function during primary neurogenesis. NumbL is involved in regulation of early neural gene expression. In addition, NumbL function is essential in the process of neuronal differentiation.

6. Bibliography

- Agius, E., Oelschläger, M., Wessely, O., Kemp, C., De Robertis, EM. (2000). Endodermal Nodal-related signals and mesoderm induction in *Xenopus*. *Development* 127, 1173-1183.
- Artavanis-Tsakonas, S., Rand, MD., Lake, RJ. (1999). Notch signaling: cell fate control and signal integration in development. *Science* 284, 770-776.
- Aruga, J., Mizugishi, K., Koseki, H., Imai, K., Balling, R., Noda, T., Mikoshiba, K. (1999). *Zic1* regulates the patterning of vertebral arches in cooperation with *Gli3*. *Mech Dev.* 89, 141-150.
- Bani-Yaghoub, M., Kubu, CJ., Cowling, R., Rochira, J., Nikopoulos, G.N., Bellum, S., Verdi, J.M. (2007). A switch in *numb* isoforms is a critical step in cortical development. *Dev Dyn.* 236, 696-705.
- Batut, J., Vandell, L., Leclerc, C., Daguzan, C., Moreau, M., Néant, I. (2005). The Ca²⁺-induced methyltransferase *xPRMT1b* controls neural fate in amphibian embryo. *Proc Natl Acad Sci U S A.* 102, 15128-15133.
- Bellefroid, E.J., Bourguignon, C., Hollemann, T., Ma, Q., Anderson, D.J., Kintner, C., Pieler, T. (1996). *X-Myt1*, a *Xenopus* C2HC-type zinc finger protein with a regulatory function in neuronal differentiation. *Cell* 87, 1191-1202.
- Bellefroid, E.J., Kobbe, A., Gruss, P., Pieler, T., Gurdon, J.B., Papalopulu, N. (1998). *Xiro3* encodes a *Xenopus* homolog of the *Drosophila* *Iroquois* genes and functions in neural specification. *EMBO J.* 17, 191-203.
- Blaikie, P., Immanuel, D., Wu, J., Li, N., Yajnik, V., Margolis, B. (1994). A region in *Shc* distinct from the SH2 domain can bind tyrosine-phosphorylated growth factor receptors. *J Biol Chem.* 269, 32031-32034.
- Boy, S., Souopgui, J., Amato, MA, Wegne, M., Pieler, T., Perron, M. (2004). *XSEB4R*, a novel RNA-binding protein involved in retinal cell differentiation downstream of bHLH proneural genes. *Development* 131, 851-862.
- Brewster, R., Lee, J., Ruiz i Altaba, A. (1998). *Gli/Zic* factors pattern the neural plate by defining domains of cell differentiation. *Nature* 393, 579-583.
- Bullock, W.O., Fernandez, J.M., Short, J.M. (1987). XL1-Blue: A high efficiency plasmid transformation *recA* *Escherichia coli* strain with betagalactosidase selection. *Biotechniques* 5, 376-379.
- Carruthers, S., Mason, J., Papalopulu, N. (2003). Depletion of the cell-cycle inhibitor 27(*Xic1*) impairs neuronal differentiation and increases the number of *ElrC(+)* progenitor cells in *Xenopus tropicalis*. *Mech Dev.* 120, 607-616.

- Chalmers, A.D., Welchman, D., Papalopulu, N. (2002). Intrinsic differences between the superficial and deep layers of the *Xenopus* ectoderm control primary neuronal differentiation. *Dev Cell*. 2, 171-182.
- Chapman, G., Liu, L., Sahlgren, C., Dahlgvist, C., Lendahl, U. (2006). High levels of Notch signaling down-regulate Numb and Numbl-like. *J Cell Biol*. 175, 535-540.
- Chien, C.T., Wang, S., Rothenberg, M., Jan, L.Y., Jan, Y.N. (1998). Numb-associated kinase interacts with the phosphotyrosine binding domain of Numb and antagonizes the function of Numb in vivo. *Mol Cell Biol*. 18, 598-607.
- Chitnis, A., Henrique, D., Lewis, J., Ish-Horowicz, D., Kintner, C. (1995). Primary neurogenesis in *Xenopus* embryos regulated by a homologue of the *Drosophila* neurogenic gene Delta. *Nature* 375, 761-766.
- Colaluca, I.N., Tosoni, D., Nuciforo, P., Senic-Matuglia, F., Galimberti, V., Viale, G., Pece, S., Di Fiore, P.P. (2008). NUMB controls p53 tumour suppressor activity. *Nature* 451, 76-80.
- Collins, B.M., McCoy, A.J., Kent, H.M., Evans, P.R., Owen, D.J. (2002) Molecular Architecture and Functional Model of the Endocytotic AP-2 complex. *Cell* 109, 523-535
- Coffman, C.R., Skoglund, P., Harris, W.A., Kintner, C.R. (1993). Expression of an extracellular deletion of Xotch diverts cell fate in *Xenopus* embryos. *Cell* 73, 659-671.
- Davis, R.L., Turner, D.L. (2001). Vertebrate hairy and Enhancer of split related proteins: transcriptional repressors regulating cellular differentiation and embryonic patterning. *Oncogene* 20, 8342-8357.
- Dawson, S.R., Turner, D.L., Weintraub, H., Parkhurst, S.M. (1995). Specificity for the hairy/enhancer of split basic helix-loop-helix (bHLH) proteins maps outside the bHLH domain and suggests two separable modes of transcriptional repression. *Mol Cell Biol*. 15, 6923-6931.
- Deblandre, G.A., Wettstein, D.A., Koyano-Nakagawa, N., Kintner, C. (1999). A two-step mechanism generates the spacing pattern of the ciliated cells in the skin of *Xenopus* embryos. *Development* 126, 4715-4728.
- Dee, C.T., Hirst, C.S., Shih, Y.H., Tripathi, V.B., Patient, R.K., Scotting, P.J. (2008). Sox3 regulates both neural fate and differentiation in the zebrafish ectoderm. *Dev Biol*. 320, 289-301.
- De la Calle-Mustienes, E., Glavic, A., Modolell, J., Gomez-Skarmeta, J.L. (2002). Xiro homeoproteins coordinate cell cycle exit and primary neuron formation by upregulating neuronal-fate repressors and downregulating the cell-cycle inhibitor XGadd45-gamma. *Mech Dev*. 119, 69-80.

- Delaune, E., Lemaire, P., Kodjabachian, L. (2005). Neural induction in *Xenopus* requires early FGF signalling in addition to BMP inhibition. *Development* 132, 299-310.
- Dent, J.A., Polson, A.G., Klymkowsky, M.W. (1989). A whole-mount immunocytochemical analysis of the expression of the intermediate filament protein vimentin in *Xenopus*. *Development* 05, 61-74.
- De Robertis, E.M., Kuroda, H. (2004). Dorsal-ventral patterning and neural induction in *Xenopus* embryos. *Annu Rev Cell Dev Biol.* 20, 285-308.
- Dho, S.E., French, M.B., Woods, S.A., McGlade, C.J. (1999). Characterization of four mammalian numb protein isoforms. Identification of cytoplasmic and membrane-associated variants of the phosphotyrosine binding domain. *J Biol Chem.* 274, 33097-33104.
- Di Marcotullio, L., Ferretti, E., Greco, A., De Smaele, E., Po, A., Sico, M.A., Alimandi, M., Giannini, G., Maroder, M., Screpanti, I., Gulino, A. (2006). Numb is a suppressor of Hedgehog signalling and targets Gli1 for Itch-dependent ubiquitination. *Nat Cell Biol.* 12, 1415-1423.
- Di Marcotullio, L., Greco, A., Mazzà, D., Canettieri, G., Pietrosanti, L., Infante, P., Coni, S., Moretti, M., De Smaele, E., Ferretti, E., Screpanti, I., Gulino, A. (2010). Numb activates the E3 ligase Itch to control Gli1 function through a novel degradation signal. *Oncogene* (Epub ahead of print).
- Dubios, L., Bally-Cuif, L., Crozatier, M., Moreau, J., Paquerereau, L., Vincent, A. (1998). XCoE2, a transcription factor of the Col/Olf-1/EBF family involved in the specification of primary neurons in *Xenopus*. *Curr Biol.* 8, 199-209.
- Ezratty, E.J., Bertaux, C., Marcantonio, E.E., Gundersen, G.G. (2009). Clathrin mediates integrin endocytosis for focal adhesion disassembly in migrating cells. *J Cell Biol.* 187, 733-747.
- Fletcher, R.B., Harland, R.M. (2008). The role of FGF signaling in the establishment and maintenance of mesodermal gene expression in *Xenopus*. *Dev Dyn.* 237, 1243-1254.
- Gawantka, V., Delius, H., Hirschfeld, K., Blumenstock, C., Niehrs, C. (1995). Antagonizing the Spemann organizer: role of homeobox gene Xvent-1. *EMBO J.* 14, 6262-6279.
- Gawantka, V., Pollet, N., Delius, H., Vingron, M., Pfister, R., Nitsch, R., Blumenstock, C., Niehrs, C. (1998). Gene expression screening in *Xenopus* identifies molecular pathways, predicts gene function and provides a global view of embryonic patterning. *Mech Dev.* 77, 95-141.

- Gerhart, J. (2001). Evolution of the organizer and the chordate body plan. *Int J Dev Biol.* 45, 133–153.
- Glinka, A., Wu, W., Delius, H., Monaghan, A.P., Blumenstock, C., Niehrs, C. (1998). Dickkopf-1 is a member of a new family of secreted proteins and functions in head induction. *Nature* 391, 357-362.
- Gulino, A., Di Marcotullio, L., Screpanti, I. (2010). The multiple functions of Numb, *Exp. Cell Res.* 316, 900–906.
- Guo, M., Jan, L.Y., Jan, Y.N. (1996). Control of daughter cell fates during asymmetric division: interaction of Numb and Notch. *Neuron.* 17, 1-4
- Hardcastle, Z., Chalmers, A.D., Papalopulu, N. (2000). FGF-8 stimulates neuronal differentiation through FGFR-4a and interferes with mesoderm induction in *Xenopus* embryos. *Curr Biol* 10, 1511-1514.
- Harland, R.M. (1991). In situ hybridization: an improved whole-mount method for *Xenopus* embryos. *Methods Cell Biol.* 36, 685-695.
- Harland, R., Gerhart, J. (1997). Formation and function of Spemann's organizer. *Annu Rev Cell Dev Biol.* 13, 611-667.
- Hartenstein, V. (1989). Early neurogenesis in *Xenopus*: the spatio-temporal pattern of proliferation and cell lineages in the embryonic spinal cord. *Neuron.* 3, 399-411.
- Haugsten, E.M., Sørensen, V., Brech, A., Olsnes, S., Wesche, J. (2005). Different intracellular trafficking of FGF1 endocytosed by the four homologous FGF receptors. *J. Cell. Sci.* 118, 3869-3881
- Heeg-Truesdell, E., LaBonne, C. (2006). Neural induction in *Xenopus* requires inhibition of Wnt-beta-catenin signaling. *Dev. Biol.* 298, 71-86.
- Holleman, T., Pieler, T. (1999). Xpitx-1: a homeobox gene expressed during pituitary and cement gland formation of *Xenopus* embryos. *Mech Dev.* 88, 249-252.
- Hopwood, N.D., Pluck, A., Gurdon, J.B. (1989). A *Xenopus* mRNA related to *Drosophila* twist is expressed in response to induction in the mesoderm and the neural crest. *Cell* 59, 893-903.
- Iemura, S., Yamamoto, T.S., Takagi, C., Uchiyama, H., Natsume, T., Shimasaki, S., Sugino, H., Ueno, N. (1998). Direct binding of follistatin to a complex of bone-morphogenetic protein and its receptor inhibits ventral and epidermal cell fates in early *Xenopus* embryo. *Proc Natl Acad Sci U S A.* 95, 9337-9342.

- Imai, T., Tokunaga, A., Yoshida, T., Hashimoto, M., Mikoshiba, K., Weinmaster, G., Nakafuku, M., Okano, H. (2001). The neural RNA-binding protein Musashi1 translationally regulates mammalian numb gene expression by interacting with its mRNA. *Mol Cell Biol* 21, 3888–3900.
- Jarman, A.P., Grau, Y., Jan, L.Y., Jan, Y.N. (1993). atonal is a proneural gene that directs chordotonal organ formation in the Drosophila peripheral nervous system. *Cell* 73, 1307-1321.
- Jarriault, S., Le Bail, O., Hirsinger, E., Pourquié, O., Logeat, F., Strong, C.F., Brou, C., Seidah, N.G., Isra, I.A. (1998). Delta-1 activation of notch-1 signaling results in HES-1 transactivation. *Mol Cell Biol*. 18, 7423-7431.
- Jen, W.C., Wettstein, D., Turner, D., Chitnis, A., Kintner, C. (1997). The Notch ligand, X-Delta-2, mediates segmentation of the paraxial mesoderm in Xenopus embryos. *Development* 124, 1169-1178.
- Jen, W.C., Gawantka, V., Pollet, N., Niehrs, C., Kintner, C. (1999). Periodic repression of Notch pathway genes governs the segmentation of Xenopus embryos. *Genes Dev*. 13, 1486-1499.
- Jonas, E., Sargent, T.D., Dawid, I.B. (1985). Epidermal keratin gene expressed in embryos of Xenopus laevis. *Proc Natl Acad Sci U S A*. 82, 5413-5417.
- Kageyama, R., Ohtsuka, T., Shimojo, H., Imayoshi, I. (2008). Dynamic Notch signaling in neural progenitor cells and a revised view of lateral inhibition. *Nat Neurosci*. 11, 1247-1251.
- Kimelman, D. (2006). Mesoderm induction: from caps to chips. *Nat Rev Genet*. 7, 360-372.
- Kintner, C.R., and Melton, D.A. (1987). Expression of Xenopus N-CAM RNA in ectoderm is an early response to neural induction. *Development* 99, 311-325.
- Kishi, M., Mizuseki, K., Sasai, N., Yamazaki, H., Shiota, K., Nakanishi, S., Sasai, Y. (2000). Requirement of Sox2-mediated signaling for differentiation of early Xenopus neuroectoderm. *Development* 127, 791-800
- Kiyota, T., Kinoshita, T. (2004). The intracellular domain of X-Serrate-1 is cleaved and suppresses primary neurogenesis in Xenopus laevis. *Mech Dev*. 121. 573-585
- Klisch, T.J., Souopgui, J., Juergens, K., Rust, B., Pieler, T., and Henningfeld, K.A. (2006). Mxi1 is essential for neurogenesis in Xenopus and acts by bridging the pan-neural and proneural genes. *Dev. Biol*. 292, 470-485.
- Kodjabachian, L., Lemaire, P. (1998). Embryonic induction: is the Nieuwkoop centre a useful concept? *Curr Biol*. 8, 918-921.

Kroll, K.L., Salic, A.N., Evans, L.M., Kirschner, M.W. (1998). Geminin, a neuralizing molecule that demarcates the future neural plate at the onset of gastrulation. *Development* 125, 3247-3258.

Kuang, W., Tan, J., Duan, Y., Duan, J., Wang, W., Jin, F., Jin, Z., Yuan, X., Liu, Y. (2009). Cyclic stretch induced miR-146a upregulation delays C2C12 myogenic differentiation through inhibition of Numb. *Biochem Biophys Res Commun.* 378, 259-263.

Kuroda, H., Wessely, O., De Robertis, E.M. (2004). Neural induction in *Xenopus*: requirement for ectodermal and endomesodermal signals via Chordin, Noggin, beta-Catenin, and Cerberus. *PLoS Biol.* 2, e92.

Kuroda, H., Fuentealba, L., Ikeda, A., Reversade, B., and De Robertis, E.M. (2005). Default neural induction: neuralization of dissociated *Xenopus* cells is mediated by Ras/MAPK activation. *Genes Dev.* 19, 1022-1027

Kyriakakis, P., Tipping, M., Abed, L., Veraksa, A. (2008). Tandem affinity purification in *Drosophila*: the advantages of the GS-TAP system. *Fly (Austin).* 2, 229-235.

Kyriazis, G.A., Belal, C., Madan, M., Taylor, D.G., Wang, J., Wei, Z., Pattisapu, J.V., Chan, S.L. (2010). Stress-induced switch in Numb isoforms enhances Notch-dependent expression of subtype-specific transient receptor potential channel. *J Biol Chem.* 285, 6811-6825.

Lamborghini, J.E. (1980). Rohon-beard cells and other large neurons in *Xenopus* embryos originate during gastrulation. *J Comp Neurol.* 189, 323-333.

Lecourtois, M., Schweisguth, F. (1995). The neurogenic suppressor of hairless DNA-binding protein mediates the transcriptional activation of the enhancer of split complex genes triggered by Notch signaling. *Genes Dev.* 9, 2598-2608.

Lee, J.E., Hollenberg, S.M., Snider, L., Turner, D.L., Lipnick, N., Weintraub, H. (1995). Conversion of *Xenopus* ectoderm into neurons by NeuroD, a basic helix-loop-helix protein. *Science.* 268, 836-844.

Lee, K.W., Moreau, M., Néant, I., Bibonne, A., Leclerc, C. (2009). FGF-activated calcium channels control neural gene expression in *Xenopus*. *Biochim Biophys Acta.* 1793, 1033-1040.

Levine, A.J., Brivanlou, A.H. (2006). GDF3, a BMP inhibitor, regulates cell fate in stem cells and early embryos. *Development.* 133, 209-216.

Levine, A.J., Levine, Z.J., Brivanlou, A.H. (2009). GDF3 is a BMP inhibitor that can activate Nodal signaling only at very high doses. *Dev Biol.* 325, 43-48.

- Leyns, L., Bouwmeester, T., Kim, S.H., Piccolo, S., De Robertis, E.M. (1997). Frzb-1 is a secreted antagonist of Wnt signaling expressed in the Spemann organizer. *Cell* 88, 747-756.
- Li, H.S., Wang, D., Shen, Q., Schonemann, M.D., Gorski, J.A., Jones, K.R., Temple, S., Jan, L.Y., Jan, Y.N. (2003). Inactivation of Numb and Numbl like in embryonic dorsal forebrain impairs neurogenesis and disrupts cortical morphogenesis. *Neuron*. 40, 1105-1118.
- Louvi, A., Artavanis-Tsakonas, S. (2006). Notch signalling in vertebrate neural development. *Nat Rev Neurosci*. 7, 93-102.
- Lu, B., Rothenberg, M., Jan, L.Y., Jan, Y.N. (1998). Partner of Numb colocalizes with Numb during mitosis and directs Numb asymmetric localization in *Drosophila* neural and muscle progenitors. *Cell* 95, 225-235.
- Lu, C.B., Fu, W., Xu, X., Mattson, M.P. (2009). Numb-mediated neurite outgrowth is isoform-dependent, and requires activation of voltage-dependent calcium channels. *Neuroscience*. 161, 403-412.
- Gaiano, N., Fishell, G. (2002). The role of notch in promoting glial and neural stem cell fates. *Annu Rev Neurosci*. 25, 471-490.
- Ma, Q., Kintner, C., Anderson, D.J. (1996). Identification of neurogenin, a vertebrate neuronal determination gene. *Cell*. 87, 43-52.
- Marchal, L., Luxardi, G., Thomé, V., Kodjabachian, L. (2009). BMP inhibition initiates neural induction via FGF signaling and Zic genes. *Proc Natl Acad Sci U S A*. 106, 17437-17442.
- McGill, M.A., McGlade, C.J. (2003). Mammalian numb proteins promote Notch1 receptor ubiquitination and degradation of the Notch1 intracellular domain. *J Biol Chem*. 278, 23196-23203.
- McGill, M.A., Dho, S.E., Weinmaster, G., McGlade, C.J. (2009). Numb regulates post-endocytic trafficking and degradation of Notch1. *J Biol Chem*. 284, 26427-26438.
- Meno, C., Saijoh, Y., Fujii, H., Ikeda, M., Yokoyama, T., Yokoyama, M., Toyoda, Y., Hamada, H. (1996). Left-right asymmetric expression of the TGF beta-family member lefty in mouse embryos. *Nature* 381, 151-155.
- Mitchell, T.S., Sheets, M.D. (2001). The FGFR pathway is required for the trunk-inducing functions of Spemann's organizer. *Dev Biol*. 237, 295-305.

- Mizuseki, K., Kishi, M., Shiota, K., Nakanishi, S., Sasai, Y. (1998)a. SoxD: an essential mediator of induction of anterior neural tissues in *Xenopus* embryos. *Neuron*. 21, 77-85.
- Mizuseki, K., Kishi, M., Matsui, M., Nakanishi, S., Sasai, Y. (1998)b. *Xenopus* Zic-related-1 and Sox-2, two factors induced by chordin, have distinct activities in the initiation of neural induction. *Development* 125, 579-587.
- Moody, S.A., Je, H.S. (2002). Neural induction, neural fate stabilization, and neural stem cells. *Scientific World Journal* 2, 1147-1166.
- Moreau, M., Néant, I., Webb, S.E., Miller, A.L., Leclerc, C. (2008). Calcium signalling during neural induction in *Xenopus laevis* embryos. *Philos Trans R Soc Lond B Biol Sci*. 363, 1371-1375.
- Moriyoshi, K., Richards, L.J., Akazawa, C., O'Leary, D.D., Nakanishi, S. (1996). Labeling neural cells using adenoviral gene transfer of membrane-targeted GFP. *Neuron*. 16, 255-260.
- Nakata, K., Nagai, T., Aruga, J., Mikoshiba, K. (1997). *Xenopus* Zic3, a primary regulator both in neural and neural crest development. *Proc Natl Acad Sci U S A*. 94, 11980-11985.
- Nieber, F. (2007). Diploma thesis: Function analysis of *Xenopus* Numb and NumbL.
- Nieber, F., Pieler, T., Henningfeld, K.A. (2009). Comparative Expression Analysis of the Neurogenins in *Xenopus tropicalis* and *Xenopus laevis*. *Dev Dyn*. 238, 451-458.
- Nieuwkoop, P.D. (1952). Activation and organization of the central nervous system in amphibians. Part III. Synthesis of a new working hypothesis. *J. Exp. Zool*. 120, 83-108.
- Nieuwkoop, P.D. (1969). The formation of mesoderm in urodelean amphibians. II. The origin of the dorso-ventral polarity of the mesoderm. *W. Roux' Arch. Entwicklungsmech. Org*. 163, 298-315.
- Niikura, Y., Tabata, Y., Tajima, A., Inoue, I., Arai, K., Watanabe, S. (2006). Zebrafish Numb homologue: phylogenetic evolution and involvement in regulation of left-right asymmetry. *Mech Dev*. 123, 407-414.
- Nishimura, T., Kaibuchi, K. (2007). Numb controls integrin endocytosis for directional cell migration with aPKC and PAR-3. *Dev Cell*. 13, 15-28.
- Okano, H., Imai, T., Okabe, M. (2002). Musashi: a translational regulator of cell fate. *J Cell Sci*. 115, 1355-1359
- Ornitz, D. M., Itoh, N. (2001). Fibroblast growth factors. *Genome Biol*. 2, 1-12

- Oschwald, R., Richter, K., Grunz, H. (1991). Localization of a nervous system-specific class II beta-tubulin gene in *Xenopus laevis* embryos by whole-mount in situ hybridization. *Int J Dev Biol.* 35, 399-405.
- Ostrakhovitch, E.A. (2009). Interplay between Numb and Notch in epithelial cancers: role for dual oxidase maturation factor. *Eur J Cancer.* 45, 2071-2076.
- Papalopulu, N., Kintner, C. (1996). A posteriorising factor, retinoic acid, reveals that anteroposterior patterning controls the timing of neuronal differentiation in *Xenopus* neuroectoderm. *Development* 122, 3409-3418.
- Pedersen, W.A., Chan, S.L., Zhu, H., Abdur-Rahman, L.A., Verdi, J.M., Mattson, M.P. (2002). Numb isoforms containing a short PTB domain promote neurotrophic factor-induced differentiation and neurotrophic factor withdrawal-induced death of PC12 Cells. *J Neurochem.* 82, 976-986.
- Penzel, R., Oschwald, R., Chen, Y., Tacke, L., Grunz, H. (1997). Characterization and early embryonic expression of a neural specific transcription factor xSOX3 in *Xenopus laevis*. *Int J Dev Biol.* 41, 667-677.
- Pera, E.M., De Robertis, E.M. (2000). A direct screen for secreted proteins in *Xenopus* embryos identifies distinct activities for the Wnt antagonists Crescent and Frzb-1. *Mech Dev.* 96, 183-195.
- Pera, E.M., Ikeda, A., Eivers, E., De Robertis, E.M. (2003). Integration of IGF, FGF, and anti-BMP signals via Smad1 phosphorylation in neural induction. *Genes Dev.* 17, 3023-3028
- Peres, J.N., Durston, A.J. (2006). Role of X-Delta-2 in the early neural development of *Xenopus laevis*. *Dev Dyn.* 235, 802-810.
- Petersen, P.H., Zou, K., Hwang, J.K., Jan, Y.N., Zhong, W. (2002). Progenitor cell maintenance requires numb and numbl like during mouse neurogenesis. *Nature.* 419(6910):929-34.
- Petersen, P.H., Zou, K., Krauss, S., Zhong, W. (2004). Continuing role for mouse Numb and Numbl in maintaining progenitor cells during cortical neurogenesis. *Nat Neurosci.* 7, 803-811.
- Piccolo, S., Agius, E., Leyns, L., Bhattacharyya, S., Grunz, H., Bouwmeester, T., De Robertis, E.M. (1999). The head inducer Cerberus is a multifunctional antagonist of Nodal, BMP and Wnt signals. *Nature* 397, 707-710.
- Pozzoli, O., Bosetti, A., Croci, L., Gonzales, G.G., Vetter, M.L. (2001). Xebf3 is a regulator of neuronal differentiation during primary neurogenesis in *Xenopus*. *Dev Biol.* 233, 495-512.

- Rennstam, K., McMichael, N., Berglund, P., Honeth, G., Hegardt, C., Rydén, L., Luts, L., Bendahl, P.O., Hedenfalk, I. (2010). Numb protein expression correlates with a basal-like phenotype and cancer stem cell markers in primary breast cancer. *Breast Cancer Res Treat.* 122, 315-324.
- Reugels, A.M., Boggetti, B., Scheer, N., Campos-Ortega, J.A. (2006). Asymmetric localization of Numb:EGFP in dividing neuroepithelial cells during neurulation in *Danio rerio*. *Dev Dyn.* 235, 934-948.
- Rhyu, M.S., Jan, L.Y., Jan, Y.N. (1994). Asymmetric distribution of numb protein during division of the sensory organ precursor cell confers distinct fates to daughter cells. *Cell* 76, 477-491.
- Sambrook and Russell (2001). *Molecular Cloning: A Laboratory Manual* (3rd ed.). Cold Spring Harbor Laboratory Press
- Santolini, E., Puri, C., Salcini, A.E., Gagliani, M.C., Pelicci, P.G., Tacchetti, C., Di Fiore, P.P. (2000). Numb is an endocytic protein. *J Cell Biol.* 151, 1345-1352.
- Sasai, Y., Lu, B., Steinbeisser, H., De Robertis, E.M. (1995). Regulation of neural induction by the Chd and BMP-4 antagonistic patterning signals in *Xenopus*. *Nature* 377, 757-759
- Sasai, Y., Lu, B., Piccolo, S., De Robertis, E.M. (1996). Endoderm induction by the organizer-secreted factors chordin and noggin in *Xenopus* animal caps. *EMBO J.* 15, 4547-4555.
- Saxen, L. and Toivonen, S. (1962). Primary Embryonic Induction. Logos Press, Academic Press (Lond.)
- Schlosser, G. (2006). Induction and specification of cranial placodes. *Dev Biol* 294, 303–351.
- Schneider, M.L., Turner, D.L., Vetter, M.L. (2001). Notch signaling can inhibit Xath5 function in the neural plate and developing retina. *Mol Cell Neurosci.* 5, 458-472.
- Seo, S., Richardson, G.A. and Kroll, K.L. (2005). The SWI/SNF chromatin remodeling protein Brg1 is required for vertebrate neurogenesis and mediates transactivation of Ngn and NeuroD. *Development* 132, 105-115.
- Seo, S., Lim, J.W., Yellajoshiyula, D., Chang, L.W., Kroll, K.L. (2007). Neurogenin and NeuroD direct transcriptional targets and their regulatory enhancers. *EMBO J.* 26, 5093-5108.
- Shibita, K., Ishimura, A., Maeno, M. (1998). GATA-1 inhibits the formation of notochord and neural tissue in *Xenopus*. *Biochem Biophys Res Commun.* 252, 241-248.

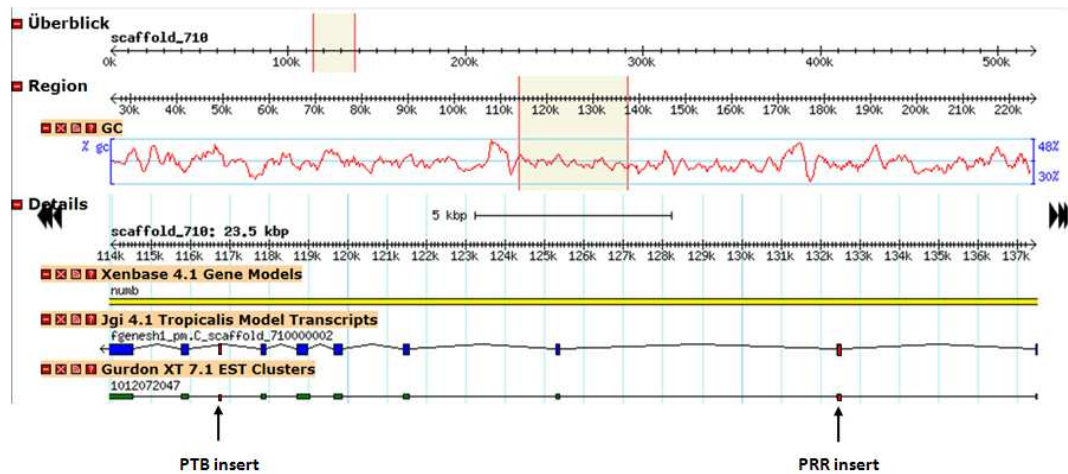
- Shivdasani, R.A. (2002). Molecular regulation of vertebrate early endoderm development. *Dev Biol.* 249, 191-203.
- Smith, W.C., Knecht, A.K., Wu, M., Harland, R.M. (1993). Secreted noggin protein mimics the Spemann organizer in dorsalizing *Xenopus* mesoderm. *Nature* 361, 547-549.
- Spemann, H., Mangold, H. (1924). Über Induktion von Embryonalanlagen durch Implantation artfremder Organisatoren. *Arch. mikr. Anat. und Entw. mech.* 100, 599-638
- Spemann, H. (1931). Das Verhalten von Organisatoren nach Zerstörung ihrer Struktur. *Verh. d. D. Zool. Ges.* 129–132.
- Sölter, M., Köster, M., Hollemann, T., Brey, A., Pieler, T., Knöchel, W. (1999). Characterization of a subfamily of related winged helix genes, XFD-12/12'/12" (XFLIP), during *Xenopus* embryogenesis. *Mech Dev.* 89, 161-165.
- Sommer, L., Ma, Q., Anderson, D.J. (1996). neurogenins, a novel family of atonal-related bHLH transcription factors, are putative mammalian neuronal determination genes that reveal progenitor cell heterogeneity in the developing CNS and PNS. *Mol Cell Neurosci.*, 8, 221-241
- Sorensen, E.B., Conner, S.D. (2008). AAK1 regulates Numb function at an early step in clathrin-mediated endocytosis. *Traffic.* 9, 1791-1800.
- Souopgui, J., Sölter, M., Pieler, T. (2002). XPak3 promotes cell cycle withdrawal during primary neurogenesis in *Xenopus laevis*. *EMBO J.* 21, 6429-39.
- Takahashi, S., Yokota, C., Takano, K., Tanegashima, K., Onuma, Y., Goto, J., Asashima, M. (2000). Two novel nodal-related genes initiate early inductive events in *Xenopus* Nieuwkoop center. *Development* 127, 5319-5329.
- Thisse, C., Thisse, B. (1999). Antivin, a novel and divergent member of the TGFbeta superfamily, negatively regulates mesoderm induction. *Development* 126, 229-240.
- Tokumitsu, H., Hatano, N., Yokokura, S., Sueyoshi, Y., Nozaki, N., Kobayashi, R. (2006). Phosphorylation of Numb regulates its interaction with the clathrin-associated adaptor AP-2. *FEBS Lett.* 580, 5797-5801.
- Tonissen, K.F., Krieg, P.A. (1993). Two neural-cell adhesion molecule (NCAM)-encoding genes in *Xenopus laevis* are expressed during development and in adult tissues. *Gene.* 127, 243-247.

- Toriya, M., Tokunaga, A., Sawamoto, K., Nakao, K., Okano, H. (2006). Distinct functions of human numb isoforms revealed by misexpression in the neural stem cell lineage in the *Drosophila* larval brain. *Dev Neurosci.* 28, 142-155.
- Uemura, T., Shepherd, S., Ackerman, L., Jan, L.Y., Jan, Y.N. (1989). numb, a gene required in determination of cell fate during sensory organ formation in *Drosophila* embryos. *Cell* 58, 349-360.
- Uwanogho, D., Rex, M., Cartwright, E.J., Pearl, G., Healy, C., Scotting, P.J., Sharpe, P.T. (1995). Embryonic expression of the chicken Sox2, Sox3 and Sox11 genes suggests an interactive role in neuronal development. *Mech Dev.* 49, 23-36.
- Van Doren, M., Powell, P.A., Pasternak, D., Singson, A., Posakony, J.W. (1992). Spatial regulation of proneural gene activity: auto- and cross-activation of achaete is antagonized by extramacrochaetae. *Genes Dev.* 6, 2592–2605.
- Verdi, J.M., Schmandt, R., Bashirullah, A., Jacob, S., Salvino, R., Craig, C.G., Program, A.E., Lipshitz, H.D., McGlade, C.J. (1996). Mammalian NUMB is an evolutionarily conserved signaling adapter protein that specifies cell fate. *Curr Biol.* 6 1134-1145.
- Verdi, J.M., Bashirullah, A., Goldhawk, D.E., Kubu, C.J., Jamali, M., Meakin, S.O., Lipshitz, H.D. (1999). Distinct human NUMB isoforms regulate differentiation vs. proliferation in the neuronal lineage. *Proc Natl Acad Sci U S A.* 96. 10472-10476.
- Vernon, A.E., Devine, C., Philpott, A. (2003). The cdk inhibitor p27Xic1 is required for differentiation of primary neurones in *Xenopus*. *Development* 130, 85-92.
- Vosper, J.M., McDowell, G.S., Hindley, C.J., Fiore-Herliche, C.S., Kucerova, R., Horan, I., Philpott, A. (2009). Ubiquitylation on canonical and non-canonical sites targets the transcription factor neurogenin for ubiquitin-mediated proteolysis. *J Biol Chem.* 284, 15458-15468.
- Wakamatsu, Y., Maynard, T.M., Jones, S.U., Weston, J.A. (1999). NUMB localizes in the basal cortex of mitotic avian neuroepithelial cells and modulates neuronal differentiation by binding to NOTCH-1. *Neuron.* 1, 71-81.
- Wang, H., Ouyang, Y., Somers, W.G., Chia, W., Lu, B. (2007). Polo inhibits progenitor self-renewal and regulates Numb asymmetry by phosphorylating Pon. *Nature* 449, 96-100.
- Wang, S., Younger-Shepherd, S., Jan, L.Y., Jan, Y.N. (1997). Only a subset of the binary cell fate decisions mediated by Numb/Notch signaling in *Drosophila* sensory organ lineage requires Suppressor of Hairless. *Development* 124, 4435-4446.
- Wegner, M., Stolt, C.C. (2005). From stem cells to neurons and glia: a Soxist's view of neural development. *Trends Neurosci.* 28, 583-588.

- Westhoff, B., Colaluca, I.N., D'Ario, G., Donzelli, M., Tosoni, D., Volorio, S., Pelosi, G., Spaggiari, L., Mazzarol, G., Viale, G., Pece, S., Di Fiore, P.P. (2009). Alterations of the Notch pathway in lung cancer. *Proc Natl Acad Sci U S A.* 106, 22293-22298.
- Wettstein, D.A., Turner, D.L., Kintner, C. (1997). The *Xenopus* homolog of *Drosophila* Suppressor of Hairless mediates Notch signaling during primary neurogenesis. *Development* 124, 693-702.
- Wills, A.E., Choi, V.M., Bennett, M.J., Khokha, M.K., Harland, R.M. (2010). BMP antagonists and FGF signaling contribute to different domains of the neural plate in *Xenopus*. *Dev Biol.* 337, 335-350.
- Wirtz-Peitz, F., Nishimura, T., Knoblich, J.A., (2008). Linking cell cycle to asymmetric division: Aurora-A phosphorylates the Par complex to regulate Numb localization. *Cell* 135, 161-173.
- Wullimann, M.F., Rink, E., Vernier, P., Schlosser, G. (2005). Secondary neurogenesis in the brain of the African clawed frog, *Xenopus laevis*, as revealed by PCNA, Delta-1, Neurogenin-related-1, and NeuroD expression. *J Comp Neurol.* 489, 387-402.
- Yan, B., Neilson, K.M., Moody, S.A. (2009)a. Notch signaling downstream of foxD5 promotes neural ectodermal transcription factors that inhibit neural differentiation. *Dev Dyn.* 238, 1358-1365.
- Yan, B., Neilson, K.M., Moody, S.A., (2009)b. foxD5 plays a critical upstream role in regulating neural ectodermal fate and the onset of neural differentiation. *Dev Biol.* 329, 80-95.
- Zhong, W., Feder, J.N., Jiang, M.M., Jan, L.Y., Jan, Y.N. (1996). Asymmetric localization of a mammalian numb homolog during mouse cortical neurogenesis. *Neuron.* 17, 43-53.
- Zhong, W., Jiang, M.M., Weinmaster, G., Jan, L.Y., Jan, Y.N. (1997). Differential expression of mammalian Numb, Numlike and Notch1 suggests distinct roles during mouse cortical neurogenesis. *Development* 124, 1887-1897.
- Zhong, W., Jiang, M.M., Schonemann, M.D., Meneses, J.J., Pedersen, R.A., Jan, L.Y., Jan, Y.N. (2000). Mouse numb is an essential gene involved in cortical neurogenesis. *Proc Natl Acad Sci U S A.* 97, 6844-6849.
- Zhou, Y., Atkins, J.B., Rompani, S.B., Bancescu, D.L., Petersen, P.H., Tang, H., Zou, K., Stewart, S.B., Zhong, W. (2007). The mammalian Golgi regulates numb signaling in asymmetric cell division by releasing ACBD3 during mitosis. *Cell* 129, 163-178.

Zimmerman, L.B., De Jesús-Escobar, J.M., Harland, R.M. (1996). The Spemann organizer signal noggin binds and inactivates bone morphogenetic protein 4. *Cell* 86, 599-606.

7. Appendix



Xt Numb cDNA:

```

ATGAACAACTGCGTCAGAGTTTTCGGCGGAAGAAAGATATCTATGTCCAGAGGCAAGCCGA
CCCACCAGTGGCAAACACTGACGAAGAATCGGTCAGGAATGGGAAATGTAGCTTTCAAGTTAAG
TATCTCGGCCATGTGGAAGTAGAGGAATCAAGAGGGATGCACATCTGCGAAGAAGCAGTGAAA
AGATTAATCTGAAAGGAAGTACTTCAAAGGCTTCTTTGCAAAAAGCGGCAAGAAAGCAATCA
AGGCCGTCCTGTGGGTTTCAGCTGATGGACTTCGAGTTGTGGATGAAAAGACAAAGGATCTTCT
GGTTGACCAGACTATTGAGAAAGTCTCCTTCTGTGCTCCAGATAGAAAATTTGACAGAGCCTTTT
CTTATATCTGTCGTGATGGTACAACACTAGGCGATGGATCTGTCACTGCTTCATGGCTGTTAAAGAT
ACGGGCGAGAGGCTCAGCCATGCTGTTGGATGTGCATTTGCTGCTTGTCTTGAGAGGAAGCAG
AAGCGGGAAAAGGAGTGTGGAGTGACTGCTACATTTGATGCCAGCAGAACTACTTTACCCCGG
GAAGGCTCTTTCAGGGTCACCACAGCCACAGAGCAAGCAGAGAGAGAGGAAGTCATGAAGCA
GATACAGGAATCCAGGAAAGAGCTGGAAGTAAAGCACCAGTCGTACCAGCAGCACCTTCAAC
AACTGTGTCTTCCACTCCAACCCAGTGCTACAATCCTCTCCAACCTCTGAGGTGTTTGTGGTCCA
GGACAGTAAAGATCTAAATTACCCCATGCAATCCCTCGAAGGCATGCTCCTGTGGAACAGCTT
GCCAGACAGGGCTCCTTCCGGGGTTTTCTGCTCTCAGCCAAAAAATGTCCCATTCAGCGTCA
GCTTTCCTTAAGGATCAATGAGCTGCCATCAACTGTTCAAAGAAAATCTGACTTTCAGGCTACAA
ATCCAGTTGCAGAGATGGAAGGAGAAAACGACAGCATAAGTGCCCTGTGTTCCAGATCACAA
ACATTTTCAGCATGCCACCTGAGGATCCATTACTTCTGCGCCCATGACTAAAGCCACCACACCA
CAGTCCCACCTTTTGAAGTAAATGGCACTGCCTCTGCATTAGTTGCTGCTGCTACACCAAC
ACCAATCTCTGTAACCAGCACCGCAGCAGCACCTGTGCGTGAGACCAACCTTGGGCAAATGCT
CCGCGGCTTCTAACTTACCAGTCACTACCCTGGGACTGTCTGTAGCCCCCTTAGTTGGTCC
TGCCCTTCATCTGGTACTCACCAGTCAAACCACAAACGAACACCCTCTGAGGCAGACCGTTGGC
TTGAAGAAGTATCCAAAACAATCATGCAAAGACAGTCTCCAGTTCCTGCAGTCCCAACTCAGCCT
ATGGTACAACCTGCCCTTGCCGCACCACAGCCTAACCCAGCCTTACCTGGCCAATGCTTATGTGAC
CTCACAGTCTATGCCTGTCTGTGTTGCCAGGTCTGCACCCTCCCTTCATGCCTGTGCAGCCACC
ATACTCTGTAGCCAATGGAATGAGCTACCAGCTCCAGTGTTCAGTGTGTTGGCATAACCCCTT
CTCAAATGGTAGCTAATGTTTTCGGAGTTGCAAGTCCACAGGTATTCCAGCCTAAGCCATCTCCA
AATTTAGCCACACAGCAAACCTATCCAACCTTATGAAGCATCCAGTGCATCCAGCAGTCCATTCTA

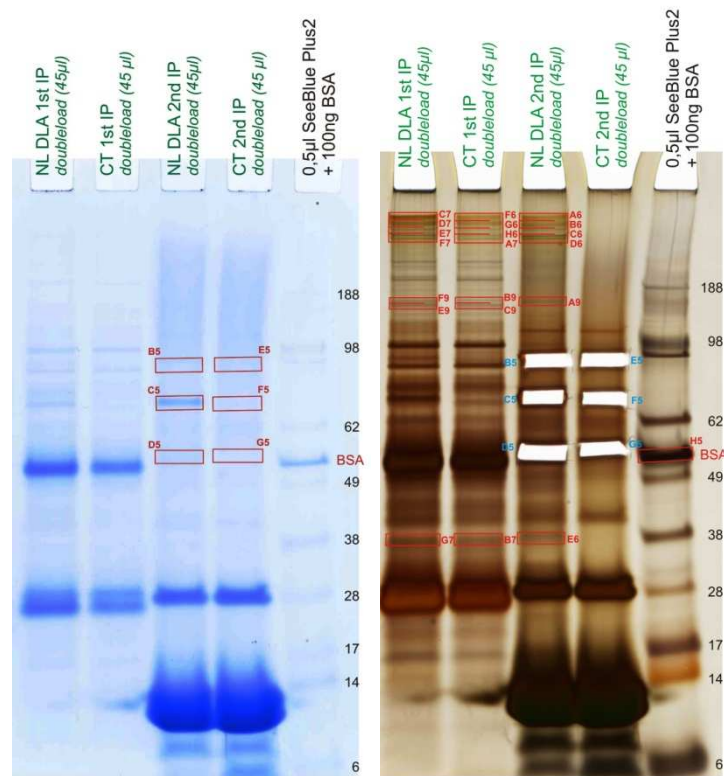
```

TAAGCCTCTGCCAGCAACAGAATGGCTCTGTTGCTTTTAATGGGGTTGAAAGTAGTGGGTGG
 GAATTGGGCGCTAAGAGCCAGCAAGCTCCAGCTGCCCTCCTCCTGTAGACCCATTTGAAGCTC
 AATGGGCAGCTCTTGAAGGCAAATCTAGACCACGTGCAAACCCATCTCCTACAAATCCTTTCTCT
 AGTGACCTTCAAAGACTTTTGAATTGAACTATAG

Xt Numb protein:

MNKLRSFRRKKDIYVPEASRPHQWQTDEESVRNGKCSFQVKYLGHVVEESRGMHICEEAVKRLK
 SERKYFKGFFAKSGKKAIAVLWVSADGLRVVDEKTKDLLVDQTIEKVSFCAPDRNFDRAFSYICRDG
 TTRRWICHCFMAVKDTGERLSHAVGCAFAACLERKQKREKECGVTATFDASRTTFTREGSFRVTTAT
 EQAEREEVMKQIQESRKELEVKAPVPPAAPSTTVSSTPTVLPVLSPTSEVFFVQDSKDLNYPHAIPRR
 HAPVEQLARQGSFRGFPALSQKMSPFKRQLSLRINELPSTVQRKSDFFQATNPVAEMEGENDSISALC
 SQITNTFSMPPEPFTSAPMTKATTPQSPPFENGTASAFSLPAATPTPISVTSTAAAPVRETNPWAN
 APAASNLPVTTTGTLSVAPLVPVPSSGTHQSNHKRTPSEADRWLEEVSKTIMQRQSPVPAVPTQPM
 VQPALAAPQPNQPYLANAYVTSQSMPVSVVPLHPPFMPVQPPYSVANGMSYPASSVPVVGITPS
 QMVANVFGVASPQVFQPKPSPNLATQQTYPTYEASSASSPFYKPPAQQQNGSVAFNGVESSGW
 ELGAKSQQAPAAPPVDPFEAQWAALEGKSRPRANPSPTNPFSSDLQKTFEIEL

Appendix Figure 1: Genomic structure of *X. tropicalis* Numb and identified insert sequences. Schematic representation of scaffold_710, 113,854 – 137,594 (*Xenopus tropicalis* genome draft 4.1), showing the *Xt Numb* gene locus. Relative positions of the PTB and the PRR exon are indicated by arrows. In the cDNA and peptide sequence of *Xt Numb*, the identified PTB insert is shown in blue and the PRR insert in green. (genome draft source: http://www.xenbase.org/fgb2/gbrowse/Xenopus_tropicalis_4_1/?name=scaffold_710:1_13854-137594, modified)



Name: Nieber, Frank
Date of Birth: 11.01.1982
Born in: Celle, Germany
Nationality: German
Address: Frank Nieber
Kaakweg 1c
37077 Göttingen, Germany
Email: Frank_Nieber@gmx.de

Education:

07.2007 – 10.2010 PhD Thesis “Function analysis of *Xenopus* NumbL in the context of primary neurogenesis” Department of Developmental Biochemistry, University of Göttingen
Advisor: Prof. Tomas Pieler, Supervisors: K.A. Henningfeld, PhD.

06.2006 – 06.2007 Diploma Thesis “Function analysis of *Xenopus* Numb and NumbL”. Department of Developmental Biochemistry, University of Göttingen,
Advisor: Prof. Tomas Pieler, Supervisor: K.A. Henningfeld, PhD

10.2002 – 05.2006 Study of Biology at the University of Göttingen. Oral diploma examinations on 12.05.2006. Major subject: Biochemistry; Minor subjects: Microbiology and Organic Chemistry.

Fellowships:

09.2008 – 01.2011 GGNB Excellence Stipend

Publications:

Frank Nieber, Tomas Pieler, Olaf Jahn, and Kristina A. Henningfeld. NumbL is essential for *Xenopus* primary neurogenesis and functions independent of Notch signaling. In preparation

Frank Nieber, Tomas Pieler, and Kristine A. Henningfeld. Comparative Expression Analysis of the Neurogenins in *Xenopus tropicalis* and *Xenopus laevis*. *Dev Dyn.* 2009 238:451–458

Göttingen, 29.11.2010